INCREASED VIP RECEPTOR EXPRESSION MEDIATES CFTR MEMBRANE LOCALIZATION IN RESPONSE TO VIP TREATMENT IN VIP KNOCKOUT MICE

by

Dustin Jeffrey Conrad

Submitted in partial fulfilment of the requirements
for the degree of Master of Science

at

Dalhousie University
Halifax, Nova Scotia
August 2011

DALHOUSIE UNIVERSITY

DEPARTMENT OF PHYSIOLOGY & BIOPHYSICS

The undersigned hereby certify that they have read and recommend to the Faculty of Graduate Studies for acceptance a thesis entitled "INCREASED VIP RECEPTOR EXPRESSION MEDIATES CFTR MEMBRANE LOCALIZATION IN RESPONSE TO VIP TREATMENT IN VIP KNOCKOUT MICE" by Dustin Jeffrey Conrad in partial fulfillment of the requirements for the degree of Master of Science.

Dated: August 23, 2011

Supervisor: _____

Readers: _____

_____

_____

DALHOUSIE UNIVERSITY

DATE: August 23, 2011

AUTHOR: Dustin Jeffrey Conrad

TITLE: INCREASED VIP RECEPTOR EXPRESSION MEDIATES CFTR MEMBRANE LOCALIZATION IN RESPONSE TO VIP TREATMENT IN VIP KNOCKOUT MICE

DEPARTMENT OR SCHOOL: Department of Physiology & Biophysics

DEGREE: MSc CONVOCATION: October YEAR: 2011

_____

Signature of Author

TABLE OF CONTENTS

LIST OF TABLES

LIST OF FIGURES

ABSTRACT

Increased VIP receptor expression mediates CFTR membrane localization in response to VIP treatment in VIP knockout mice

Cystic Fibrosis (CF) is caused by mutations in CFTR, a protein for chloride efflux in epithelial cells. VIP is a peptide that activates CFTR and improves membrane stability; VIP has 3 receptors $VPAC_1$, $VPAC_2$ and PAC_1 that can cause CFTR phosphorylation. VIP-knockout (VIPKO) mice experience inflammation and reduced CFTR membrane localization comparable to CF phenotypes, that's reversible after 3 weeks of VIP treatment (VIPKOT). In this thesis western blotting showed $VPAC_1$ and $VPAC_2$ expression increased in VIPKO and VIPKOT lung and duodenum tissues. The expression and maturation of CFTR was unchanged in both VIPKO and VIPKOT tissues. The results showed absence of VIP caused increased receptor expression in VIPKO mice, after VIP treatment VIPKO mice maintained increased receptor expression. VIP treatment reduces inflammation and restores existing CFTR membrane localization in VIPKO mice. VIP receptor expression may be important for future treatment of CF for CFTR localization and reducing tissue inflammation.

LIST OF ABBREVATIONS USED

ΔF508-CFTR	Deletion of phenylalanine at position 508 on CFTR protein
ABC	ATP-Binding Cassette
ASL	Airway Surface Liquid
ATP	Adenosine Triphosphate
BHK	Baby Hamster Kidney
BSA	Bovine Serum Albumin
CaCC	Calcium Activated Chloride Channels
Calu-3	Human bronchial serous cell line
cAMP	Cyclic Adenosine Monophosphate
CF	Cystic Fibrosis
CFTR	Cystic Fibrosis Transmembrane Regulator
CNS	Central Nervous System
ddH20	Double Deionized Water
EC_{50}	Half maximal effective concentration
ENaC	Epithelial Sodium Channels
GPCR	G-Protein-Coupled Receptor
JME/CF15	Human nasal epithelial cell line derived from ΔF508 CF Patient
NBD	Nucleotide Binding Domain
ns	non significant
ORCC	Outwardly Rectifying Chloride Channels
PAC_1	PACAP specific receptor 1
PACAP	Pituitary Adenylate Cyclase-Activating Peptide
PAH	Pulmonary Arterial Hypertenstion
PBS	Phosphate Buffered Saline
PCL	Periciliary Liquid
PKA	Protein Kinase A
PKC	Protein Kinase C
PLC	Phospholipase C
PLD	Phospholipase D
PNS	Peripheral Nervous System
ROMK	Renal Potassium Channels
RD	Regulatory Domain
RT	Room Temperature
RT-PCR	Reverse Transcription Polymerase Chain Reaction
SCN	Suprachiasmatic Nucleus
TBS	Tris Buffered Saline
TTBS	Tris-Tween Buffered Saline
TMD	Transmembrane Spanning Domain
VIP	Vasoactive Intestinal Peptide
VIPKO	Mice with deleted VIP gene
VIPKOT	Mice with deleted VIP gene, that received exogenous VIP injections
$VPAC_1$	VIP receptor 1
$VPAC_2$	VIP receptor 2
WT	Wild Type

ACKNOWLEDGEMENTS

I would like to express my most sincere gratitude to all the people involved during the course of my Master's project. To my supervisor Dr. Valerie Chappe her continued support and guidance has been invaluable during the course of this project and her passion and dedication to Cystic Fibrosis research has been inspiring. I thank the former and current members of the lab especially Frederick Chappe, Nicole Alcolado and Adrienne Ackermann. Thank you to Dr. Sami Said (SUNY, NY, USA) for generously providing the VIPKO and VIPKOT mice samples used in this study. I would like to thank the labs of Dr. Younes Anini, Dr. Robert Rose and Dr. Stefan Krueger for providing technical support and equipment. I would also like to thank NSERC for funding through the CGS award as well as funding from the granting agencies CFC, CIHR, CFI and DMRF. Finally I would like to acknowledge the support of my family and friends during the course of my studies.

CHAPTER 1: INTRODUCTION

1.1 Cystic Fibrosis

The most common fatal genetic autosomal recessive disease found in individuals of European linage is Cystic Fibrosis (CF); however CF is also prevalent across many other origins and cultures worldwide (Bobadilla et al. 2002). In Canada, 1/25 people have one defective allele in the gene that is ultimately responsible for CF and currently 1/3,600 children born in Canada will have CF (Cystic Fibrosis Canada 2011; Dupis et al. 2005). CF affects the physiology of numerous organs including the lungs, intestine, pancreas, reproductive tract, sweat glands and liver (Tizzano and Buchwald 1995).

In CF, electrolyte transport in exocrine epithelium lining the organs is defective, specifically the movement of chloride ions from within epithelial cells across the apical membrane to the lumen is deficient (Quinton 1999). The chloride ion movement is largely mediated by the channel forming protein Cystic Fibrosis Transmembrane Conductance Regulator (CFTR) that when functioning correctly regulates ionic composition of the mucus layer at the apical membrane. The movement of chloride ions through CFTR and sodium ions through the epithelial sodium channel (ENaC) is extremely important because it influences the movement of water that hydrates the extracellular mucus layers. The correct hydration of the mucus layer is vital for functions such as pericellular clearance in the lung and digestive enzyme secretions into the intestine from the pancreas (Rowe et al. 2005; Moskowitz et al. 2001).

The clinical complications of CF can develop *in utero* at approximately 17 weeks of gestation presenting with a blockage in the ileum known as meconium ileus.

Meconium ileus occurs in 15-20% of children born with CF and usually requires an operation to help improve function (Brock and Barron 1986; Grosse et al. 2004). Infants with CF also show characteristics such as reoccurring cough, abdominal discomfort and failure to thrive (Accurso et al. 2005). Approximately 60% of patients with CF in Canada will be diagnosed within the first 12 months after birth and 90% will be diagnosed before 10 years of age (Cystic Fibrosis Canada 2011).

The organ most commonly associated with CF is the lungs because over 90% of patients who succumb to CF are the result of chronic bacterial infections that manifest in the lungs (Aris et al. 1997). In CF affected airways, CFTR function is compromised causing a decrease in the volume of the air surface liquid (ASL), the ASL is a fluid layer resting overtop of airway epithelial cells composed of a pericellular layer (PCL) and mucus layer. The PCL is in direct contact with the epithelium and its protruding cilia while the muscus layer is located above the PCL and functions to capture small particles and bacteria. The volume regulation of the ASL is crucial in airways, when correctly hydrated it allows the cilia that line the airways to beat in unison and perform mucociliary clearance, a process that removes foreign particles and microorganism that have collected in the mucus layer (Boucher 2002; Robinson 2002). When the ASL has a reduced volume, mucociliary clearance is impaired because the cilia can no longer move freely and transport the mucus, allowing for chronic colonization of microorganism such as *Haemophilus influenza*, *Staphylococcus aureus* and *Pseudomonas aeruginosa* which cause infection of the lungs (Rogers et al. 2008).

Other organs with altered function in CF patients are the exocrine pancreas and small intestine both involved in digestion and absorption of nutrients. The pancreas

secretes a bicarbonate rich solution into the duodenum that contains enzymes to facilitate digestion of fats and proteins (Taylor and Aswani 2002). The small intestine is the site where the broken down nutrients are absorbed; CFTR maintains the fluidity of the small intestine allowing normal absorption and bolus passage. When CFTR is compromised the digestive secretions from the pancreas precipitate in the ducts leading to the duodenum causing blockages, the enzymes proceed to cause destruction of the exocrine pancreas replacing it with fibrotic tissue (Krysa and Steger 2007; Morton et al. 2009). The resulting pancreatic insufficiency fails to deliver the necessary secretions for proper digestion of nutrients and causes increased levels of the enzyme trypsinogen in the serum, a marker of CF (Krysa and Steger 2007). Complications in the small intestine contribute to thickened mucus causing poor nutrient absorption, inflammation and gastrointestinal blockages (Littlewood et al. 2006).

1.2 Treatment of Cystic Fibrosis

There is currently no cure for people suffering from CF, although through dedicated research efforts treatments are available that can elevate the symptoms of the disease. Treatment of the airways in CF patients can include chest physical therapy which involves repetitive percussions to the chest and back in order to loosen the mucus build up and facilitate its movement out of the airways (Hodson 2000; CFC 2011). Other lung therapy regimes may call for use of antibiotics, anti-inflammatory, mucus thinning agents and bronchodilators (Sheils et al. 1996; Friedlander et al. 2010; Ibrahim et al. 2011). Each of these treatments is aimed at to either prevent or reducing the swelling and inflammation of the airways or promoting the loosening and removal of the thick

dehydrated airway mucus. In severe conditions with decreased lung function a lung transplant may be performed to restore airway function.

Current therapies to help manage the complications of pancreatic insufficiency and poor nutrient absorption are administration of oral pancreatic enzymes and nutrient supplements of vitamins A, D, E and K (Anthony et al. 1999). A diet consisting of high calorie shakes to provide further increased nutrient intake in conjunction with mucus thinning medications is also common among CF patients (Gardner 2007; Kremer et al. 2008). If intestinal complications become more severe, a build up of dehydrated mucus can occur blocking a segment of the intestine which may require surgery to clear the blockage (Speck and Charles 2008).

Although these forms of treatment have been successful in increasing the life expectancy of CF patients to over 40 years of age (Hodson 2000; CFC 2011), there still needs to be a focus on correcting CFTR defects to restore normal function in patients with CF and not just medications targeting the symptoms of the disease.

1.3 Cystic Fibrosis Transmembrane Conductance Regulator

CFTR is a 1480 amino acid protein and member of the ATP Binding Cassette (ABC) superfamily of transporters (Riordan et al. 1989). A defining process that ABC transporters employ is the binding and hydrolysis of adenosine triphosphate (ATP) to provide energy for gating (Ko and Pedersen 2001; Mehta 2005). Although the ABC transporter superfamily transports a wide range of molecules and ions, CFTR is the only member of the ABC family that acts as an ion channel when activated and facilitates the movement of chloride ions (Dean et al. 2001). CFTR is also capable of transporting

bicarbonate which may be important not only for fluid secretion but also pH balance of the mucus layer (Fischer and Widdicombe 2006).

1.3.1 Structure of CFTR

CFTR has 5 distinct domains that organize together to form a functioning channel. The transmembrane domains (TM) are membrane spanning regions of the protein that each containing six alpha helices (Farinha et al. 2004). The TM domains come together to give CFTR its structure and functions to form the pore region which facilitates the transport of the chloride ions and bicarbonate (Akabas et al. 1997). The TM domains also form interactions with the intracellular domains that are important for the facilitation of CFTR channel gating (Zhang et al. 2000). CFTR also contains 2 nuclear binding domains (NBD) that are located on the cytosolic intracellular region of the CFTR protein when present at the plasma membrane. The NBDs are responsible for the binding and hydrolysation of ATP, a crucial process to provide the energy for CFTR gating and NBDs can also receive phosphorylation by protein kinases (Howell et al. 2000; Aleksandrov et al. 2001). The last domain of the CFTR protein is the regulatory domain more commonly referred to as the R domain. The R domain is the major site of phosphorylation by protein kinase A (PKA) and protein kinase C (PKC) of the CFTR protein, this phosphorylation is essential for activation and regulation of CFTR channel gating (Chappe et al. 2003; Seavilleklein et al. 2008).

1.3.2 CFTR gating and regulation through PKA and PKC

At resting or non-stimulated conditions the majority of CFTR channels present at the membrane are inactive and closed. The regulation of CFTR is a complex process involving the binding and hydrolysis of ATP in the NBDs as well as phosphorylation by PKA and PKC (Fig. 1.1) (Gadsby et al. 2006). At rest CFTR is inhibited by the unphosphorylated R domain, CFTR activation occurs when there is an increase in cellular cAMP causing activation of PKA that can in turn phosphorylate residues in the CFTR R domain (Winter and Welsh 1997; Sheppard and Welsh 1999). The phosphorylation of the R domain is believed to cause conformation changes to CFTR allowing the NBDs to dimerize in a head-to-tail conformation. With the change in conformation, ATP can gain access and bind to specialized sequences called Walker motifs in the NBDs, the Walker motif sequence is an identifying characteristic found in all ABC transporters (Stratford et al. 2007). When both NBDs have ATP bound and have dimerized it allows channel opening and the conductance of chloride ions. After channel opening the ATP bound to the catalytically active NBD_2 is hydrolysed and causes incomplete dissociation of the NBD dimer and subsequent channel closing (Gadsby et al. 2006; Hwang and Sheppard 2009).

Phosphorylation by PKC along can activate CFTR at approximately 1-2% of PKA activation in baby hamster kidney (BHK) cell line transfected with CFTR (Chappe et al. 2003). Phosphorylation by PKC is also important for CFTR activation because it potentiates further PKA phosphorylation and channel activity, but also may contribute to channel inhibition through activation of other accessory proteins of CFTR (Raghuram et al. 2003; Chappe et al. 2004). Additionally PKC phosphorylation increases CFTR

membrane stability and density once at the plasma membrane enhancing CFTR mediated chloride secretion (Winpenny et al. 1995; Chappe et al. 2003; Chappe et al. 2008; Rafferty et al. 2009). There are 11 PKC isoforms, previous work in BHK cells and JME/CF15 derived from human nasal epithelium of a CF patient showed the epsilon isoform is important for the CFTR response due to PKC phosphorylation (Liedtke et al. 2002; Alcolado et. al 2011).

1.3.3 CFTR expression and regulation of membrane proteins

CFTR expression is primarily found in epithelial cells lining the exocrine organs of the body. In the airway epithelium CFTR is expressed throughout, however there are also specialized areas of epithelial cells indenting the tracheal and bronchial regions known as submucosal glands. Submucosal glands contain both mucus cells and high CFTR expressing serous cells that are situated below the airway but are connected by a collecting duct (Engelhardt et al. 1992). The submucosal glands supply watery mucus secretions to the surface of the airways and are regulated by inputs of the autonomic nervous system (Rogers 2001). Complimentary to submucosal glands in the lung are Brunners glands of the duodenum which also contain dense CFTR expression. Brunners glands function to lubricate the intestinal wall and provide basic pH secretions that promote activation of digestive enzymes (Jakab et al. 2011).

CFTR is also expressed in non-epithelial cells including smooth muscle, cardiomyocytes, endothelium and T-lymphocytes (Kleizen et al. 2000; Vandebrouck et al. 2006). The expression level of CFTR in non-epithelial cells is generally much lower compared to epithelial cells and has not been thoroughly investigated. CF does not appear

to cause major complications in the non-epithelial cells expressing defective CFTR suggesting the possible compensation by other genes for the loss of CFTR function (Trezise 2006).

Regulation of other ion channels such as calcium activated chloride channels (CaCC), outwardly rectifying chloride channels (ORCC), ROMK potassium channels and epithelial sodium channels (ENaC) is another important function of CFTR (Kleizen et al. 2000). In CF epithelium an increase in CaCC activity occurs, possibly to compensate for the loss of chloride efflux through CFTR however CaCC is not successful in restoring the ASL to a functioning level in CF airways (Tarran et al. 2002). In CF, the ORCC is unable to receive proper phosphorylation to extrude chloride ions from epithelium when CFTR is defective due to loss of interactions with NBD_1 at the apical membrane (Schwiebert et al. 1999). The regulation of CFTR on ENaC has been studied extensively due to the colocalization of both proteins at the apical membrane, in CF epithelium with defective CFTR regulation there is an increase in ENaC function (Ji et al. 2000;Rubenstein et al. 2011). Under normal conditions CFTR inhibits the function of ENaC at the apical membrane preventing an influx of sodium ions. In CF, CFTR regulation of ENaC is lost and sodium ions influx into the epithelium causing water to follow, further dehydrating the mucus layer of the epithelium (Matsui et al. 1998).

1.3.4 CFTR membrane life cycle

The life cycle of CFTR begins with transcription of the CFTR gene located on chromosome 7 and is completed when CFTR is targeted for lysosomal degradation. There

are key steps and waypoints in-between that CFTR experiences during its life as a chloride transporter in epithelial cells (Ameen et al. 2007). After transcription the CFTR protein is moved to the endoplasmic reticulum where it is folded and undergoes glycosylation during its translocation through vesicles of the Golgi apparatus and eventually traffics to the plasma membrane (Wang et al. 2004). When CFTR is present at the plasma membrane it undergoes cycles of internalization into recycling endosomes just under the plasma membrane and reinsertion of the recycled CFTR back into the plasma membrane (Ameen et al. 2007). When CFTR has served its lifetime which was found to be ~48 hours in cells lines for WT-CFTR at the plasma membrane, it is ubiquitinilated marking it for degradation (Heda et al. 2001). Upon internalization, the vesicle containing CFTR fuses with lysosomes degrading the contents. The life time of CFTR at the plasma membrane can be influenced by PKA and PKC phosphorylation, this form of regulation varies between cell types and agonists used to stimulate phosphorylation (Silvis et al. 2009).

1.3.5 Cystic Fibrosis and mutations of CFTR

CF is caused by mutations in the CFTR gene that cause alterations of the gene expression or amino acid composition in the primary sequence of CFTR. Currently there are over 1,800 mutations of the CFTR gene found in every intron and exon (CFMD, 2011). In CF patients there exists a large array of phenotypes associated with certain mutations ranging from asymptomatic to severe symptoms (McKone et al. 2006). Although the pathology of CF stems from genetic mutations, the correlation between specific mutants and phenotype is not precise. Other factors such as environment and

secondary genetic factors may account for variation of pathology seen in patients with the same CF genetic mutations (Zielenski 2000).

At the molecular level, mutated CFTR can be identified into 6 different classes based upon the molecular process that is found to be defective. The classes of mutations are grouped into defects in (1) synthesis, (2) trafficking, (3) regulation, (4) channel conductance, (5) abundance and (6) membrane stability (Kreindler 2010).

Despite the existence of over 1.800 mutations in the CFTR gene, the ΔF508 mutation which has a deleted phenylalanine amino acid at position 508 is the most frequent mutation, found in at least 1 allele in 85% of CF patients (Boucher 2002; Cystic Fibrosis Canada 2011). The molecular defect associated with ΔF508 mutation is a failure to traffic to the plasma membrane due to misfolding of CFTR in the endoplasmic reticulum preventing proper processing and maturation. The vast majority of ΔF508-CFTR is retained in the endoplasmic reticulum and degraded by proteosomes however a small amount of ΔF508-CFTR does mature to the plasma membrane (Riordan 1999; Belcher and Vij 2010). When ΔF508-CFTR is present at the plasma membrane it has a reduced conductance and reduced open probability compared to WT-CFTR. The membrane stability of ΔF508-CFTR has been shown to be significantly less with a half life of 4 hours compared to 48 hours for WT-CFTR (Heda et al. 2001). Taken together the molecular processes affected in ΔF508-CFTR contribute to decreased protein lifespan and decreased chloride efflux which facilitate the complications observed in the organs affected by CF.

1.4 Vasoactive Intestinal Peptide

Vasoactive intestinal peptide (VIP) is a neuropeptide 28 amino acids in length after post translational modifications by enzymatic cleavages. VIP is conserved across many species being identical in humans, rats, goats, dogs and pigs; amino acid substitutions in VIP within other species are also conserved and do not cause changes in bioactivity (Dockray 1994). VIP shares similarities in sequence with other peptides including pituitary adenyl cyclase activating polypeptide (PACAP), secretin, calcitonin, parathyroid hormone and glucagon all belonging to the secretin family of peptides (Sherwood et al. 2000; Chapter et al. 2010). VIP was discovered in 1970 by Said and Mutt who had previously attempted to isolate an agent responsible for vasodilatation from injurious lung; however the isolation of the agent proved difficult. During embryonic formation the lung and duodenum originate from the same embryonic bud thus focus turned to the duodenum where the vasodilation agent was isolated and named VIP (Said and Mutt 1970). Shortly after VIP was isolated from the duodenum it was additionally characterized as a smooth muscle relaxant and stimulator of electrolyte secretion in the gut (Barbezat and Grossman 1971)

Since the discovery of VIP in the duodenum it has been found to have widespread distribution all throughout the body. VIP has been found in the central nervous system (CNS) and peripheral nervous system (PNS) as well as peripheral tissues. In the brain VIP distribution is found in the cerebral cortex, hippocampus, suprachiasmatic nucleus, amygdala and hypothalamus (Said 2000; Fahrenkrug and Hannibal 2004). In the peripheral tissues VIP distribution is found in lung, intestine, genitor-urinary tracts and in exocrine epithelia (Dickson and Finlayson 2009). VIP in peripheral tissues is delivered

from neurons of the PNS; the VIP neurons have direct innervations to smooth muscle, endothelial and epithelial tissues in gastrointestinal, respiratory, and genital tracts (Power et al. 1988).

1.4.1 Physiological Functions of VIP

VIP not only has widespread distribution throughout the body but also engages in an array of different functions depending on tissue type. Early studies showed effects of VIP on the respiratory, cardiovascular, circulatory and metabolic systems (Dickson and Finlayson 2009). The effects on the cardiovascular system include increased heart rate, increased coronary arterial blood flow, vascular tone regulation, increased ventricular contractility and reduced mean arterial pressure (Smitherman et al. 1989). In the circulatory system VIP acts as a major vasodilatation agent, 50-100 times more potent than acetylcholine (Fahrenkrug 1989). In the respiratory system VIP was found to be the most potent endogenous bronchodilator of the airways in addition to its role in airway mucus secretion. VIP's involvement in airway mucus secretion has been studied extensively due to dense VIP innervations found around the submucosal glands (Dey et al. 1981; Wu et al. 2011). VIP is the primary stimulus for CFTR mediated secretions in exocrine epithelium in organs such as the lungs, pancreas and intestine (Chastre et al. 1989; Said 1991). Metabolically, VIP can influence blood glucose levels by stimulating insulin secretion from the pancreas and causes prolactin release from the pituitary gland as well as release of catecholamines from the adrenal glands (Kato et al. 1994; Chapter et al. 2010). A major system influenced by VIP is the immune system; VIP directly inhibits pro-inflammatory cytokine production and increases production of interleukin 10 (IL-10)

an anti-inflammatory molecule. VIP also inhibits T-cell differentiation into Th_1 cells involved in mediation of an immune response while preserving Th_2 cells which further produce IL-10 and IL-13 which can limit inflammation (Delgado et al. 2004).

VIP has been found to have neuroprotective effects, it counters pathways leading to cell apoptosis and can reduce oxidative stress damages in the lungs (Said and Dickman 2000; Delgado and Ganea 2003). VIP is also important to stimulate electrolyte secretions through membrane channels from the epithelium; VIP function in epithelial tissue is important as VIP is the main physiological stimulus for CFTR mediated secretions which allows pancreatic enzyme secretions, digestion in the duodenum and maintenance of ASL volume in the airways (Chappe et al. 2008; Dickson and Finlayson 2009).

1.4.2 VIP Receptors and Signalling

The receptors that facilitate the VIP response are members of the G protein coupled receptor (GPCR) family. GPCRs are an enormous family of proteins and are frequently the targets of new and emerging pharmacologies. GPCR's are subdivided into classes labelled A-F based on the homology of the primary sequence, however only A-C are found in mammalian systems (Kolakowski 1994). The family of receptors for VIP binding belong to family B, commonly known as the secretin-like receptor family. There are 3 primary receptors that VIP binds to; $VPAC_1$, $VPAC_2$ and PAC_1 which among other places are distributed on the basolateral membrane of polarized epithelial cells (Laburthe et al. 2002; Derand et al. 2004). All 3 receptors are capable of binding both VIP and PACAP. However the affinities measured for VIP varies with an EC_{50} for $VPAC_1$ is 0.01-0.1 nM, 2 nM for $VPAC_2$ and 40 nM for PAC_1. PACAP binds to PAC_1 with an EC_{50} of

0.2 nM, a much higher affinity compared to VIP binding (Buscail et al. 1990; Dickson and Finlayson 2009).

When VIP binds to one of its receptors a signalling cascade follows, however there are multiple pathways that can be activated (Dickson and Finlayson 2009). When the VIP receptor couples to the Gαs subunit of the G-protein complex it initiates activation of the adenylyl cyclase (AC) enzyme which increases intracellular levels of cAMP through conversion of ATP (Fig. 1.1)(Laburthe et al. 2002). Increased intracellular cAMP causes the regulatory subunits of PKA to release their inhibition, allowing the catalytic domain to phosphorylate targets in the cell. VIP receptors also stimulate other cellular signalling cascades that involve increases in calcium signalling, phospholipase C and PKC activation (Dickson and Finlayson 2009; Rafferty et al. 2009). Phospholipase D is also indirectly activated through the VIP receptors but only when mediated through Adenosine-diphosphate ribosylation factor (ARF) or PKC dependant pathways (McCulloch et al. 2001).

1.4.3 Regulation of VIP Receptors

The presence of VIP receptors at the basolateral membrane of epithelial cells is common, although the receptors are constantly undergoing internalization and redistribution at the membrane (Shetzline et al. 2002). Upon VIP activation of the receptor, a rapid response occurs to phosphorylate the receptor through two different mechanisms causing internalization to a submembrane pool of recycling endosomes (Shetzline et al. 2002). The first method is through G-protein coupled receptor kinases

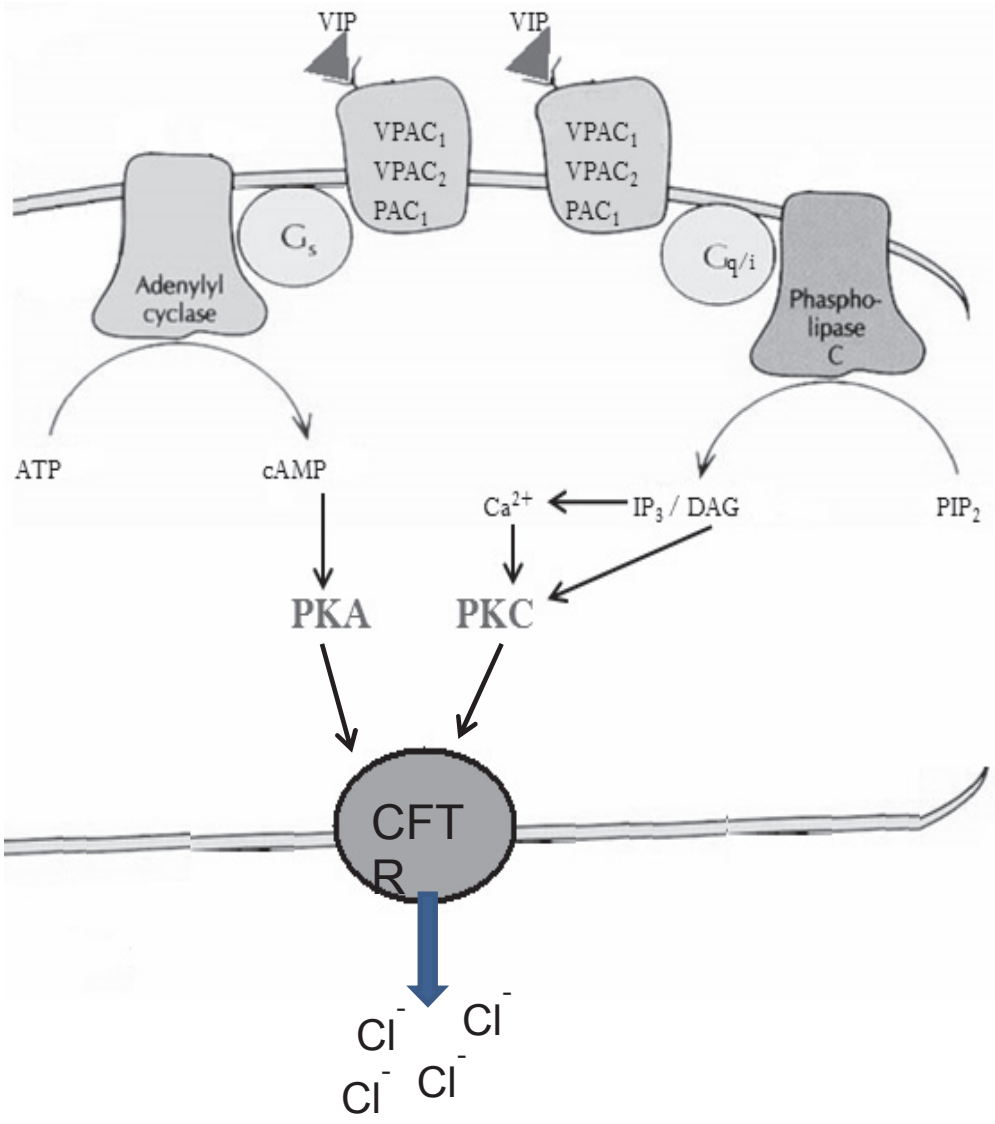

Figure 1.1 Vasoactive intestinal peptide signalling pathways through the G_s and $G_{q/I}$ proteins causes increases in cAMP and DAG/Ca^{2+} resulting in activation of PKA and PKC. Both PKA and PKC then phosphorylate CFTR causing channel activation and increased membrane stability.

(GRK) and the second method of receptor phosphorylation is mediated through second messenger activated kinases. Once the receptor is phosphorylated, binding of β-arrestin can occur initiating the process of receptor internalization via clatherin coated pits (McDonalad et al. 1998).

VIP desensitization and internalization of the $VPAC_1$ receptor was observed in human HT-29 colonic carcinoma cells and was found to occur within 10 minutes of VIP binding (Boissard et al. 1986). It was determined that $VPAC_1$ was internalized into an endosomal pool below the plasma membrane. When VIP was cleared from the media, a redistribution of the $VPAC_1$ receptors occurred within 60 minutes returning them to the membrane able to respond to further VIP activation (Boissard et al. 1986). The $VPAC_1$ receptor phosphorylation and internalization was also studied in human colonic carcinoma cells and GRK 5 / GRK 6 were identified as the kinases involved in internalization (Shetzline et al 2002). The regulation of $VPAC_2$ was also examined in cell lines that were transfected with $VPAC_2$. After VIP binding $VPAC_2$ desensitization was determined to be mediated through a cAMP dependant kinase however the role of GRK phosphorylation which regulates $VPAC_1$ was not examined for $VPAC_2$ regulation and may also be important for desensitization and internalization (McDonald et al. 1998; Shetzline et al 2002).

Regulation of VIP receptor expression has been previously examined *in vivo* in a study of smokers with chronic bronchitis, where an increase of VIP nerve fibres and hyper secretion were reported (Miotto et al. 2004). Bronchial epithelium was found to have significantly increased levels of $VPAC_1$ but not $VPAC_2$ receptor expression. The

submuscosal layer revealed that both receptors had elevated expression in patients with chronic bronchitis (Miotto et al. 2004).

1.4.4 Distribution of VIP Receptors

The VIP receptors are expressed throughout the brain, respiratory, digestive, immune and reproductive systems. In the brain VIP receptor expression is present throughout with $VPAC_1$ localized to the cerebral cortex and hippocampus (Vertongenet et al. 1997). $VPAC_2$ is found in thalamus, hippocampus, suprachiasmatic nucleus and dorsal root ganglia (Vertongenet et al. 1997) and PAC_1 in olfactory bulb, thalamus, hippocampus and cerebellum (Hashimoto et al. 1996).

The expression of VIP receptors in the immune system has been examined previously to understand VIPs effects on cytokine formation and immune cell differentiation. Rodent peritoneal macrophages were shown to express $VPAC_1$ and PAC_1 receptors which inhibited the adverse effects of TNF-α (Delgado et al. 1999). In the differentiation of CD4+ and CD8+ T-lymphocytes the action of VIP was found to be mediated through expression of both $VPAC_1$ and $VPAC_2$ (Delgado et al. 2004).

In C57Bl/6 mouse airways $VPAC_1$ was found to be localized to the tracheal and bronchial epithelium where as $VPAC_2$ was found to be largely expressed in the alveoli and smooth muscle tissue (Harmar et al. 2004). In the C57Bl/6 mice $VPAC_2$ expression was also found throughout the vasculature, skeletal and smooth muscle tissues in the periphery while $VPAC_1$ expression was predominantly expressed in epithelium throughout the periphery (Harmar et al. 2004). PAC_1 is also expressed in the lung

however localization within the lung tissue has not been previously examined (Kastin 2006).

The VIP receptors are also expressed throughout the small intestine of C57Bl/6 mice. In the duodenum, jejunum and ileum $VPAC_1$ is expressed in the mucosa while $VPAC_2$ expression is located primarily in the smooth muscle layer (Harmar et al. 2004). PAC_1 expression has been detected in the myenteric plexus of the duodenum however expression has not been extensively studied in the regions of the small intestine (Kirchgessner and Liu 2001).

1.4.5 VIP in Cystic Fibrosis and CFTR Regulation

The potential for use of VIP in the airways for treatment of diseases such as asthma, chronic obstructive pulmonary disease (COPD) and pulmonary hypertension has been studied previously (Ollerenshaw et al. 1989; Petkov et al 2003; Miotto et al. 2004). VIP has also been shown *in vitro* and *in vivo* to inhibit proliferation of small cell lung cancer without exposing the body to the levels of toxicity that are associated with current anti-cancer treatments (Maruno et al. 1998). The potential use of VIP in CF has also been studied over the past decade on the basis that VIP not only activates the CFTR channel but can also increase its stability at the membrane (Derand et al. 2004; Chappe et al. 2008; Rafferty et al. 2009; Alcolado et al. 2011). The connection between VIP and CF was first examined in the 1980's when CF patients were found to have decreased VIP innervation to sweat glands, nasal epithelium and intestinal mucosa (Heinz-Erian et al. 1985; Wattchow et al. 1988). Furthermore the Said group also found that circulating VIP levels were elevated in CF patients along with VIP binding antibodies, suggesting

abnormalities in VIP regulation in CF patients (Heinz-Erian and Said 1988). With the discovery of the CFTR gene in 1989 many studies followed to understand the function and regulation of CFTR, it was found CFTR requires ATP, PKC and cAMP elevations for PKA activation for optimal activation and function (Fig 1.1) (Riordan et al. 1989; Hwang et al. 1989; Cheng et al. 1991). VIP was already known to be a stimulator of electrolyte secretion in epithelium and was quickly found to stimulate chloride efflux through the CFTR channel upon its discovery (Sinaasappel et al. 1990).

The effect that VIP exerts on CFTR has since been found to extend beyond channel activation. In excised shark rectal glands VIP stimulation increased not only channel activity but maturation of CFTR to the membrane (Lehrich et al. 1998). In rat duodenal epithelial cells, VIP was found to cause an increase in plasma membrane insertion and reduced internalization of mature CFTR at the membrane (Ameen at al. 1999). The mechanism by which VIP stabilizes CFTR at the membrane is attributed to PKC phosphorylation (Bajnath et al. 1993; Chappe et al 2008). In the human bronchial epithelial cell line Calu-3, CFTR membrane stability was found to increase due to phosphorylation by PKC not PKA (Chappe et al. 2008). The mechanism was found to be a reduction in endocytosis of CFTR; the same mechanism was reported for ΔF508-CFTR in the human nasal epithelial cell line JME/CF15 (Rafferty et al 2009). VIP was also found to promote maturation of ΔF508-CFTR in a PKA dependant manner in the JME/CF15 cell line (Rafferty et al. 2009).

1.4.6 VIPKO Mice

A knockout mouse was developed to study the physiological role of VIP, the mice were developed through backcrossing with the C57BL/6 mice. The VIP knockout (VIPKO) mice have the gene responsible for VIP production deleted from their genome resulting in loss of VIP production. The phenotype knockout mice experienced from the loss of VIP included altered circadian rhythms, pulmonary hypertension, airway and intestinal inflammation and hyperresponsiveness (Aton et al. 2005; Szema et al. 2006).

Previous work in the Chappe laboratory (Nicole Alcolado, Masters Thesis, Dalhousie University) with adult VIPKO mice determined, using pathological assessments, the level of goblet cell formation and inflammatory cell abundance in lung and duodenum tissues. In lung and duodenum tissues of WT C57BL/6 mice, goblet cell formation was minimal and there was little evidence of inflammatory cell infiltration. In VIPKO mice an increase in both goblet and inflammatory cell presence was detected. VIPKO mice that received intraperitoneal injections of 500 mg/kg VIP every other day for 3 weeks showed a reduction in both lung and duodenum tissues of goblet and inflammatory cells. CFTR membrane localization was also examined in these tissues using immunoflurescence labelling and confocal microscopy for WT, VIPKO and VIPKO treated mice. In WT mice tissues, localization of CFTR at the apical membrane of epithelial cells was observed, while in VIPKO mice tissues, reduced apical membrane localization was found as CFTR was distributed uniformly throughout the epithelial cells. After treatment of VIPKO mice with VIP, the apical membrane localization of CFTR was restored. This provided the first evidence that VIP plays a physiological role in

maintaining CFTR localized to the membrane in epithelial cells and helps to control inflammation in the lung and duodenum.

1.5 Study Objectives

VIP is the primary stimulus *in vivo* of CFTR mediated chloride secretions. The effect of VIP on CFTR acts not only to activate the channel by phosphorylation but also to improve its stability at the plasma membrane. In some cell lines VIP was also shown to promote trafficking of CFTR in a PKA-dependant manner. VIPKO mice experience lung and duodenum tissue inflammation and reduced CFTR apical membrane localization which can be reversed with VIP treatment. The expression of the VIP receptors in these tissues has not been studied and it is unclear how receptor expression may play a role for increased CFTR membrane localization in response to VIP stimulation.

The first objective of the current study was to examine the changes in the expression of $VPAC_1$, $VPAC_2$ and PAC_1 receptors in lung and duodenum of WT, VIPKO and VIPKO treated mice. When VIP binds to its receptor it produces second messengers in the cell, these second messengers play a role in negative feedback through phosphorylation of the VIP receptor (Shetzline et al 2002). Phosphorylation of the receptor causes desensitization and internalization before its degradation (Ferguson et al 1998; Shetzline et al 2002). It was hypothesised that receptor expression would increase in VIPKO tissues due to loss of VIP signalling and negative feedback of receptor expression. The second objective of the study was to examine CFTR expression and maturation between the groups. It was hypothesised that CFTR expression would remain constant as would maturation of CFTR.

CHAPTER 2: MATERIALS AND METHODS

2.1 Materials

2.1.1 Chemicals

Antibodies: Monoclonal anti-$VPAC_1$ (AS59), monoclonal anti-$VPAC_2$ (AS69), monoclonal anti-PAC_1 (1B5) and Actin-horse radish peroxidase (C2) were from Santa Cruz Biotechnology Inc. (Santa Cruz, CA, USA). The monoclonal anti-CFTR antibody MM13-4 was from Upstate (Charlottesville, VA, USA).

Mouse Dissection Buffer: Phosphate buffered saline (PBS) was prepared with 137 mM NaCl, 10 mM Na_2, 2.7 mM KCl, 1.7 mM KH_2PO_4, I*soflurothane and heparin were from* Sigma (Sigma, St. Louis, MO,USA).

Reverse Transcriptase PCR : The iTaq™ DNA Polymerase kit (Bio-Rad, Mississauga, ON, Canada) provided the 10x iTaq buffer, 50 mM $MgCl_2$ and iTaq DNA Polymerase. The 10 mM dNTP mix was also purchased from Bio-Rad. Primers were designed spanning exon-exon junctions of the mRNA using Primer-BLAST (http://www.ncbi.nlm.nih.gov/tools/primer-blast/). All sequences had 100% homology with *Mus musculus* sequence for the VIP receptors.

Agarose Gel Electorphoresis: The agarose was UltraPure™ Agarose (Invitrogen™, Carlsbad, CA, USA) and 10x Tris-Borate-EDTA (TBE) buffer from Sigma (St. Louis, MO,USA). The Ethidum Bromide Solution (10 mg/ml) came from

Invitrogen™(Carlsbad, CA, USA) and 6x Loading dye was purchased from Thermo Fisher Scientific (Burlington, ON, Canada).

Radioimmunopercipitation Assay Buffer (RIPA): RIPA buffer for mouse tissue homogenization and protein extraction was made with 0.15 M NaCl, 10 mM Tris, 1 mM EDTA, 1% TritonX-100, 0.08% Deoxycholic Acid, 0.01% SDS, pH 7.5 and a Protease Inhibitor Cocktail (Roche, Laval, QC, Canada)was added to prevent protein degradation.

Buffers for Western Blotting: The following chemicals were from Bio-Rad (Mississauga, ON, Canada): 30% acrylamide/Bis solution, 29:1 (3.3% C), 1x running buffer (192 mM Glycine, 25 mM Tris, 0.1% SDS, pH 8.3), 10x transfer buffer (Tris Glycine Buffer (192 mM Glycine, 25 mM Tris, pH 8.3), 1x TBS (500 mM NaCl, 20 mM Tris, pH 7.5) and 1x TTBS (500 mM NaCl, 20 mM Tris, 1% Tween-20, pH 7.5). To make 1x transfer buffer (100 ml 10x transfer buffer, 200 ml methanol and 700 ml ddH20). Purchased from Sigma (St. Louis, MO,USA) was the methanol, ammonium persulfate (APS), 10% sodium dodecyl sulphate solution (SDS) and tetramethylethylene-diamine (TEMED). The 5x sample buffer for sample preparation and Restore™ PLUS Western Blot Stripping buffer was from Thermo Fisher Scientific (Burlington, ON, Canada). The chemiluminescence kit used was ECL Plus Western Blotting Detection System from GE Health Care Life Sciences (Piscataway, NJ, USA).

2.2 Methods

2.2.1 Mice Tissues

Wild type C57BL/6 mouse tissues were obtained from Dr. Robert Rose (Dalhousie University, Halifax, NS, Canada). All mice were fully mature male mice aged 14-20 weeks and kept in Dalhousie animal care facility at Sir Charles Tupper Medical Building. VIP knockout (VIPKO) mice were fully mature aged 16-20 weeks, littermates and all male. The VIPKO mice had the VIP gene deleted from their genome resulting in the absence of VIP production. The VIP knockout treated (VIPKOT) mice received treatments of intraperinatal injections of 500 mg/kg VIP every other day for a period of 3 weeks. VIPKO and VIPKOT mice were raised and had lung and duodenum tissue harvested by the Dr. Sami Said laboratory at State University New York (SUNY), Stone Brook, NY, USA. The upper lobe of the right lung was collected and the proximal 1 cm of the small intestine was collected for duodenum samples; tissues were immediately flash frozen with liquid nitrogen and stored at -80°C.

2.2.2 Mouse Tissue Dissection

All experimental procedures performed in the current study were in accordance with The Canadian Council on Animal Care and were approved by the University Committee on Laboratory Animals at Dalhousie University. Mice were injected with 0.2 ml heparin (1000 U/ml) and moved into a small plastic box before application of anaesthesia. Briefly a Q-tip was saturated in isoflurothane and placed inside the enclosed

container until the mouse lost consciousness. To ensure loss of sensation mechanical cervical dislocation was employed using forceps. An incision was made extending from the upper chest to the lower pelvis followed by removal of the ribcage. The lungs were immediately extracted and rinsed in ice cold phosphate buffered saline (PBS) to remove excess blood before being placed in a cryo tube and flash frozen in liquid nitrogen. The small intestine was excised and washed in ice cold PBS, the lumen of the small intestine was rinsed with ice cold PBS using a P200 pipette with a long reach tip. The pipet tip was inserted into the proximal opening of the small intestine and the PBS was gently dispensed to push out debris, this process was repeated two more times. The proximal 1 cm of the duodenum was excised from the small intestine and was placed into a cryo tube and flash frozen in liquid nitrogen, both lung and small intestine samples were stored at -80°C until homogenization.

2.2.3 RNA Extraction From Mouse Tissue

RNA extraction was performed following the manufacturer's instructions for RNeasy mini kit (Qiagen, Mississauga, ON, Canada) according to the protocol: *Purification of Total RNA from Animal Tissues*. All experiments were performed using RNAse free tips, RNAse free water and in the vicinity of an open flame to prevent any contamination, all buffers were supplied with RNeasy mini kit.

WT, VIPKO or VIPKOT tissue was removed from the -80°C freezer and placed in liquid nitrogen to keep frozen until ready for processing. A small portion of tissue weighing between 20 – 30 mg was immediately placed into 600 µl of RTL buffer (1 M Dithiothreitol was added to the RTL buffer in a 1:30 dilution). Tissue was homogenized

using rotor –stator homogenizer (PRO scientific Inc., model AHS 200, Oxford, CT, USA) on high for 30 seconds. Tissue lysate was then centrifuged for 3 minutes with 13,000 rpm at 4°C and the supernatant was carefully removed by pipetting as to not disturb the pellet. The supernatant was added to an equal volume of 70% ethanol and thoroughly mixed by repeated pipetting. 700 µl of the mixed sample was transferred to an RNeasy spin column placed inside a 2 ml collection tube and centrifuged for 15 seconds at 10,000 rpm. The flow through was discarded and 700 µl of RW1 buffer was added to the spin column and centrifuged for 15 seconds at 10,000 rpm and flow through discarded . 500 µl of RPE buffer was added to the spin column and centrifuged 15 seconds at 10,000 rpm and flow through discarded. An additional 500 µl of RPE buffer was added to the spin column and centrifuged for 2 minutes at 10,000 rpm to ensure ethanol was washed away and not carried over to RNA elution. The spin column was placed in a new 1.5 ml tube and 34 µl of RNase-free water was added to the spin column and spun for 1 minute at 10,000 rpm to recover the RNA. Recovered RNA concentration was determined using UV spectrometry (Unico, Dayton, NJ, USA) by measuring optical density (OD) at 260 nm and 280 nm, the ratio of 260/280 was required to be above 1.8 for RNA purity. RNA was then stored at -20°C until use.

2.2.4 Conversion of RNA to cDNA

To convert recovered RNA to cDNA the iScript^{TM} cDNA Synthesis Kit (Bio-Rad, Mississauga, ON, Canada) was used and protocol was followed according to manufacturer directions, all buffers and reagents were supplied with the kit. A PCR reaction tube was prepared containing 4 µl of 5x iScript reaction mix, 1 µl of iScript

reverse transcriptase, 1 µg of RNA and addition of Nuclease-free water to bring the total volume of the mixture to 20 µl. The reaction tube was then place in a thermocycler (MyCycler™, Bio-Rad) and underwent 1 cycle of the following program: 5 minutes at 25°C, 30 minutes at 42°C and 5 minutes at 85°C. The reaction tube containing the newly synthesised RNA was removed from the thermocycler and stored at -20°C until use.

2.2.5 Reverse Transcriptase Polymerase Chain Reaction (RT-PCR)

Reactions were prepared in PCR tubes using the iTaq™ DNA Polymerase kit (Bio-Rad). On ice the following was added to a PCR tube: 5 µl of 10x iTaq buffer, 1.5 µl $MgCl_2$ (50 mM), 1 µl of forward primer (50 mM), 1 µl of reverse primer (50 mM), 1 µg cDNA template, 1 µl dNTP mix (10 mM), 0.25 µl iTaq DNA Polymerase and sterile ddH20 to complete total reaction volume to 50 µl. Reaction tubes were briefly spun down with a micro centrifuge to ensure the total 50 µl volume was at base of the PCR tube. Reaction tubes were placed into a thermo cycler (MyCycler™, Bio-Rad) and underwent the following heat cycle program for DNA amplification: 95°C for 3 minutes once for polymerase activation, 40 cycles of 95°C for 30 seconds to denature DNA, 55-60°C for 30 seconds to allow primer annealing and 72°C for 50 seconds to allow for product elongation. Following the completion of the 40 cycles an additional step of 72°C for 4 minutes was applied to allow elongation of any incomplete products before the temperature was decrease to 4°C indefinitely to stabilize DNA until it can be frozen and stored at -20°C.

2.2.6 Agarose Gel Electrophoresis

Agarose gel electrophoresis was used to image the products produced from RT-PCR experiments. 0.8% agarose gels were prepared using 0.24 g agarose and 30 ml of 1x Tris-Borate-EDTA (TBE) buffer placed in a 200 ml glass bottle. The mixture was microwaved on high for 1 minute with intermissions every 15 seconds for swirling. The agarose mixture was allowed to cool down to a luke warm temperature before the addition of 1.3 µl of Ethidum Bromide Solution (10 mg/ml) and thorough mixing. The agarose mixture was poured into a horizontal casting system followed by the insertion of a well comb and allowed to sit at room temperature for approximately 30 minutes to solidify. The PCR samples were prepared in separate tubes using 2µl of 6x loading dye and 10 µl of PCR product before receiving a brief vortex and micro centrifuge to collect the total volume at the bottom of tube. The Φx marker was prepared using 2 µl of stock Φx molecular weight marker, 2 µl of 6x loading dye and 3 µl ddH20. Marker and samples were loaded into the lanes of the solidified agarose gel which was submerged in TBE buffer in an electrophoresis cell (Mini-Sub Cell GT Cell, Bio-Rad). The gel was run at 89 V for approximately 1.5 hours or until samples had migrated a sufficient distance to allow imaging. Gels were imaged using an ultraviolet imaging box and digital camera in combination with the AlphaDigiDoc® (Cell Biosciences, Toronto, ON, Canada) software-imaging program.

Table 2.1 – Forward and reverse primers designed for detection of VIP receptors by RT-PCR. PKC α was used as a positive control for the PCR reaction.. The expected product size is shown in base pairs (bp) and annealing temperature (Tm) is indicated.

VIP Receptor	Primer Sequence (5'-> 3')	Product Size (bp)	Tm (°C)	Locus (NCBI)
$VPAC_1$	Forward Primer: ATTTCGGGTGCTGGGACACCAT Reverse Primer: TTTGAGGGCAGGCGGTTTGCTT	804	61.3	NM_011702
$VPAC_2$	Forward Primer: ACCTTCTGATCGGATGGGGCAT Reverse Primer: TCCATAGGCATGCGTTGGGTGT	969	60.7	NM_009511
PAC_1	Forward Primer: AGCATCTACTTCAGCTGCGTGC Reverse Primer: AGTACAGCCACCACAAAGCCCT	245	60.9	NM_007407
PKC Aplha (+ Control)	Forward Primer: TGCCGGCCAGTGGATGGTAT Reverse Primer: TGCACATCCCAAAGTCGGCG	651	57.9	NM_011101

2.2.7 Mouse Tissue Homogenization

Tissue was removed from -80°C freezer and placed in liquid nitrogen to keep frozen and prevent protein degradation. The upper lobe of lung tissue and proximal 1 cm for duodenal tissue was immediately weighed and immersed in RIPA buffer, 100 µl for every 10 mg of tissue. The tissue was homogenized with rotor –stator homogenizer (PRO scientific Inc., model AHS 200, Oxford, CT, USA) for 45-60 seconds, followed by 15 minutes of gentle shaking, 30 seconds of vortexing and 15 additional minutes of gentle shaking all at 4°C. The tissue lysate was vortexed for 30 seconds and underwent sonication (Ultrasonic Homogenizer 4710 series, Model ASI probe, Cole-Parmer Instrument Co, Chicago, IL, USA) at 30% power output on ice for 3 cycles of 20 seconds. Tissue lysate was centrifuged at 8,000 rpm for 10 minutes at 4°C to removed large debris, the supernatant was recovered with gentle pipetting without disturbing pellet. To improve membrane protein recovery the samples underwent gentle shaking for an additional 30 minutes at 4°C with vortexing at 15 minutes. Finally samples were centrifuged at 13,000 rpm for 20 minutes at 4°C to remove any remaining debris before supernatant was recovered and stored at -20°C.

2.2.8 Protein Assay

The protein concentration of the homogenized tissue lysate was determined using the Bradford protein assay technique. A standard curve was constructed using bovine serum albumin (BSA) standards with increasing protein concentrations of 0, 2, 5, 10, 15 µg. Standards were mixed in 1.5 ml eppendorph tubes containing 480 µl of ddH20, 10 µl

of RIPA (diluted to 1:4 in ddH20), stock BSA (2 µg/µl) was diluted in ddH20 to make 10 µl aliquots for each protein standard concentration and added to the mixture. Finally 500 µl of Quick Start™ Bradford 1x dye reagent (Bio-Rad, Mississauga, ON, Canada) was added to mixture to produce protein dependant colour change. Tissue samples were prepared with 490 µl ddH20, 10 µl of tissue sample (diluted 1:4 in ddH20) and 500 µl Bradford 1x dye. Standard and sample tubes were quickly vortexed and incubated at room temperature for 30 minutes before the optical densities were measured. A spectrophotometer (2802 UV/VIS Spectrophotometer, Unico®) with wavelength set to 595 nm was used to determine the optical density of each standard and sample in duplicate. The optical densities for the standards of known concentration were entered into a software program (Protein & DNA Assays by Spectrophotometry Software, copyrights: Frederic & Valerie Chappe) using linear regression a standard curve was constructed. The results for the tissue lysate samples were plotted against the standard curve to give the total protein concentration of each tissue lysate sample.

2.2.9 Western Blotting

All polyacrylamide gels used for western blots contained a 5% stacking gel with 10 wells. The resolving gels used for detection of VIP receptors were made with 7.5% acrylamide and for CFTR detection, gradient gels consisting of 6%,12% and 14% acrylamide layers were used (see table 2.2 for gel composition). Tissue protein samples were prepared by adding 50 µg of lysate mixed with an equal volume of ddH20 and 5x sample buffer to reduce the proteins. Samples probed for VIP receptors underwent heating at 90°C for 10 minutes to further denature the proteins before loading into the

gel; samples probed for CFTR were not heated due to denaturation of the CFTR protein under high temperatures. Samples were loaded next to Benchmark™ Prestained Protein Standard (Invitrogen, Burlington, ON, Canada) and underwent sodium dodecyl sulfate polyacrylamide gel electrophoresis (SDS-PAGE). The gels were exposed to 90 V submerged in 1x running buffer until samples had migrated into resolving gel, the voltage was increased to 120 V for the remaining part of migration. Proteins were transferred from the polyacrylamide gels onto nitrocellulose membranes using a blotting chamber (Thermo Scientific OWL, Rochester, NY, USA) at 45 V for 2 hours in 1x transfer buffer. Membranes were blocked by saturation with 5% milk in 1x TTBS with gentle shaking for 1 hour at room temperature. Membranes were then rinsed off with 1x TBS before addition of the primary antibody for respective protein of interest; $VPAC_1$ 1/200, $VPAC_2$ 1/200, PAC_1 1/1000 or CFTR 1/1000. Membranes were incubated with primary antibody overnight at 4°C with gentle shaking. Upon removal of primary antibody membrane were washed 3 times with 1x TTBS for 15 minutes each 1 more wash with 1x TBS for 15 minutes, all at room temperature with moderate shaking. The secondary antibody used was peroxidase-conjugated, goat anti-mouse light chain specific IgG (1/5,000 in TBS, 0.5% milk) added to membranes for 2 hours with gentle shaking at room temperature. Secondary antibody was removed and membrane washed 3x with TTBS and once with TBS for 15 minutes each at room temperature and moderate shaking. Proteins were revealed using chemiluminescence, 1.5 ml Reagent A (ECL^+ substrate) and 40 µl of Reagent B (Acridan in Dioxane and Ethanol) mixed in a light protected tube. The mixture was distributed evenly over the membrane for 2 minutes to allow enzyme activation before exposure using Kodak X-Ray films and development using X-Ray

processor. X-Ray films were scanned and protein band density was measured with *ImageJ* software program (National Institute of Health, http://rsbweb.nih.gov/ij/). After completion of lung tissue western blots the membrane was stripped of antibodies, using 10 ml of western blot stripping buffer under gentle shaking for 30 minutes at room temperature. Membranes were then washed three times with 1x TTBS for 15 minutes and moderate shaking. Membranes were then blocked with 5% milk in 1x TTBS for 1 hour with gentle shaking before a rapid wash with 1x TBS and application of 1/200 actin antibody conjugated to horseradish peroxidise to probe for actin as an internal control of total protein loading. Membranes were then imaged and scanned as described above.

2.3 Statistics

The values reported are means ± SEM, n = number of independent experiments where the WT group had 8 mice tested and VIPKO and VIPKOT had 5 mice tested. For each mouse tissues extracted were tested a minimum of 3 times and values obtained were averaged for statistical analysis. Statistical differences between groups were assessed using 1 way ANOVA analysis and the post hoc Tukey multiple comparison tests with $p < 0.05$ considered significant(*).

Table 2.2 – Composition of acrylamide resolving gels used for western blotting.

	5% Gel (6 ml)	6% Gel (3.5 ml)	7.5% Gel (7.5 ml)	14% Gel (2ml)	12% Gel (2 ml)
DDH20	3.35	1.842	3.575	0.518	0.653
30% Acrylamide	1	0.7	1.875	0.935	0.8
1.5 M Tris	1.5 (0.5M Tris)	0.885	1.9	0.505	0.505
10% SDS	0.06	0.035	0.075	0.02	0.02
10% APS	0.06	0.035	0.075	0.02	0.02
TEMED	0.006	0.03	0.006	0.002	0.002

CHAPTER 3: RESULTS

3.1 Detection of VIP receptor mRNA in WT, VIPKO and VIPKOT mouse lung

Previous work in human airway epithelial cell lines identified that the $VPAC_1$ was the receptor bound by VIP to activate CFTR and improve membrane stability, however in mouse lung tissue VIP receptor expression is unknown (Derand et al. 2004; Rafferty et al. 2009).

To identify which VIP receptors might be expressed in WT, VIPKO and VIPKOT mouse lung, mRNA was extracted from each tissue and converted to cDNA (see *Materials and Methods*). Specific primers designed to identify sequences of mouse $VPAC_1$, $VPAC_2$ and PAC_1 were used in RT-PCR (see *Materials and Methods*). Controls were performed to ensure that cDNA conversion for each group had worked and products were amplified in the reaction. The positive control used PKCα which is known to have mRNA expression in the lung and duodenum tissues. The negative controls had the primers omitted to eliminate the possibility of non-specific product amplification from the tissue mRNA (Fig. 3.1). Detection of $VPAC_1$ product at 804 bp was found in all 3 mouse groups (Fig. 3.2A), as was the 969 bp product of $VPAC_2$ (Fig. 3.2B) and the 245 bp product of PAC_1 (Fig. 3.2C). Therefore WT, VIPKO and VIPKOT mouse lungs all express the mRNA for production of the 3 VIP receptors.

3.2 $VPAC_1$, $VPAC_2$ and PAC_1 protein expression in WT, VIPKO and VIPKOT mouse lung

3.2.1 $VPAC_1$

$VPAC_1$ receptor expression has been studied using western blotting in human epithelium, rat brain tissue and mice lungs, there is a range of reported sizes for the $VPAC_1$ protein ranging from 49-80 kDa (Shetzline et al. 2002; El Karim et al. 2006; Hilaire et al. 2010). The mRNA of the $VPAC_1$ receptor was detected in the lung of all mice groups (Fig. 3.2A-C) however the presence of a proteins mRNA does not strongly correlate with the level of production of the protein. To assess the level of expression in the lungs of WT, VIPKO and VIPKOT mice, immunoblotting was used (see *Materials and Methods*).

The protein concentration for homogenized lung lysate was determined and 50 μg of total protein were loaded into each lane of a polyacrylamide electrophoresis gel. $VPAC_1$ was revealed with probing of monoclonal $VPAC_1$ antibody (AS58). To validate that the band detected was specific and not the result from background binding of the secondary antibody, negative controls were performed by omitting the primary antibody (Fig. 3.3). No background signal from the secondary antibody was detected in lung or duodenum tissue lysates from WT (lane 1-2), VIPKO (lane 3-4) and VIPKOT (lane 5-6) mice (Fig. 3.3).

In WT lung tissue $VPAC_1$ expression was measured in 8 different WT mice, the $VPAC_1$ band was faintly detected at ~72 kDa (Fig. 3.4A). Actin was reprobed in each sample to be used as an internal control for the amount of protein loaded. The $VPAC_1$

bands were measured using densitometry and turned into a percent of the actin band. Values for $VPAC_1$ as a percentage of actin ranged from 8.1% in WT mouse 1 to 36.8% in WT mouse 6 (Fig 3.4B).

Expression of $VPAC_1$ was examined by western blotting in the lung of 5 VIPKO mice and revealed a prominent band at ~72 kDa and a weaker band at ~47 kDa (Fig. 3.5A). The presence of 2 bands with different sizes has been reported previously and is attributed to differences in glycosylation with the 72 kDa band being the mature receptor found at the membrane which binds VIP (Bajo et al. 2000; Barberi et al. 2007). The 72 kDa was measured with densitometry and represented as a percentage of the actin internal control (Fig. 3.5B). The variability of $VPAC_1$ in VIPKO lung ranged from 25% in mouse 3 to 107.4% in mouse 2 demonstrating a wide range of expression of $VPAC_1$ in the lungs of VIPKO mice.

$VPAC_1$ receptor expression was also tested in VIPKOT mice which had received 500 mg/kg VIP every other day by intraperitoneal injections. Western blots showed similar bands for $VPAC_1$ in VIPKOT lungs as was observed in the VIPKO lungs (Fig. 3.6A). Mouse 4 showed the lowest percent of $VPAC_1$ to actin at 55.5% and the largest expression was found in mouse 1 at 112.5% again showing a wide range of $VPAC_1$ expression in the VIPKO mouse lung.

The $VPAC_1$ expression was averaged for each group and a total value was obtained from WT, VIPKO and VIPKOT lungs. The average WT $VPAC_1$ expression in the lung was found to be 23.6 ± 3.6 %, in VIPKO average expression was 75.2 ± 16.5% and in VIPKOT 81.6 ± 9.7% (Fig 3.7). Using one way ANOVA, the Tukey's multiple comparison test showed significant differences existed between WT vs. VIPKO groups

and WT vs. VIPKOT groups. The level of significance for WT vs. VIPKO was $p < 0.01$ and for WT vs. VIPKOT was $p < 0.001$. The results demonstrate that $VPAC_1$ expression is increased in VIPKO mice and remains significantly higher than WT even after treatment with VIP for 3 weeks as seen in the VIPKOT samples.

3.2.2 $VPAC_2$

Previously, $VPAC_2$ has been studied in human and rodent lung with a reported molecular weight between 43 - 80 kDa (Busto et al. 1999 ; Hilaire et al. 2010) .In the current study the $VPAC_2$ receptor expression was revealed with monoclonal $VPAC_2$ antibody (AS69) by western blotting.

The expression of $VPAC_2$ in WT lung tissue was found to be very weak (Fig 3.8A). In 8 WT mice examined, the highest expression was found in mouse 1 to be 11.3% percent of the actin band and the lowest expression was found in mouse 8 to be 5.2%.

In VIPKO mouse lung $VPAC_2$ expression was found to be increased compared to WT $VPAC_2$ expression. A distinct band was detected at ~70 kDa and a less dense band at ~47 kDa (Fig. 3.9A). The larger 70 kDa band was measured as it represents to mature receptor present at the plasma membrane in the same manner as the WT band and represented as a percent of actin. The means ranged from 29.6% in mouse 3 to 115.1% in mouse 2 (Fig. 3.9B) again demonstrating the variability of receptor expression in tissues without VIP.

The VIPKOT lung also revealed the bands observed in the VIPKO at ~47 and ~70 kDa but also showed a third band located at ~83 kDa (Fig. 3.10A). The ~47 and ~70 kDa bands are the result of differences in glycosylation of the $VPAC_2$ protein, the heavier ~70

kDa band indicates more glycosylation which is found in proteins at the membrane (Bajo et al. 2000). The addition of the 83 kDa band may be due to phosphorylation or ubiquitination of the $VPAC_2$ receptor at the membrane in preparation for degradation. The band located at ~70 kDa showed greatest density and was taken as the mature $VPAC_2$ and measured using densitometry. The means for $VPAC_2$ in the VIPKOT lung was at the lowest found in mouse 4 (71.2%) and the highest found in mouse 5 (115.7%) (Fig. 3.10B), showing a lower amount of variance than $VPAC_1$ expression in VIPKOT lung.

Comparing the averages from WT, VIPKO and VIPKOT groups as described for $VPAC_1$ it was determined that significant differences existed in $VPAC_2$ receptor expression (Fig. 3.11). The WT lung $VPAC_2$ expression average was 9.2 ± 1.7% and when compared to the average VIPKO lung expression 85.4 ± 15.1% a significance of $p < 0.0001$ was found. When the WT lung was compared to the average $VPAC_2$ expression in VIPKOT lung (81.6 ± 9.7) the significance level was found to be $p < 0.0001$. The results for expression of $VPAC_2$ in mouse lung indicates that under normal conditions $VPAC_2$ expression is maintain low, as was seen with $VPAC_1$. When the lung is challenged in an inflammatory state as seen in VIPKO lungs, the expression of $VPAC_2$ is increased and after treatment with VIP the elevated levels of $VPAC_2$ remain as demonstrated in the VIPKOT lung.

3.2.3 PAC_1

The expression of a third receptor for VIP, the PAC_1 receptor was also examined in the lung of WT, VIPKO and VIPKOT mice. Although more commonly associated

with its primary ligand PACAP, VIP binding can still signal through PAC_1 and therefore changes in expression may have effects on the physiological response by VIP. PAC_1 has been examined using western blotting before in rodents and was shown to produce bands between 55-75 kDa (Joo et al. 2004).

The expression of PAC_1 was found using the same immunoblotting technique as $VPAC_1$ and $VPAC_2$ receptors. PAC_1 was shown to produce a single robust band at ~70 kDa in all 8 WT mice samples examined (Fig 3.12A). Expression was again measured as a percent of the total actin band, Mouse 1 demonstrated the lowest expression (107.5%) and mouse 8 showed the largest expression (186.4%) (Fig. 3.12B). PAC_1 receptor expression in WT lung was easily detectable with western blotting unlike the $VPAC_1$ and $VPAC_2$ receptors.

Expression of PAC_1 was observed in VIPKO mouse lung to determine if the absence of VIP would influence PAC_1 receptor expression. In VIPKO one band was detected at ~70 kDa (Fig. 3.13A) similar to the results of PAC_1 in WT lung. Measurement of PAC_1 as a percent of actin gave a consistent expression of PAC_1 across all 5 mice examined (Fig. 3.13B). The range exhibited from the VIPKO group was 117.4% in mouse 3 to 146.1% in mouse 4.

Finally the PAC_1 expression was examined in the VIPKOT group to assess if any PAC_1 expression changes occurred with exogenous VIP stimulation. As seen in WT and VIPKO mice, a band was detected at ~70 kDa in the lung of VIPKOT mice with consistent expression among all 5 mice examined (Fig. 3.14A). Bands were once again measured with densitometry and expressed as a percent of actin. In VIPKOT lung the mouse 1 (135.7%) and mouse 2 (126.5%) showed slightly higher expression then mouse

3 (116%), mouse 4 (112%) and mouse 5 (113%). Overall the expression of the PAC_1 receptor was consistent throughout the entire group with little variability.

The average PAC_1 expression for WT, VIPKO and VIPKOT lung was determined and analyzed for significant differences. The value given by ANOVA analysis was $p > 0.5$ which indicated that no significant differences existed between any groups (Fig 3.15). The results of PAC_1 expression in WT, VIPKO and VIPKOT lungs demonstrate that PAC_1 expression is constant even in the absence of VIP in VIPKO or when exogenous VIP is introduced to VIPKO mice.

3.3 CFTR expression in WT, VIPKO and VIPKOT mouse lung

Previous work has shown that VIP stimulation is important *in vivo* for stimulation of CFTR mediated chloride secretion (Ameen et al. 1999). VIP also influences the stability and lifetime of CFTR at the membrane, an effect that has been observed both in human epithelial cell lines and *in vivo* in rat duodenum epithelial cells (Ameen et al. 1999; Chappe et al. 2008; Rafferty et al. 2009). The molecular weight of CFTR in human epithelial cells is frequently reported at ~180 kDa for mature gylcosylated CFTR and ~150 for immature core glyscosylated CFTR. In other species such as mouse the molecular weight of CFTR has been reported at a range of molecular weights between 130-180 kDa for mature CFTR (Kopito 1999; Hernandez-Gonzalez et al. 2007). The tissue lysate was prepared with the same method used for the VIP receptors analysis by western blots except that lysate boiling was omitted to prevent degradation of the CFTR protein. CFTR was examined in WT, VIPKO and VIPKOT lung tissues to determine if the expression of total CFTR was altered between the groups and to examine if the

maturation of CFTR differed in absence of VIP or after exogenous VIP was injected to VIPKO mice.

The CFTR protein is very temperature sensitive; if the lysate is heated CFTR will be degraded or form aggregates that do not enter the gel when using SDS-PAGE, thus lysates probed for CFTR were not boiled.

Detection of CFTR in WT lung lysate showed strong bands at ~140 kDa and ~82 kDa in 8 WT mice (Fig. 3.16). The band located at 140 kDa was considered to be the mature mouse CFTR band and was measured by densitometry and represented as a percent of total actin in the sample. Mouse 2 averaged the lowest expression at 119.8%, while mouse 6 averaged 327% expression. We observed a large variability of CFTR expression in these WT mouse lung tissue lysates.

The expression of CFTR in VIPKO lung showed 2 bands, one at ~140 kDa and at ~82 kDa similar to the WT lung (Fig. 3.18A). Measurement of the mature band as a percent of actin showed CFTR expression to range from 176.3% in mouse 3 to 244.1% in mouse 4 (Fig. 3.18B).

The VIPKOT showed similar band expression of CFTR as compared to WT and VIPKO lung tissue (Fig. 3.19A). When measured with densitometry as a percent of actin, VIPKOT ranged from 159.3% in mouse 4 to 294% in mouse 3 (Fig. 3.19B).

There was a large variability of CFTR expression in the lungs for each group tested; the average expression of each group was calculated. The average CFTR expression for WT lung was 226.6%, 218.5% for VIPKO and 220.5% for VIPKOT. No significant differences were detected between any of the groups examined, indicating that CFTR expression does not change between groups.

3.4 Detection of VIP receptors mRNA in WT, VIPKO and VIPKOT mouse duodenum

The mRNA expression of the VIP receptors in mouse duodenum tissues was examined for WT, VIPKO and VIPKOT mice. Tissues underwent RT-PCR after RNA extraction and conversion to cDNA (see *Materials and Methods*). Specific primers used for identification of VIP receptor mRNA in the lung were also used for identification in the duodenum. Negative controls showed that non-specific products were not being amplified and positive controls (PKC α) demonstrated the integrity of the cDNA (Fig. 3.20). $VPAC_1$ (804 bp), $VPAC_2$ (969 bp) and PAC_1 (245 bp) were detected in every group at their respective sizes (Fig. 3.21A-C). Duodenum tissue from WT, VIPKO and VIPKOT mice all express the mRNA for production of the VIP receptors.

3.5 $VPAC_1$, $VPAC_2$ and PAC_1 receptor expression in WT, VIPKO and VIPKOT mouse duodenum

With every VIP receptor mRNA detected in the duodenum, the protein expression was to be determined. Previous work in the duodenum of VIPKO showed increased inflammation and reduced CFTR apical membrane localization (Nicole Alcolado, Masters Thesis, Dalhousie University). After treatment for 3 weeks of VIPKO mice byintraperitoneal injection of VIP, inflammation observed in duodenum histology slides, was reduced and CFTR localization returned to the apical membrane. Western blotting was then used to detect which VIP receptors protein is present and may be involved in the observed effects. We tried to detect the actin content as before with the lung tissues, but

were unsuccessful. Therefore samples tested in the duodenum do not have densitometry measurements and statistical analysis as was performed for the lung. Also, WT mouse 1 duodenum lysate was omitted from VIP receptor probing in duodenum because lysate was compromised due to prolonged exposure to room temperature.

3.5.1 $VPAC_1$

The study of $VPAC_1$ expression in duodenum lysates showed that WT mice expression was too low to be detected by western blotting (Fig. 3.22A). In VIPKO mice $VPAC_1$ expression was detected showing bands at ~72 and ~47 kDa (Fig. 3.22B) similar to $VPAC_1$ in the VIPKO lung. After VIP treatment, $VPAC_1$ remained detectable in VIPKOT in all 5 mince examined (Fig. 3.22C). The expression of $VPAC_1$ is increased in VIPKO compared to WT mice in the duodenum. VIPKO and VIPKOT mice express $VPAC_1$ bands at ~72 and ~47 kDa, the expression appears to be higher in the VIPKO samples compared to the VIPKOT samples. The loss of $VPAC_1$ expression in the VIPKOT may be the result of internalization and degradation of the receptor as a result of prolonged VIP treatment.

3.5.2 $VPAC_2$

Duodenum $VPAC_2$ was also examined by western blotting in all mice groups. Similar to the results from $VPAC_1$, the $VPAC_2$ receptor was not detectable in WT duodenum (Fig. 3.23A). In VIPKO and VIPKOT duodenum samples $VPAC_2$ expression appeared increased when compared to WT duodenum (Fig. 3.23B-C). In VIPKO mouse 2 a dense $VPAC_2$ band was detected compared to all other VIPKO samples tested. The

expression of $VPAC_2$ in VIPKO samples excluding mouse 2 and the expression of $VPAC_2$ in VIPKOT samples have similar band intensities at both the 70 and 47 kDa bands. Thus $VPAC_2$ protein expression is increased in VIPKO duodenum and remains at a comparable level even after 3 weeks of VIP treatment.

3.5.3 PAC_1

The PAC_1 receptor was detected in duodenum of WT mouse 4,5,6 and 8 but not detected in WT mouse 2,3 and 7 (Fig. 3.24A). PAC_1 was not detected in VIPKO duodenum and only mouse 1 of the VIPKOT group showed PAC_1 expression (Fig. 3.24B-C). The PAC_1 receptor expression level was variable in the WT group but detected in more than half of the samples tested. In the VIPKO and VIPKOT groups PAC_1 expression was lost possibly indicating a role for VIP or inflammation in regulation of PAC_1 in the duodenum.

3.6 CFTR expression in WT, VIPKO and VIPKOT mouse duodenum

CFTR expression in the duodenum was examined by western blotting as before; the lysates could not undergo boiling to denature samples because the CFTR signal would be lost.

In WT duodenum a band was detected at ~140 kDa in all 7 WT mice tested (Fig. 3.25). In the VIPKO and VIPKOT a band was also detected at ~140 kDa. In the VIPKO group mouse 1 and mouse 3 showed weaker expression and mouse 4 had lower expression in the VIPKOT samples. The expression does not appear to change between groups with CFTR expression present in each group for a qualitative perspective,

however the failure to detect actin in the intestinal samples make it impossible to make any quantitative observations.

CHAPTER 4: DISCUSSION

Previously the lung and duodenum tissues used in the current study underwent a pathological assessment to determine inflammatory cell infiltration and tissue integrity (Nicole Alcolado, Masters Thesis, Dalhousie University). The CFTR localization in the epithelium was also examined with immunofluorescence and confocal microscopy. Results from the Alcolado study demonstrated increased inflammation and reduced CFTR membrane localization in the VIPKO mice (Nicole Alcolado, Masters Thesis, Dalhousie University). When the VIPKO mice received intraperitoneal injections of VIP, inflammation was reduced and CFTR apical membrane localization was restored, resembling the condition of WT tissues. In CF patients with the ΔF508 mutation also experience loss of CFTR at the apical membrane and experience inflammation in the lung and intestine. Taken together the VIPKO mouse model demonstrates VIPs physiological role in CFTR membrane localization and control of inflammation in the lung and duodenum tissues modeling the phenotype seen in CF. In the previous study it was unknown which VIP receptors were expressed in each tissue and if the changes in CFTR localization after VIP injections were from increased expression or redistribution of existing CFTR.

The current study first identified the expression of the 3 VIP receptors ($VPAC_1$, $VPAC_2$ and PAC_1) in these tissues and compared the changes in VIP receptor expression between each group. Additionally the current study also examined CFTR protein expression in the tissues to understand if VIP stimulation or lack thereof altered CFTR tissue expression.

Western blotting showed in the lung and duodenum tissues that $VPAC_1$ and $VPAC_2$ receptors have low expression in WT mice and increased expression in VIPKO and VIPKOT tissues. In the lung PAC_1 receptor expression did not differ between the WT, VIPKO and VIPKOT mice, however in the duodenum PAC_1 expression was detected in WT mice but not in VIPKO or VIPKOT mice. The expression of CFTR did not change in the lung or duodenum of WT, VIPKO and VIPKOT mice.

4.1 VIP influences CFTR membrane insertion

The role of VIP stimulation has been previously studied for CFTR mediated mucus secretions and CFTR membrane stability in both cells lines and animal tissues. In the human epithelial cell lines Calu-3 and JME/CF15 expressing WT-CFTR and ΔF508-CFTR respectively, VIP was shown to improve CFTR membrane insertion and function through PKA and PKC dependant mechanisms (Chappe et al. 2008; Rafferty et al. 2009; Alcolado et al. 2011). In the JME/CF15 cells, VIP stimulation was also observed to promote trafficking of ΔF508-CFTR to the plasma membrane, a process that was found to be dependent on PKA stimulation alone (Rafferty et al. 2009). Previous work has shown that VIP stimulation causes increased apical membrane insertion of mature WT-CFTR from the sub membrane recycling endosomes. This effect was observed in epithelium from rat duodenum and jejunum and also in shark rectal glands (Ameen et al. 1999; Ameen et al. 2004; Lehrich et al. 1998). Previous work by the Chappe laboratory has also demonstrated in VIPKO C57Bl/6 mice that VIP is required to maintain CFTR apical membrane localization in the lung and duodenum (Nicole Alcolado, Masters Thesis, Dalhousie University). In VIPKO mice lung and duodenum CFTR apical

membrane localization is compromised with CFTR distributed throughout the epithelial cells, however when VIPKO mice received intraperitoneal injections of 500 mg/kg of exogenous VIP every other day for 3 weeks, CFTR localization was restored to favour the apical membrane.

In the human Calu-3 and JME/CF15 cell lines the VIP receptor $VPAC_1$ was identified as the only receptor expressed and thus VIP signalling was credited to be through this receptor (Derand et al. 2004; Rafferty et al. 2009; Alcolado et al. 2011). In the C57Bl/6 VIPKO mice it was unknown which VIP receptors were expressed in the lung and duodenum tissues responding to VIP treatment. Additionally with increased CFTR apical membrane localization it was unknown if existing mature CFTR was redistributed to the apical membrane or if maturation of immature CFTR was influenced by VIP stimulation.

4.2 VIP receptors in the lung of C57Bl/6 mice

Previous work has identified $VPAC_1$ receptor expression in both human and rodent lung. In human lung $VPAC_1$ receptor expression was monitored by immunostaining and western blotting in both normal healthy individuals and patients with primary pulmonary hypertension (PPH). Compared to healthy individuals, the PPH group had inflammation and showed increased amounts of $VPAC_1$ and $VPAC_2$ receptor expression (Petkov et al. 2003). Previously in the lung of WT mice $VPAC_1$ mRNA expression was quantified using real time RT-PCR and was found to have a low level of expression compared to other organs such as the brain and intestine (Karacay et al. 2001). These results are consistent with what we have found for $VPAC_1$and $VPAC_2$ expression

in the lungs of WT and VIPKO mice. In the present study low levels of $VPAC_1$ expression were detected in the WT mouse lung compared to the VIPKO lung.

In VIPKOT mice lung we found $VPAC_1$ expression to be approximately 3 times greater compared to WT mice. In studies using cell lines it was determined that the VIP receptors are internalized after binding with VIP, but were recycled back into the membrane shortly after VIP was cleared from the media (Boissard et al. 1986). *In vivo* VIP is reported to have a short half-life due to enzyme degradation (Domschke et al.1978; Hassan et al. 1994). The increased level of $VPAC_1$ found in the lung of VIPKOT mice may be due to VIPs short half-life in circulation of approximately 2 minutes *in vivo.* If VIP is eliminated from circulation shortly after injection, then the tissue may favour recycling of the receptors rather than degradation, which could explain our results of maintained receptor expression post VIP treatment. However the half-life of VIP or related peptides in the intraperitoneal cavity has not been examined and may have effects on the efficacy of VIP compared to VIP in the bloodstream. If VIP were administered on a continuous basis to VIPKO mice, a reduction of the $VPAC_1$ receptor may yield an expression level closer to the findings in WT mice. It should also be noted that while tissue inflammation was reduced in VIPKOT mice compared to untreated VIPKO mice, there was still evidence of inflammation which may be sufficient to maintain increased $VPAC_1$ receptor expression.

The expression of $VPAC_2$ mimicked that of $VPAC_1$ in WT, VIPKO and VIPKOT mice groups examined. Previous studies have detected $VAPC_2$ in the murine lung using the radioligand technique, where a specifically designed agonist for only the $VPAC_2$ receptor is applied to mouse lung tissue slices (Harmer et al. 2004). Through this method

it is known that $VAPC_2$ is expressed in the murine lung however the level of protein expression of the $VPAC_2$ receptor was unknown. Conversely in human airways $VPAC_2$ receptor expression has been observed to be low when examined with western blotting and northern blotting techniques (Busto et al. 1999; Groneberg et al. 2001). In our study $VPAC_2$ had a low level of expression in lung of WT mice; this result is consistent with the level of protein expression found in human lung and is the first analysis of $VPAC_2$ protein expression in the murine lung.

The expression of the PAC_1 receptor in the lung did not change between WT, VIPKO and VIPKOT mice in the current study. In VIPKO mice VIP is absent but PACAP the primary agonist for PAC_1 is still produced. The effects of signalling through PAC_1 have been studied in PAC_1 knockout mice and showed inflammation and increased amount of the pro-inflammatory cytokines (Martinez et al. 2002). In the present study PAC_1 was the most abundant receptor in WT mouse lung and expression levels did not change in the lung of VIPKO or VIPKOT mice. The results indicate that in the absence of VIP, PACAP which can bind to the $VPAC_1$ and $VPAC_2$ receptors although at a much lower affinity than VIP is not able to compensate for the loss of VIP. Furthermore when VIP is absent the PAC_1 receptor does not change its expression in the murine lung. This finding is supported by a study by Jiang et al. which identified the $VPAC_1$ and $VPAC_2$ receptors mediate the immune response in mouse more than the PAC_1 receptor (Jiang et al. 1998). Although in another study the mRNA level of PAC_1 was observed to increase in mouse lung with ovalbumine induced inflammation, however protein expression was not analysed in this study (Lauenstein et al. 2011).

The VIPKOT mice tissues used in the current study were previously studied to assess the role of VIPs effect on tissue inflammation and were assessed by pathologist Dr. Zhaolin Xu (Department of Pathology, QEII Health-Sciences Centre) where it was determined that 4 out of 5 VIPKOT mice used in the current study showed reversal of inflammation after VIP treatment. The one mouse, which did not respond to VIP treatment and showed no reversal of inflammation was VIPKOT mouse 4. Interestingly, VIP receptor expression analysis showed that VIPKOT mouse 4 had the lowest expression levels in the lung of all 3 VIP receptors. This may provide the first insight into the importance of increased $VPAC_1$ and $VPAC_2$ receptor expression in compromised tissue for VIP treatment to be effective. Our results are consistent to studies performed in mice lacking the $VPAC_2$ receptor.

4.3 VIP Receptors in the duodenum of C57Bl/6 mice

In the duodenum of WT mice $VPAC_1$ and $VPAC_2$ receptors were not detected using western blotting. However in the VIPKO and VIPKOT groups both receptors were detected at the expected sizes. The regulation is similar to what was found in the lung, where when VIP is absent there is an increase in both $VPAC_1$ and $VPAC_2$ receptors. In another study similar to our findings, in WT rat duodenum the expression of $VAPC_1$ was also not detected using *in stitu* hybridization; however different from our results $VPAC_2$ was detected in the muscular layers and in the epithelium (Usdin et al. 1994). The difference from our results could be explained from using different techniques where the threshold of detection is different or from the use of different species of rodents.

The expression of PAC_1 in the intestine has been difficult to ascertain from previous publications. Studies using radioligand binding and mRNA detection have produced mixed results in rodents, a potential reason for these finding may be due to the identification of different splice variants of the PAC_1 receptor (Ekblad et al. 2000). The results of the current study were also diverse, in WT mice the PAC_1 receptor was only detected in mice 4,5,6 and 8, while no PAC_1 receptor was detected in the VIPKO group and in the VIPKOT group only mouse 1 showed expression. Given the results PAC_1 receptor regulation may be diverse in the presence or absence of VIP signalling. There were also differences in the tissue integrity between the groups examined, the regulation of splice variants of PAC_1 are unknown and may dependant on gene expression influenced by factors released during an immune response. The anti-PAC_1 antibody (1B5) used in this study may only be able to detect select splice variants of the PAC_1 receptor and thus other variants would not be detected.

The detection of the VIP receptors in this study is a first step to identify expression in the lung and duodenum. The tissue preparations used were whole tissue lysates meaning all tissue layers were included in the samples. Thus the results demonstrate the dynamic changes in receptor presence, however cannot determine if the expression changes are occurring at the epithelial, sub mucosal, muscle or endothelial levels. Other techniques such as immunohistochemistry or radioligand binding are required to determine the exact location where the receptors are located.

In this study, for lung tissue actin was probed to serve as an internal control for protein loading. However, in the duodenum samples actin could not be detected in any of the groups examined suggesting a tissue specific complication. Similar to PAC_1 having

spice variants, actin has different isofroms that are expressed in tissue. The antibody used in this study was unable to detect actin in the intestine possibly because a different isoform expressed in the duodenum of C57Bl/6 mice. The lysate preparation of the duodenum tissue was different from the lung as duodenum samples had to undergo additional sonication immediately before gel loading for protein to enter the gel. The actin protein may have also been susceptible to aggregations in this tissue that would result in failure to enter the gel.

4.4 Inflammation can increase VIP receptor expression

The expression of the VIP receptors in tissue is not limited a specific cell type. VIP receptors have previous reported expression in numerous cell types (Delgado et al. 2004). In the immune system it is established to have VIP receptor expression in T-cells, macrophages and mast cells (Delgado et al. 2004). The VIP receptors when stimulated can influence the immune response to favour release of anti-inflammatory molecules (Delgado et al. 1999). However during inflammation cytokines are released which can influence VIP receptor expression in surrounding tissues through activation of nuclear transcription factors. An example is Nuclear Factor kappa-B (NFκB) which is activated during inflammation in response to signals from reactive oxygen species, tumor necrosis factor alpha (TNFα) and interleukin 1-beta (IL1β) (Chandel et al. 2000). NFκB is known bind to the promoter of the $VPAC_1$ gene and increases cellular expression of the $VPAC_1$ receptor (Karacay et al. 2000).

The results of the current study support this finding as both $VPAC_1$ and $VPAC_2$ receptor expression increased in VIPKO mice that had increased inflammation. The

increased receptor expression was initially thought to be due in part to increased immune cell presence in conjunction with increased expression in the tissues themselves. In the VIPKOT mice tissues $VPAC_1$ and $VPAC_2$ have greater expression than WT tissues and similar expression to VIPKO tissues, although pathological assessments showed in WT and VIPKOT tissues show very little or no immune cell infiltration. The increased receptor expression in the VIPKOT tissues show reduced inflammation and support the hypothesis that increased receptor expression is occurring within the tissues and not from immune cell infiltration.

The role of the $VPAC_1$ and $VPAC_2$ receptors has been previously examined using knockout mice for each receptor. Interestingly, it was found that the receptors had opposing effects on inflammation in the intestine. The $VPAC_2$ receptor was important for anti-inflammation while $VAPC_1$ was found to induce inflammation (Yadav et al 2011). In relation to our study to determine the receptor responsible for the anti-inflammation and CFTR membrane localization, pharmacological agonist specific for either $VPAC_1$ or $VPAC_2$ could be used.

4.5 Mature CFTR expression is constant in WT,VIPKO and VIPKOT mice

The connection between deficient VIP nerve innervations and CF was first reported in human sweat glands of CF patients (Heinz-Erain et al. 1985). The reduced presence of nerves containing VIP was further reported in nasal and intestinal mucosa of CF patients (Wattchow et al. 1988). VIPKO mice were first used to study the effect of VIP regulation of circadian rhythms (Colwell et al. 2003) but have also been used in the

study of diseases such as asthma and pulmonary hypertension (Szema et al. 2006; Hamidi et al. 2006).

Recently VIPKO mice have been used to assess the role of VIP *in vivo* on CFTR membrane localization where it was found that VIP is required for CFTR apical membrane localization (Nicole Alcolado, Masters Thesis, Dalhousie University). It was unknown if the increased CFTR membrane localization was due to insertion of existing mature CFTR from sub membrane vesicles as was previously seen in rat duodenum and jejunum (Ameen et al. 1999; Ameen et al. 2000) or the result of increased trafficking of immature CFTR from the endoplasmic reticulum which has been observed in the human nasal JME/CF15 cell line for ΔF508-CFTR (Rafferty et al. 2009). Using western blotting our results showed that in lysates from all tissues in the 3 groups of mice examined, no significant differences in total CFTR (mature and immature forms) level was observed. We concluded that in tissue from VIPKO mice, which received VIP treatment for 3 weeks, the restoration of CFTR localization to the apical membrane was due to the increased insertion of existing mature CFTR rather than an increase in trafficking of immature CFTR. This conclusion is based up consistent levels of mature CFTR found across all mice groups in this study.

4.6 Conclusions

This study has reported that in lung and duodenum of VIPKO mice, increased expression of the $VPAC_1$ and $VPAC_2$ receptors is found however no changes were observed for PAC_1 receptor expression. When the VIPKO mice receive VIP treatment, it effectively reversed the inflammation in the lung and duodenum. This is the first time that

VIP receptor expression has been studied in whole tissues of the VIPKO and VIPKOT mice and identified the important changes of their expression in parallel to VIP mediated effects on tissue integrity. Interestingly the regulation of the VIP receptors is maintained at elevated levels even after treatment with VIP for 3 weeks, suggesting that VIP can be used chronically and still have receptors present to mediate a response.

The importance of VIP stimulation on CFTR membrane localization is also a critical process to maintain CFTR at the apical membrane where it can function to regulate the ion composition of mucus layer. Previously in mice the mechanism of VIP action on CFTR membrane localization was not clear *in vivo.* We have shown that this mechanism is most likely due to the retention of already mature CFTR at the cell membrane rather than an increase in immature CFTR trafficking or increased CFTR expression. These finding provide the first analysis of VIP receptor expression in a VIPKO mouse model. The VIPKO mouse demonstrates lung inflammation similar to the pathology of CF airways. In CF patients VIP nerve innervations have been shown to be reduced compared to healthy individuals. This study found in VIPKO mice that the receptors for VIP showed increased expression in tissues that were inflamed and lacking VIP. If CF patients experience a similar increase in VIP receptor expression then treatment with exogenous VIP may be beneficial not only to control inflammation but also to maintain CFTR at the apical membrane.

4.7 Future Studies

The localization of VIP receptor expression in lung and duodenum tissues needs to be further investigated to ascertain the precise regions in the tissue where increased

receptor expression occurs and especially to determine if it is in CFTR expressing cells. There are currently multiple CF mouse models, one model is a CFTR knockout and others are homozygotes for the ΔF508 and G551D mutations (Zeither et al. 1995; Delany et al. 1996). The CF mice do not exhibit the same lung pathology as human CF lungs because mice have other ion channels that can compensate for the loss of CFTR (Ianowski et al. 2007). The efforts to develop an animal model of CF have been directed towards a porcine model because of increased similarities to human CF pathology. The VIPKO mice have been shown to have similar pathologies in the lung, intestine and pancreas that are observed in human CF tissues, demonstrating the importance of VIP not only in CFTR membrane localization but also overall tissue health. It is currently not known about VIP receptor expression in either CF mice or human CF patients, to determine if VIP may be a suitable molecule for treatment the level of receptor expression in CF tissues should be studied. In this study VIPKO mice were treated and examined after 3 weeks of 500 mg/kg VIP injections every other day, other treatment lengths and alternate VIP doses should be examined for effects on VIP receptor expression and CFTR membrane localization.

REFERENCES

Accurso FJ, Sontag MK, Wagener JS. Complications associated with symptomatic diagnosis in infants with cystic fibrosis. J Pediatr. 2005 Sep;147(3 Suppl):S37-41.

Akabas MH, Cheung M, Guinamard R. Probing the structural and functional domains of the CFTR chloride channel. J Bioenerg Biomembr. 1997 Oct;29(5):453-63.

Alcolado N, Conrad DJ, Rafferty S, Chappe FG, Chappe VM. VIP-dependent increase in F508del-CFTR membrane localization is mediated by PKC{varepsilon}. Am J Physiol Cell Physiol. 2011 Jul;301(1):C53-65.

Alcolado N. Regulation of CFTR membrane localization by vasoactive intestinal peptide peptide (VIP). Masters Thesis, Dalhousie University. 2010.

Aleksandrov L, Aleksandrov AA, Chang XB, Riordan JR. The First Nucleotide Binding Domain of Cystic Fibrosis Transmembrane Conductance Regulator Is a Site of Stable Nucleotide Interaction, whereas the Second Is a Site of Rapid Turnover. J Biol Chem. 2002 May 3;277(18):15419-25.

Ameen N, Silvis M, Bradbury NA. Endocytic trafficking of CFTR in health and disease. J Cyst Fibros. 2007 Jan;6(1):1-14.

Ameen NA, Marino C, Salas PJ. cAMP-dependent exocytosis and vesicle traffic regulate CFTR and fluid transport in rat jejunum in vivo. Am J Physiol Cell Physiol. 2003 Feb;284(2):C429-38.

Ameen NA, Martensson B, Bourguinon L, Marino C, Isenberg J, McLaughlin GE. CFTR channel insertion to the apical surface in rat duodenal villus epithelial cells is upregulated by VIP in vivo. J Cell Sci. 1999 Mar;112(Pt 6):887-94.

Anthony H, Collins CE, Davidson G, Mews C, Robinson P, Shepherd R, Stapleton D. Pancreatic enzyme replacement therapy in cystic fibrosis: Australian guidelines. Pediatric Gastroenterological Society and the Dietitians Association of Australia. J Paediatr Child Health. 1999 Apr;35(2):125-9.

Aris RM, Gilligan PH, Neuringer IP, Gott KK, Rea J, Yankaskas JR. The effects of panresistant bacteria in cystic fibrosis patients on lung transplant outcome. Am J Respir Crit Care Med. 1997 May;155(5):1699-704.

Aton SJ, Colwell CS, Harmar AJ, Waschek J, Herzog ED. Vasoactive intestinal polypeptide mediates circadian rhythmicity and synchrony in mammalian clock neurons. Nat Neurosci. 2005 Apr;8(4):476-83.

Bajo AM, Juarranz MG, Valenzuela P, Martínez P, Prieto JC, Guijarro LG. Expression of vasoactive intestinal peptide (VIP) receptors in human uterus. Peptides. 2000 Sep;21(9):1383-8.

Barbezat GO, Grossman MI. Intestinal secretion: stimulation by peptides. Science. 1971 Oct 22;174(7):422-4.
Belcher CN, Vij N. Protein processing and inflammatory signaling in Cystic Fibrosis: challenges and therapeutic strategies. Curr Mol Med. 2010 Feb;10(1):82-94.

Bobadilla JL, Macek M Jr, Fine JP, Farrell PM. Cystic fibrosis: a worldwide analysis of CFTR mutations--correlation with incidence data and application to screening. Hum Mutat. 2002 Jun;19(6):575-606.

Boissard C, Marie JC, Hejblum G, Gespach C, Rosselin G. Vasoactive intestinal peptide receptor regulation and reversible desensitization in human colonic carcinoma cells in culture. Cancer Res. 1986 Sep;46(9):4406-13.

Boucher RC. An overview of the pathogenesis of cystic fibrosis lung disease. Adv Drug Deliv Rev. 2002 Dec 5;54(11):1359-71.

Boucher RC. Regulation of airway surface liquid volume by human airway epithelia. Pflugers Arch. 2003 Jan;445(4):495-8.

Brock DJ, Barron L. Biochemical analysis of meconium in fetuses presumed to have cystic fibrosis. Prenat Diagn. 1986 Jul-Aug;6(4):291-8.

Buscail L, Gourlet P, Cauvin A, De Neef P, Gossen D, Arimura A, Miyata A, Coy DH, Robberecht P, Christophe J. Presence of highly selective receptors for PACAP (pituitary adenylate cyclase activating peptide) in membranes from the rat pancreatic acinar cell line AR 4-2J. FEBS Lett. 1990 Mar 12;262(1):77-81.

Busto R, Carrero I, Guijarro LG, Solano RM, Zapatero J, Noguerales F, Prieto JC. Expression, pharmacological, and functional evidence for PACAP/VIP receptors in human lung. Am J Physiol. 1999 Jul;277(1 Pt 1):L42-8.

Chandel NS, Trzyna WC, McClintock DS, Schumacker PT. Role of oxidants in NF-kappa B activation and TNF-alpha gene transcription induced by hypoxia and endotoxin. J Immunol. 2000 Jul 15;165(2):1013-21.

Chappe F, Loewen ME, Hanrahan JW, Chappe V. Vasoactive intestinal peptide increases cystic fibrosis transmembrane conductance regulator levels in the apical membrane of Calu-3 cells through a protein kinase C-dependent mechanism. J Pharmacol Exp Ther. 2008 Oct;327(1):226-38.

Chappe V, Hinkson DA, Howell LD, Evagelidis A, Liao J, Chang XB, Riordan JR, Hanrahan JW. Stimulatory and inhibitory protein kinase C consensus sequences regulate the cystic fibrosis transmembrane conductance regulator. Proc Natl Acad Sci USA. 2004 Jan 6;101(1):390-5.

Chappe V, Hinkson DA, Zhu T, Chang XB, Riordan JR, Hanrahan JW. Phosphorylation of protein kinase C sites in NBD1 and the R domain control CFTR channel activation by PKA. J Physiol. 2003 Apr 1;548(Pt 1):39-52.

Chapter MC, White CM, DeRidder A, Chadwick W, Martin B, Maudsley S. Chemical modification of class II G protein-coupled receptor ligands: frontiers in the development of peptide analogs as neuroendocrine pharmacological therapies. Pharmacol Ther. 2010 Jan;125(1):39-54.

Chastre E, Bawab W, Faure C, Emami S, Muller F, Boué A, Gespach C. Vasoactive intestinal peptide and its receptors in fetuses with cystic fibrosis. Am J Physiol. 1989 Oct;257(4 Pt 1):G561-9.

Cheng SH, Rich DP, Marshall J, Gregory RJ, Welsh MJ, Smith AE. Phosphorylation of the R domain by cAMP-dependent protein kinase regulates the CFTR chloride channel. Cell. 1991 Sep 6;66(5):1027-36.

Colwell CS, Michel S, Itri J, Rodriguez W, Tam J, Lelievre V, Hu Z, Liu X, Waschek JA. Disrupted circadian rhythms in VIP- and PHI-deficient mice. Am J Physiol Regul Integr Comp Physiol. 2003 Nov;285(5):R939-49.

Cystic Fibrosis Canada, The Canadian Facts & Figures on Cystic Fibrosis http://www.cysticfibrosis.ca/en/aboutCysticFibrosis/CfStatistics.php. Accessed in July 2011.

Cystic Fibrosis Mutation Database (CFMD) 2011. http://genet.sickkids.on.ca/StatisticsPage.html. Accessed in July 2011.

Dean M, Hamon Y, Chimini G. The human ATP-binding cassette (ABC) transporter superfamily. J Lipid Res. 2001 Jul;42(7):1007-17.

Delaney SJ, Alton EW, Smith SN, Lunn DP, Farley R, Lovelock PK, Thomson SA, Hume DA, Lamb D, Porteous DJ, Dorin JR, Wainwright BJ. Cystic fibrosis mice carrying the missense mutation G551D replicate human genotype-phenotype correlations. EMBO J. 1996 Mar 1;15(5):955-63.

Delgado M, Ganea D. Neuroprotective effect of vasoactive intestinal peptide (VIP) in a mouse model of Parkinson's disease by blocking microglial activation.FASEB J. 2003 May;17(8):944-6.

Delgado M, Pozo D, Ganea D. The significance of vasoactive intestinal peptide in immunomodulation. Pharmacol Rev. 2004 Jun;56(2):249-90.

De Lisle RC, Isom KS, Ziemer D, Cotton CU. Changes in the exocrine pancreas secondary to altered small intestinal function in the CF mouse. Am J Physiol Gastrointest Liver Physiol. 2001 Oct;281(4):G899-906.

Dérand R, Montoni A, Bulteau-Pignoux L, Janet T, Moreau B, Muller JM, Becq F. Activation of VPAC1 receptors by VIP and PACAP-27 in human bronchial epithelial cells induces CFTR-dependent chloride secretion. Br J Pharmacol. 2004 Feb;141(4):698-708.

Dey RD, Shannon WA Jr, Said SI. Localization of VIP-immunoreactive nerves in airways and pulmonary vessels of dogs, cat, and human subjects. Cell Tissue Res. 1981;220(2):231-8.
Dickson L, Finlayson K. VPAC and PAC receptors: From ligands to function. Pharmacol Ther. 2009 Mar;121(3):294-316.

Dockray GJ. Vasoactive Intestinal Polypeptide and related Peptides. In: Gut Hormones: Biochemistry and Physiology, 1st ed, Walsh JH, Dockray GJ. (Eds), Raven Press, Ltd. New York 1994. p.447

Domschke S, Domschke W, Bloom SR, Mitznegg P, Mitchell SJ, Lux G, Strunz U. Vasoactive intestinal peptide in man: pharmacokinetics, metabolic and circulatory effects. Gut. 1978 Nov;19(11):1049-53.

Dupuis A, Hamilton D, Cole DE, Corey M. Cystic fibrosis birth rates in Canada: a decreasing trend since the onset of genetic testing. J Pediatr. 2005 Sep;147(3):312-5.

Ekblad E, Jongsma H, Brabet P, Bockaert J, Sundler F. Characterization of intestinal receptors for VIP and PACAP in rat and in PAC1 receptor knockout mouse. Ann N Y Acad Sci. 2000;921:137-47.

El Karim IA, Lamey PJ, Ardill J, Linden GJ, Lundy FT. Vasoactive intestinal polypeptide (VIP) and VPAC1 receptor in adult human dental pulp in relation to caries. Arch Oral Biol. 2006 Oct;51(10):849-55.

Engelhardt JF, Yankaskas JR, Ernst SA, Yang Y, Marino CR, Boucher RC, Cohn JA, Wilson JM. Submucosal glands are the predominant site of CFTR expression in the human bronchus. Nat Genet. 1992 Nov;2(3):240-8.

Fahrenkrug J. VIP and autonomic neurotransmission. Pharmacol Ther. 1989;41(3):515-34.

Fahrenkrug J, Hannibal J. Neurotransmitters co-existing with VIP or PACAP. Peptides. 2004 Mar;25(3):393-401.

Farinha CM, Penque D, Roxo-Rosa M, Lukacs G, Dormer R, McPherson M, Pereira M, Bot AG, Jorna H, Willemsen R, Dejonge H, Heda GD, Marino CR, Fanen P, Hinzpeter A, Lipecka J, Fritsch J, Gentzsch M, Edelman A, Amaral MD. Biochemical methods to assess CFTR expression and membrane localization. J Cyst Fibros. 2004 Aug;3 Suppl 2:73-7.

Ferguson SS, Zhang J, Barak LS, Caron MG. Molecular mechanisms of G protein-coupled receptor desensitization and resensitization. Life Sci. 1998;62(17-18):1561-5.

Fischer H, Widdicombe JH. Mechanisms of acid and base secretion by the airway epithelium. J Membr Biol. 2006;211(3):139-50.

Friedlander AL, Albert RK. Chronic macrolide therapy in inflammatory airways diseases. Chest. 2010 Nov;138(5):1202-12.

Gadsby DC, Vergani P, Csanády L. The ABC protein turned chloride channel whose failure causes cystic fibrosis. Nature. 2006 Mar 23;440(7083):477-83.
Gardner J. What you need to know about cystic fibrosis. Nursing. 2007 Jul;37(7):52-5.

Groneberg DA, Hartmann P, Dinh QT, Fischer A. Expression and distribution of vasoactive intestinal polypeptide receptor VPAC(2) mRNA in human airways. Lab Invest. 2001 May;81(5):749-55.

Grosse SD, Boyle CA, Botkin JR, Comeau AM, Kharrazi M, Rosenfeld M, Wilfond BS. Centers for Disease Control and Prevention. Newborn screening for cystic fibrosis: evaluation of benefits and risks and recommendations for state newborn screening programs. MMWR 2004;53(No. RR-13):1-35.

Hamidi SA, Szema AM, Lyubsky S, Dickman KG, Degene A, Mathew SM, Waschek JA, Said SI. Clues to VIP function from knockout mice. Ann N Y Acad Sci. 2006 Jul;1070:5-9.

Harmar AJ, Sheward WJ, Morrison CF, Waser B, Gugger M, Reubi JC. Distribution of the VPAC2 receptor in peripheral tissues of the mouse. Endocrinology. 2004 Mar;145(3):1203-10.

Hassan M, Refai E, Andersson M, Schnell PO, Jacobsson H. In vivo dynamical distribution of 131I-VIP in the rat studied by gamma-camera. Nucl Med Biol. 1994 Aug;21(6):865-72.

Heda GD, Tanwani M, Marino CR. The Delta F508 mutation shortens the biochemical half-life of plasma membrane CFTR in polarized epithelial cells. Am J Physiol Cell Physiol. 2001 Jan;280(1):C166-74.

Heinz-Erian P, Dey RD, Flux M, Said SI. Deficient vasoactive intestinal peptide innervation in the sweat glands of cystic fibrosis patients. Science. 1985 Sep 27;229(4720):1407-8.

Heinz-Erian P, Said SI. Vasoactive intestinal peptide as a regulator of exocrine function and as a possible factor in cystic fibrosis. Ann N Y Acad Sci. 1988;527:568-73.

Hodson ME. Treatment of cystic fibrosis in the adult. Respiration. 2000;67(6):595-607.

Howell LD, Borchardt R, Cohn JA. ATP hydrolysis by a CFTR domain: pharmacology and effects of G551D mutation. Biochem Biophys Res Commun. 2000 May 10;271(2):518-25.

Hwang TC, Lu L, Zeitlin PL, Gruenert DC, Huganir R, Guggino WB. Cl- channels in CF: lack of activation by protein kinase C and cAMP-dependent protein kinase. Science. 1989 Jun 16;244(4910):1351-3.

Hwang TC, Sheppard DN. Gating of the CFTR Cl- channel by ATP-driven nucleotide-binding domain dimerisation. J Physiol. 2009 May 15;587(Pt 10):2151-61.
Ianowski JP, Choi JY, Wine JJ, Hanrahan JW. Mucus secretion by single tracheal submucosal glands from normal and cystic fibrosis transmembrane conductance regulator knockout mice. J Physiol. 2007 Apr 1;580(Pt 1):301-14.

Ibrahim BM, Tsifansky MD, Yang Y, Yeo Y. Challenges and advances in the development of inhalable drug formulations for cystic fibrosis lung disease. Expert Opin Drug Deliv. 2011 Apr;8(4):451-66.

Jakab RL, Collaco AM, Ameen NA. Physiological relevance of cell-specific distribution patterns of CFTR, NKCC1, NBCe1, and NHE3 along the crypt-villus axis in the intestine. Am J Physiol Gastrointest Liver Physiol. 2011 Jan;300(1):G82-98.

Ji HL, Chalfant ML, Jovov B, Lockhart JP, Parker SB, Fuller CM, Stanton BA, Benos DJ. The cytosolic termini of the beta- and gamma-ENaC subunits are involved in the functional interactions between cystic fibrosis transmembrane conductance regulator and epithelial sodium channel. J Biol Chem. 2000 Sep 8;275(36):27947-56.

Jiang X, Wang HY, Yu J, Ganea D. VIP1 and VIP2 receptors but not PVR1 mediate the effect of VIP/PACAP on cytokine production in T lymphocytes. Ann N Y Acad Sci. 1998 Dec 11;865:397-407.

Karacay B, O'Dorisio MS, Summers M, Bruce J. Regulation of Vasoactive intestinal peptide receptor expression in developing nervous systems. Ann N Y Acad Sci. 2000;921:165-74.

Karacay B, O'Dorisio MS, Kasow K, Hollenback C, Krahe R. Expression and fine mapping of murine vasoactive intestinal peptide receptor 1. J Mol Neurosci. 2001 Dec;17(3):311-24.

Kato I, Suzuki Y, Akabane A, Yonekura H, Tanaka O, Kondo H, Takasawa S, Yoshimoto T, Okamoto H. Transgenic mice overexpressing human vasoactive intestinal peptide (VIP) gene in pancreatic beta cells. Evidence for improved glucose tolerance and enhanced insulin secretion by VIP and PHM-27 in vivo. J Biol Chem. 1994 Aug 19;269(33):21223-8.

Kirchgessner AL, Liu MT. Pituitary adenylate cyclase activating peptide (PACAP) in the enteropancreatic innervation. Anat Rec. 2001 Jan 1;262(1):91-100.

Kleizen B, Braakman I, de Jonge HR. Regulated trafficking of the CFTR chloride channel. Eur J Cell Biol. 2000 Aug;79(8):544-56.

Ko YH, Pedersen PL. Cystic fibrosis: a brief look at some highlights of a decade of research focused on elucidating and correcting the molecular basis of the disease. J Bioenerg Biomembr. 2001 Dec;33(6):513-21.

Kolakowski LF Jr. GCRDb: a G-protein-coupled receptor database. Receptors Channels. 1994;2(1):1-7.

Kreindler JL. Cystic fibrosis: exploiting its genetic basis in the hunt for new therapies. Pharmacol Ther. 2010 Feb;125(2):219-29.
Kremer TM, Zwerdling RG, Michelson PH, O'Sullivan P. Intensive care management of the patient with cystic fibrosis. J Intensive Care Med. 2008 May-Jun;23(3):159-77.

Krysa J, Steger A. Pancreas and cystic fibrosis: the implications of increased survival in cystic fibrosis. Pancreatology. 2007;7(5-6):447-50.

Laburthe M, Couvineau A. Molecular pharmacology and structure of VPAC Receptors for VIP and PACAP. Regul Pept. 2002 Oct 15;108(2-3):165-73.

Lauenstein HD, Quarcoo D, Plappert L, Schleh C, Nassimi M, Pilzner C, Rochlitzer S, Brabet P, Welte T, Hoymann HG, Krug N, Müller M, Lerner EA, Braun A, Groneberg DA. Pituitary adenylate cyclase-activating peptide receptor 1 mediates anti-inflammatory effects in allergic airway inflammation in mice. Clin Exp Allergy. 2011 Apr;41(4):592-601.

Lehrich RW, Aller SG, Webster P, Marino CR, Forrest JN Jr. Vasoactive intestinal peptide, forskolin, and genistein increase apical CFTR trafficking in the rectal gland of the spiny dogfish, Squalus acanthias. Acute regulation of CFTR trafficking in an intact epithelium. J Clin Invest. 1998 Feb 15;101(4):737-45.

Liedtke CM, Yun CH, Kyle N, Wang D. Protein kinase C epsilon-dependent regulation of cystic fibrosis transmembrane regulator involves binding to a receptor for activated C kinase (RACK1) and RACK1 binding to Na+/H+ exchange regulatory factor. J Biol Chem. 2002 Jun 21;277(25):22925-33.

Littlewood JM. Gastrointestinal complications in cystic fibrosis. Journal of the Royal Society of Medicine Supplement. 1992; 85(18):13-7.

Littlewood JM, Wolfe SP, Conway SP. Diagnosis and treatment of intestinal malabsorption in cystic fibrosis. Pediatr Pulmonol. 2006 Jan;41(1):35-49.

Martinez C, Abad C, Delgado M, Arranz A, Juarranz MG, Rodriguez-Henche N, Brabet P, Leceta J, Gomariz RP. Anti-inflammatory role in septic shock of pituitary adenylate cyclase-activating polypeptide receptor. Proc Natl Acad Sci U S A. 2002 Jan 22;99(2):1053-8.

Maruno K, Absood A, Said SI. Vasoactive intestinal peptide inhibits human small-cell lung cancer proliferation in vitro and in vivo. Proc Natl Acad Sci USA. 1998 Nov 24;95(24):14373-8.

Matsui H, Grubb BR, Tarran R, Randell SH, Gatzy JT, Davis CW, Boucher RC. Evidence for periciliary liquid layer depletion, not abnormal ion composition, in the pathogenesis of cystic fibrosis airways disease. Cell. 1998 Dec 23;95(7):1005-15.

McCulloch DA, Lutz EM, Johnson MS, Robertson DN, MacKenzie CJ, Holland PJ, Mitchell R. ADP-ribosylation factor-dependent phospholipase D activation by VPAC receptors and a PAC(1) receptor splice variant. Mol Pharmacol. 2001 Jun;59(6):1523-32.

McDonald TP, Dinnis DM, Morrison CF, Harmar AJ. Desensitization of the human vasoactive intestinal peptide receptor (hVIP2/PACAP R): evidence for agonist-induced receptor phosphorylation and internalization. Ann N Y Acad Sci. 1998 Dec 11;865:64-72.

McKone EF, Goss CH, Aitken ML. CFTR genotype as a predictor of prognosis in cystic fibrosis. Chest. 2006 Nov;130(5):1441-7.

Mehta A. CFTR: more than just a chloride channel. Pediatr Pulmonol. 2005 Apr;39(4):292-8.

Miotto D, Boschetto P, Bononi I, Zeni E, Cavallesco G, Fabbri LM, Mapp CE. Vasoactive intestinal peptide receptors in the airways of smokers with chronic bronchitis. Eur Respir J. 2004 Dec;24(6):958-63.

Morton JR, Ansari N, Glanville AR, Meagher AP, Lord RV. Distal intestinal obstruction syndrome (DIOS) in patients with cystic fibrosis after lung transplantation. J Gastrointest Surg. 2009 Aug;13(8):1448-53.

Moskowitz SM, Chmiel JF, Sternen DL, Cheng E, Cutting GR. CFTR-Related Disorders. 2001. Pagon RA, Bird TD, Dolan CR,Stephens K, editors. GeneReviews. Seattle (WA): University of Washington, Seattle; 1993.

Ollerenshaw S, Jarvis D, Woolcock A, Sullivan C, Scheibner T. Absence of immunoreactive vasoactive intestinal polypeptide in tissue from the lungs of patients with asthma. N Engl J Med. 1989 May 11;320(19):1244-8.

Petkov V, Mosgoeller W, Ziesche R, Raderer M, Stiebellehner L, Vonbank K, Funk GC, Hamilton G, Novotny C, Burian B, Block LH. Vasoactive intestinal peptide as a new drug for treatment of primary pulmonary hypertension. J Clin Invest. 2003 May;111(9):1339-46.

Power RF, Bishop AE, Wharton J, Inyama CO, Jackson RH, Bloom SR, Polak JM. Anatomical distribution of vasoactive intestinal peptide binding sites in peripheral tissues investigated by in vitro autoradiography. Ann N Y Acad Sci. 1988;527:314-25.

Quinton PM. Physiological basis of cystic fibrosis: a historical perspective. Physiol Rev. 1999 Jan;79(1 Suppl):S3-S22.

Raghuram V, Hormuth H, Foskett JK. A kinase-regulated mechanism controls CFTR channel gating by disrupting bivalent PDZ domain interactions. Proc Natl Acad Sci USA. 2003 Aug 5;100(16):9620-5.
Riordan JR. Cystic fibrosis as a disease of misprocessing of the cystic fibrosis transmembrane conductance regulator glycoprotein. Am J Hum Genet. 1999 Jun;64(6):1499-504.

Riordan JR, Rommens JM, Kerem B, Alon N, Rozmahel R, Grzelczak Z, Zielenski J, Lok S, Plavsic N, Chou JL, et al. Identification of the cystic fibrosis gene:cloning and characterization of complementary DNA. Science. 1989 Sep8;245(4922):1066-73.

Robinson M, Bye PT. Mucociliary clearance in cystic fibrosis. Pediatr Pulmonol. 2002 Apr;33(4):293-306.

Rogers DF. Motor control of airway goblet cells and glands. Respir Physiol. 2001 Mar;125(1-2):129-44.

Rogers GB, Stressmann FA, Koller G, Daniels T, Carroll MP, Bruce KD. Assessing the diagnostic importance of nonviable bacterial cells in respiratory infections. Diagn Microbiol Infect Dis. 2008 Oct;62(2):133-41.

Rowe SM, Miller S, Sorscher EJ. Cystic fibrosis. N Engl J Med. 2005 May 12;352(19):1992-2001.

Rubenstein RC, Lockwood SR, Lide E, Bauer R, Suaud L, Grumbach Y. Regulation of endogenous ENaC functional expression by CFTR and ΔF508-CFTR in airway epithelial cells. Am J Physiol Lung Cell Mol Physiol. 2011 Jan;300(1):L88-L101.

Said SI. The Viktor Mutt Memorial Lecture. Protection by VIP and related peptides against cell death and tissue injury. Ann N Y Acad Sci. 2000;921:264-74.

Said SI. Vasoactive intestinal polypeptide (VIP) in asthma. Ann N Y Acad Sci. 1991;629:305-18.

Said SI, Dickman KG. Pathways of inflammation and cell death in the lung: modulation by vasoactive intestinal peptide. Regul Pept. 2000 Sep 25;93(1-3):21-9.

Said SI, Mutt V. Polypeptide with broad biological activity: isolation from small intestine. Science. 1970 Sep 18;169(951):1217-8.

St Hilaire RC, Murthy SN, Kadowitz PJ, Jeter JR Jr. Role of VPAC1 and VPAC2 in VIP mediated inhibition of rat pulmonary artery and aortic smooth muscle cell proliferation. Peptides. 2010 Aug;31(8):1517-22.

Schwiebert EM, Benos DJ, Egan ME, Stutts MJ, Guggino WB. CFTR is a conductance regulator as well as a chloride channel. Physiol Rev. 1999 Jan;79(Suppl):S145-66.

Seavilleklein G, Amer N, Evagelidis A, Chappe F, Irvine T, Hanrahan JW, Chappe V. PKC phosphorylation modulates PKA-dependent binding of the R domain to other domains of CFTR. Am J Physiol Cell Physiol. 2008 Nov;295(5):C1366-75.

Sheils CA, Käs J, Travassos W, Allen PG, Janmey PA, Wohl ME, Stossel TP. Actin filaments mediate DNA fiber formation in chronic inflammatory airway disease. Am J Pathol. 1996 Mar;148(3):919-27.

Sheppard DN, Welsh MJ. Structure and function of the CFTR chloride channel. Physiol Rev. 1999 Jan;79(1 Suppl):S23-45.

Sherwood NM, Krueckl SL, McRory JE. The origin and function of the pituitary adenylate cyclase-activating polypeptide (PACAP)/glucagon superfamily. Endocr Rev. 2000 Dec;21(6):619-70.

Shetzline MA, Walker JK, Valenzano KJ, Premont RT. Vasoactive intestinal polypeptide type-1 receptor regulation. Desensitization, phosphorylation, and sequestration. J Biol Chem. 2002 Jul 12;277(28):25519-26.

Silvis MR, Bertrand CA, Ameen N, Golin-Bisello F, Butterworth MB, Frizzell RA, Bradbury NA. Rab11b regulates the apical recycling of the cystic fibrosis transmembrane conductance regulator in polarized intestinal epithelial cells. Mol Biol Cell. 2009 Apr;20(8):2337-50.

Sinaasappel M, Veeze HJ, De Jonge HR. New insights into the pathogenesis of cystic fibrosis. Scand J Gastroenterol Suppl. 1990;178:17-25.

Smitherman TC, Popma JJ, Said SI, Krejs GJ, Dehmer GJ. Coronary hemodynamic effects of intravenous vasoactive intestinal peptide in humans. Am J Physiol. 1989 Oct;257(4 Pt 2):H1254-62.

Speck K, Charles A. Distal intestinal obstructive syndrome in adults with cystic fibrosis: a surgical perspective. Arch Surg. 2008 Jun;143(6):601-3.

Stratford FL, Ramjeesingh M, Cheung JC, Huan LJ, Bear CE. The Walker B motif of the second nucleotide-binding domain (NBD2) of CFTR plays a key role in ATPase activity by the NBD1-NBD2 heterodimer. Biochem J. 2007 Jan 15;401(2):581-6.

Szema AM, Hamidi SA, Lyubsky S, Dickman KG, Mathew S, Abdel-Razek T, Chen JJ, Waschek JA, Said SI. Mice lacking the VIP gene show airway hyperresponsiveness and airway inflammation, partially reversible by VIP. Am J Physiol Lung Cell Mol Physiol. 2006 Nov;291(5):L880-6.

Tarran R, Loewen ME, Paradiso AM, Olsen JC, Gray MA, Argent BE, Boucher RC, Gabriel SE. Regulation of murine airway surface liquid volume by CFTR and Ca2+-activated Cl- conductances. J Gen Physiol. 2002 Sep;120(3):407-18.

Taylor CJ, Aswani N. The pancreas in cystic fibrosis. Paediatr Respir Rev. 2002 Mar;3(1):77-81.

Tizzano EF, Buchwald M. CFTR expression and organ damage in cystic fibrosis. Ann Intern Med. 1995 Aug 15;123(4):305-8.

Trezise A, Exquisite and Multilevel Regulation of CFTR Expression. In: A Bush, EWFW Alton, JC Davies, U Griesenbach, A Jaffe, eds. Cystic Fibrosis in the 21st Century. Progressive Respiratory Research, vol 34. Basel: Karger; 2006: 11-20.

Usdin TB, Bonner TI, Mezey E. Two receptors for vasoactive intestinal polypeptide with similar specificity and complementary distributions. Endocrinology. 1994 Dec;135(6):2662-80.

Vandebrouck C, Melin P, Norez C, Robert R, Guibert C, Mettey Y, Becq F. Evidence that CFTR is expressed in rat tracheal smooth muscle cells and contributes to bronchodilation. Respir Res. 2006 Aug 28;7:113

Wang X, Matteson J, An Y, Moyer B, Yoo JS, Bannykh S, Wilson IA, Riordan JR, Balch WE. COPII-dependent export of cystic fibrosis transmembrane conductance regulator from the ER uses a di-acidic exit code. J Cell Biol. 2004 Oct 11;167(1):65-74.

Wattchow DA, Furness JB, Gibbons IL, Little KE, Carter RF. Vasoactive intestinal peptide immunoreactive nerve fibres are deficient in intestinal and nasal mucosa affected by cystic fibrosis. J Gastro Hepat. 1988 Dec;3(6):549-555.

Winpenny JP, McAlroy HL, Gray MA, Argent BE. Protein kinase C regulates the magnitude and stability of CFTR currents in pancreatic duct cells. Am J Physiol. 1995 Apr;268(4 Pt 1):C823-8.

Winter MC, Welsh MJ. Stimulation of CFTR activity by its phosphorylated R domain. Nature. 1997 Sep 18;389(6648):294-6.

Wu D, Lee D, Sung YK. Prospect of vasoactive intestinal peptide therapy for COPD/PAH and asthma: a review. Respir Res. 2011 Apr 11;12:45.

Zeiher BG, Eichwald E, Zabner J, Smith JJ, Puga AP, McCray PB Jr, Capecchi MR, Welsh MJ, Thomas KR. A mouse model for the delta F508 allele of cystic fibrosis. J Clin Invest. 1995 Oct;96(4):2051-64.

Zhang ZR, McDonough SI, McCarty NA. Interaction between permeation and gating in a putative pore domain mutant in the cystic fibrosis transmembrane conductance regulator. Biophys J. 2000 Jul;79(1):298-313.

Zielenski J. Genotype and phenotype in cystic fibrosis. Respiration. 2000;67(2):117-33.

APPENDIX A: Figures

Figure 3.1 Positive and negative controls in wild type (WT), VIP knockout (VIPKO) and VIP knockout treated (VIPKOT) C57BL/6 mouse lung using RT-PCR after RNA was extracted and converted to cDNA. Positive control primer was designed using the GenBank sequence specific to *Mus musculus* for PKC α and negative controls had no primer added to the reaction . All products were run using 0.8% agarose gel electrophoresis and using the φx molecular marker. Positive controls for PKC α are shown on left panels and negative controls on right panels. **A)** WT lung controls, positive control PKC α on the left and negative control on the right. **B)** VIPKO lung controls, positive control PKC α on the left and negative control on the right. **C)** VIPKOT lung controls, positive control PKC α on the left and negative control on the right. The expected size in base pair (bp) is displayed above each lane.

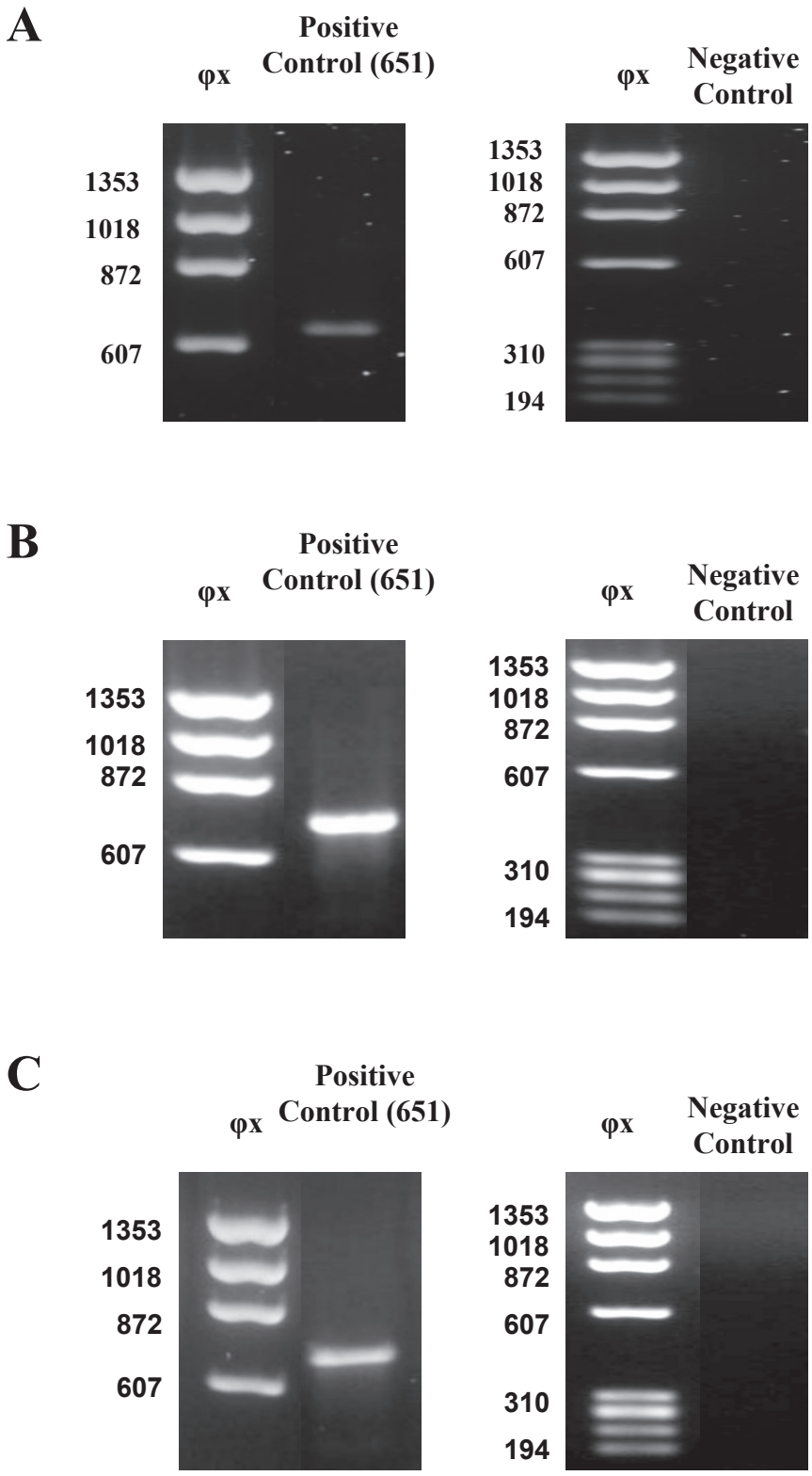
A
φx
Positive Control (651)
1353
1018
872
607
φx
Negative Control
1353
1018
872
607
310
194
B
φx
Positive Control (651)
1353
1018
872
607
φx
Negative Control
1353
1018
872
607
310
194
C
φx
Positive Control (651)
1353
1018
872
607
φx
Negative Control
1353
1018
872
607
310
194

Figure 3.2 Detection of VIP receptor cDNA in Positive and negative controls in wild type (WT), VIP knockout (VIPKO) and VIP knockout treated (VIPKOT) C57BL/6 mouse lung using RT-PCR after RNA extraction and conversion to cDNA. All primers were designed using GenBank sequences specific to *Mus musculus* for each VIP receptor and PKC α. All products were run using 0.8% agarose gel electrophoresis and using the φx molecular marker. **A)** $VPAC_1$ receptor cDNA detection in WT (left), VIPKO (center) and VIPKOT (right) mouse lung. **B)** $VPAC_2$ receptor cDNA detection in WT (left), VIPKO (center) and VIPKOT (right) mouse lung. **C)** PAC_1 receptor cDNA detection in WT (left), VIPKO (center) and VIPKOT (right) mouse lung. The expected size in base pair (bp) is displayed above each lane.

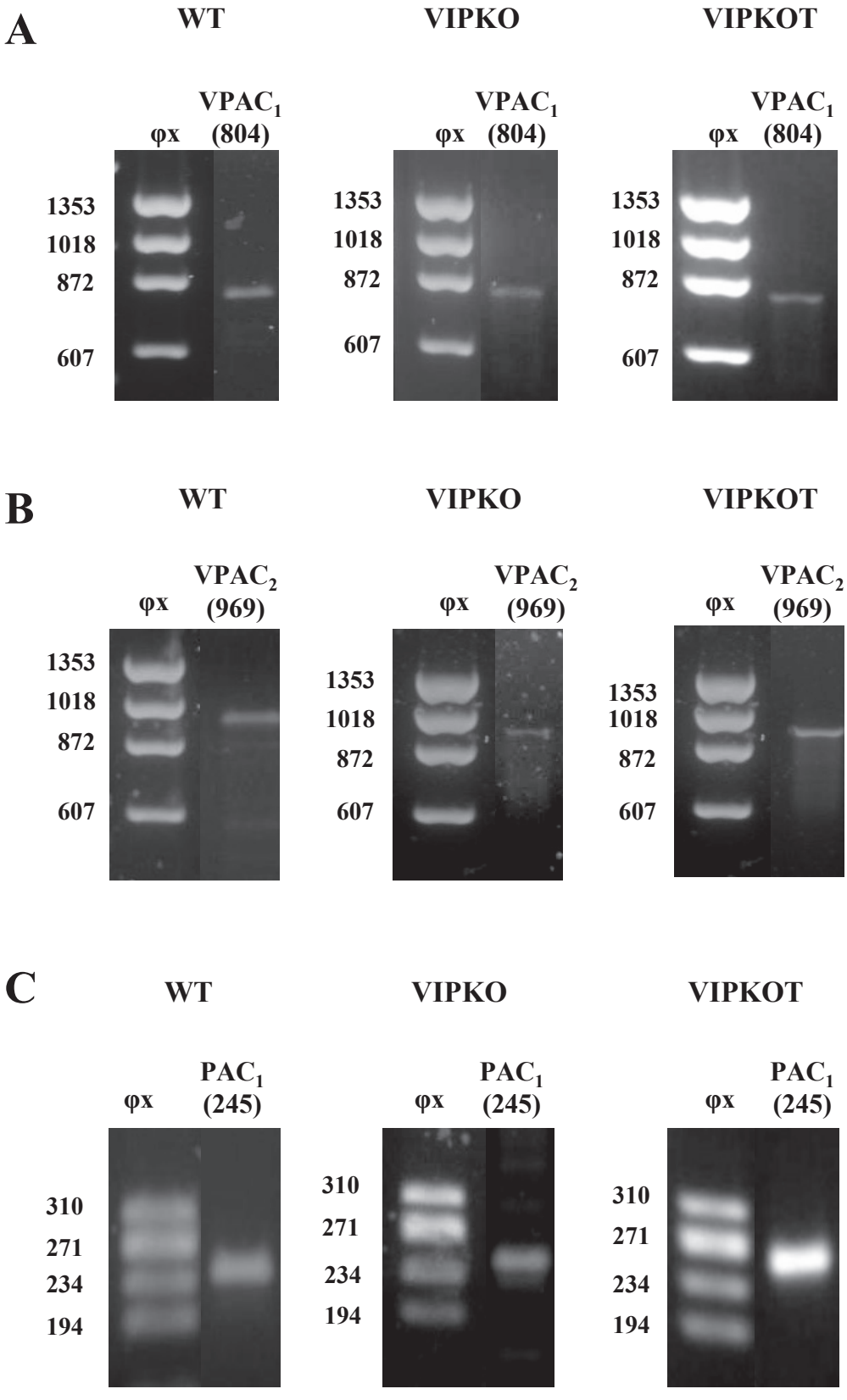
A
WT
VIPKO
VIPKOT
VPAC1 (804)
φx
1353
1018
872
607
B
WT
VIPKO
VIPKOT
VPAC2 (969)
φx
1353
1018
872
607
C
WT
VIPKO
VIPKOT
PAC1 (245)
φx
310
271
234
194

Figure 3.3 Western blot negative controls, membranes were probed with secondary antibody only. **A)** Samples were boiled at 90°C for 10 minutes to denature proteins. WT lung (lane 1), WT duodenum (lane 2), VIPKO lung (lane 3), VIPKO duodenum (lane 4), VIPKO treated lung (lane 5) and VIPKO treated duodenum (lane 6).

A

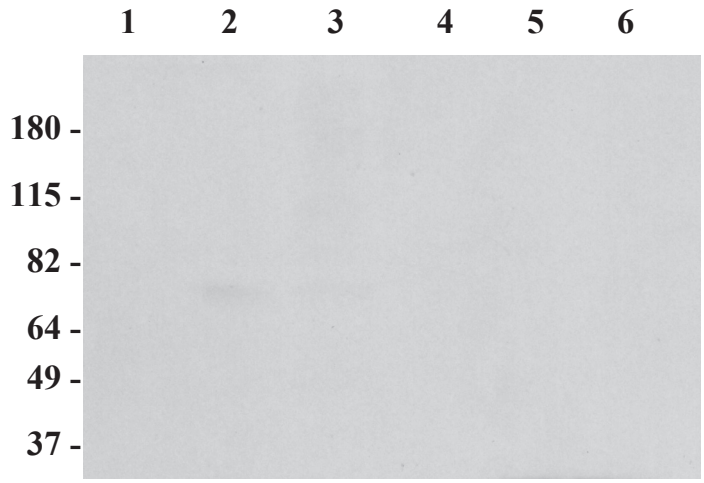

Figure 3.4 $VPAC_1$ receptor expression in whole lung tissue lysate from wild type mice. **A)** Representative western blot of 8 wild type mouse lung samples revealed with the monoclonial $VPAC_1$ (AS58) antibody. Each lane contains 50 μg of total protein. Membrane was then stripped and re-probed for actin as an internal control (lower panel). **B)** Densitometry values from western blots comparing the percent of the $VPAC_1$ band to actin band ± SEM of n= 3 independent experiments on each mouse lung sample. Arrow indicates expected size of $VPAC_1$ band.

A

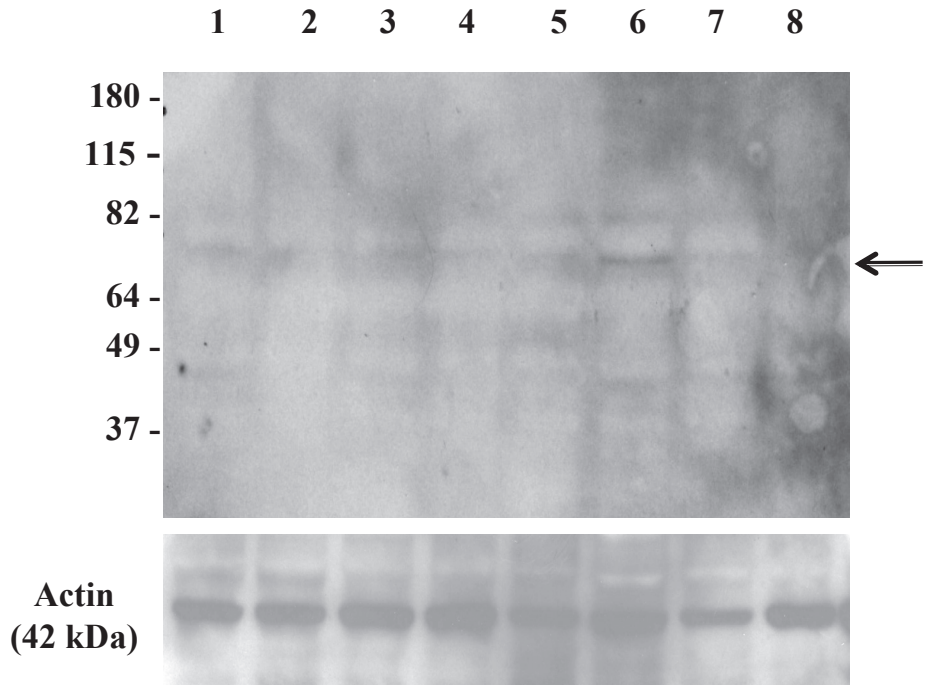
1 2 3 4 5 6 7 8
180 -
115 -
82 -
64 -
49 -
37 -
Actin
(42 kDa)

B

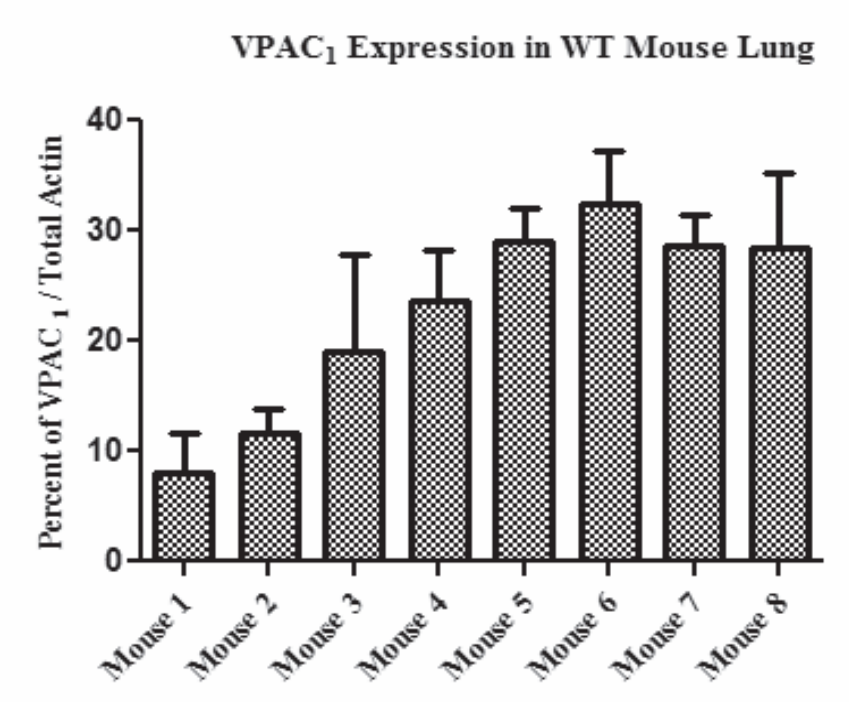
VPAC1 Expression in WT Mouse Lung
Percent of VPAC 1 / Total Actin
40
30
20
10
0
Mouse 1
Mouse 2
Mouse 3
Mouse 4
Mouse 5
Mouse 6
Mouse 7
Mouse 8

Figure 3.5 $VPAC_1$ receptor expression in whole lung tissue lysate from VIP knockout mice (VIPKO). **A)** Representative western blot of 5 VIPKO mouse lung samples revealed with the monoclonial $VPAC_1$ (AS58) antibody. Each lane contains 50 μg of total protein. Membrane was then stripped and re-probed for actin as an internal control (lower panel). **B)** Densitometry values from western blots comparing the percent of the $VPAC_1$ band to actin band ± SEM of n= 4-5 independent experiments on each mouse lung sample. Arrow indicates expected size of $VPAC_1$ band.

A

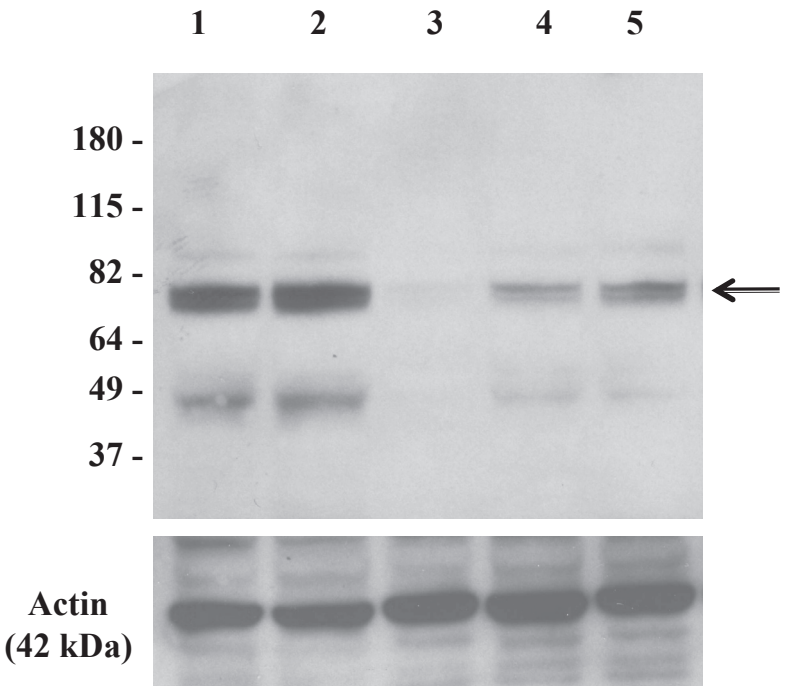
1
2
3
4
5
180 -
115 -
82 -
64 -
49 -
37 -
Actin
(42 kDa)

B

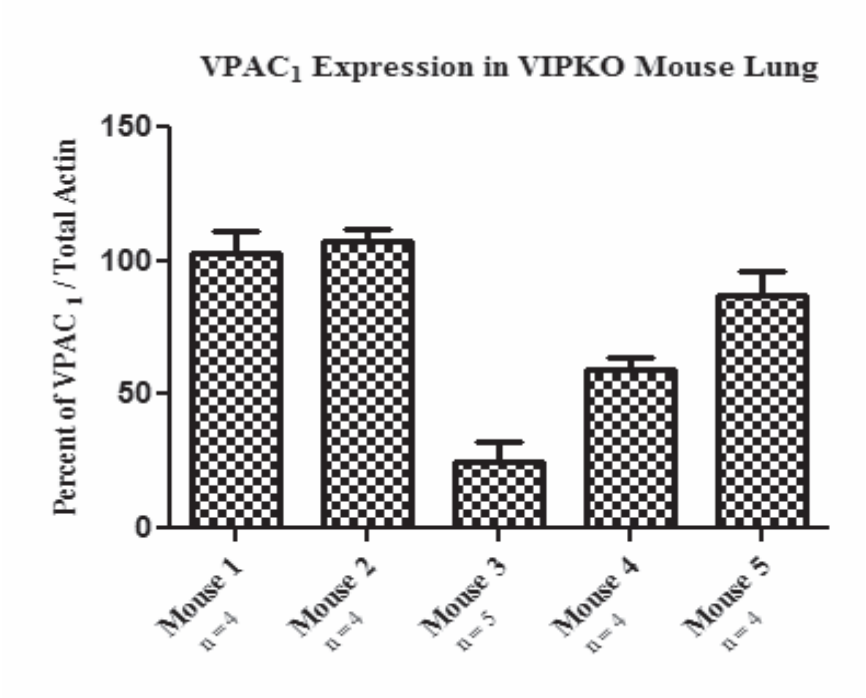
VPAC1 Expression in VIPKO Mouse Lung
Percent of VPAC1 / Total Actin
150
100
50
0
Mouse 1
n = 4
Mouse 2
n = 4
Mouse 3
n = 5
Mouse 4
n = 4
Mouse 5
n = 4

Figure 3.6 $VPAC_1$ receptor expression in whole lung tissue lysate from VIP knockout treated mice (VIPKOT) that received 500 mg/kg VIP every other day for 3 weeks . **A)** Representative western blot of 5 VIPKOT mouse lung samples revealed with the monoclonial $VPAC_1$ (AS58) antibody. Each lane contains 50 μg of total protein. Membrane was then stripped and re-probed for actin as an internal control (lower panel). **B)** Densitometry values from western blots comparing the percent of the $VPAC_1$ band to actin band ± SEM of n= 3-5 independent experiments on each mouse lung sample. Arrow indicates expected size of $VPAC_1$ band.

A

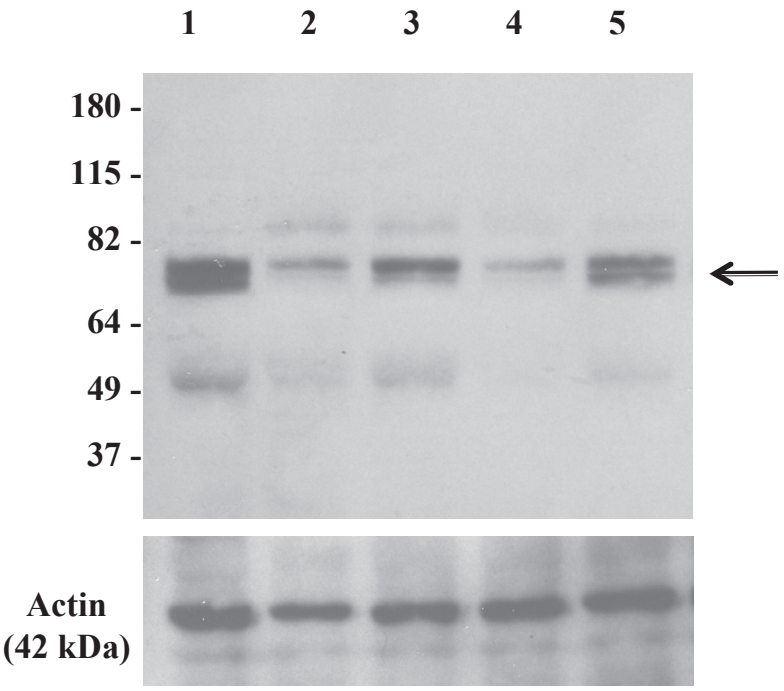
1
2
3
4
5
180 -
115 -
82 -
64 -
49 -
37 -
Actin
(42 kDa)

B

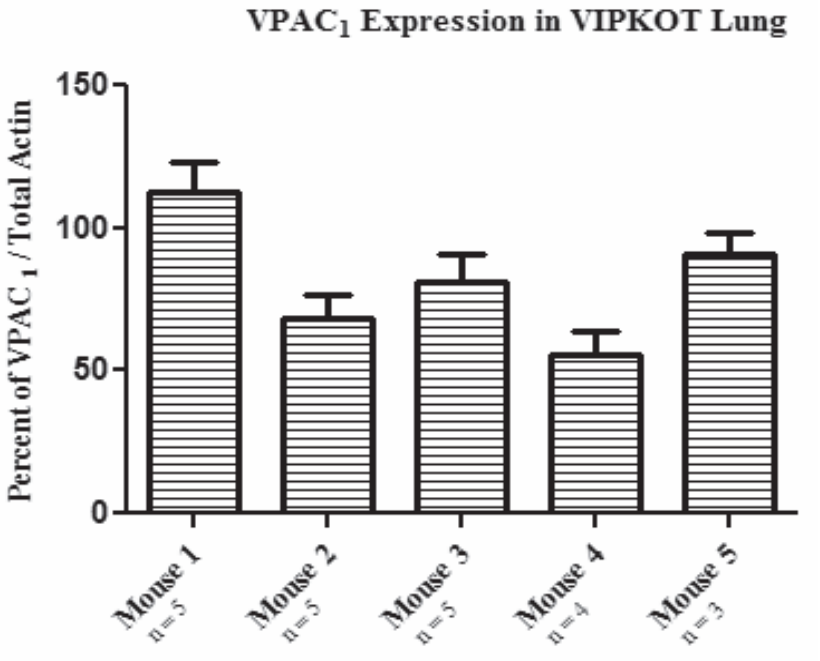
VPAC1 Expression in VIPKOT Lung
Percent of VPAC 1 / Total Actin
150
100
50
0
Mouse 1
n = 5
Mouse 2
n = 5
Mouse 3
n = 5
Mouse 4
n = 4
Mouse 5
n = 3

Figure 3.7 Average $VPAC_1$ lung expression for all combined samples tested in WT, VIPKO and VIPKO treated groups by western blotting. $VPAC_1$ band was normalized against actin comparing the percent of the $VPAC_1$ band to actin band ± SEM . n= 8 for WT group, n=5 for VIPKO and VIPKOT groups. Statistical analysis for WT vs VIPKO or VIPKOT ** $p < 0.01$, *** $p < 0.0001$

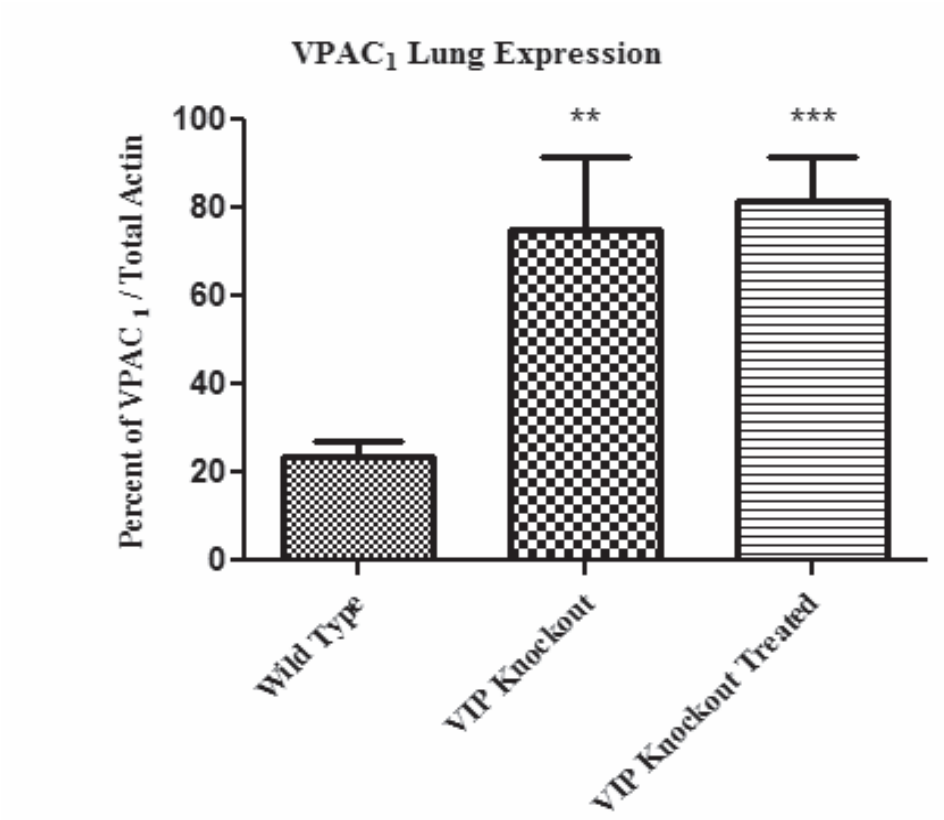
VPAC1 Lung Expression
Percent of VPAC 1 / Total Actin
100
80
60
40
20
0
**
***
Wild Type
VIP Knockout
VIP Knockout Treated

Figure 3.8 $VPAC_2$ receptor expression in whole lung tissue lysate from wild type mice. **A)** Representative western blot of 8 wild type mouse lung samples revealed with the monoclonial $VPAC_2$ (AS69) antibody. Each lane contains 50 μg of total protein. Membrane was then stripped and re-probed for actin as an internal control (lower panel). **B)** Densitometry values from western blots comparing the percent of the $VPAC_2$ band to actin band ± SEM of n= 3 independent experiments on each mouse lung sample. Arrow indicates expected size of $VPAC_2$ band.

A

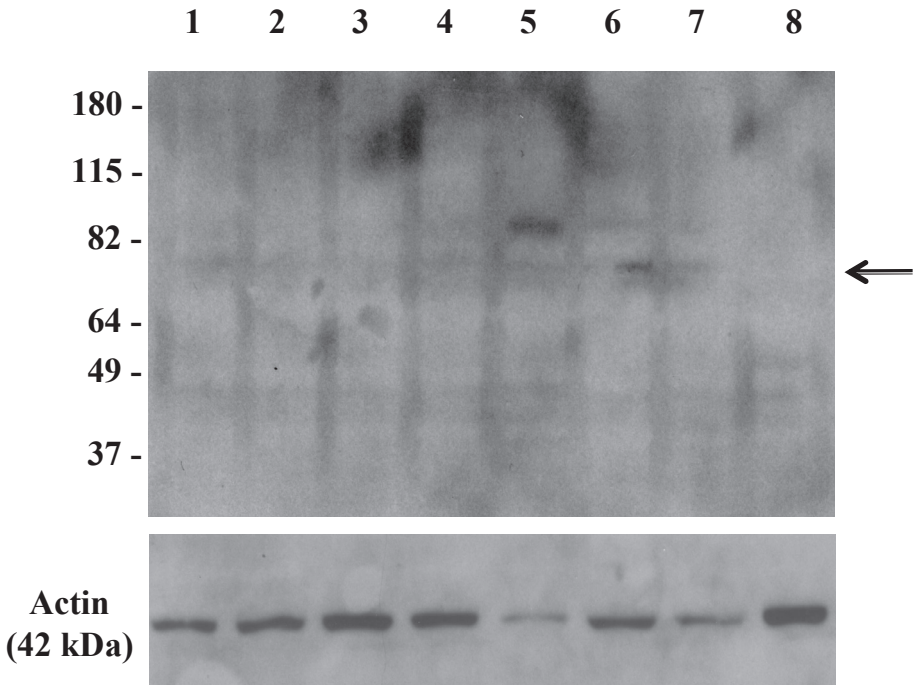
1 2 3 4 5 6 7 8
180 -
115 -
82 -
64 -
49 -
37 -
Actin
(42 kDa)

B

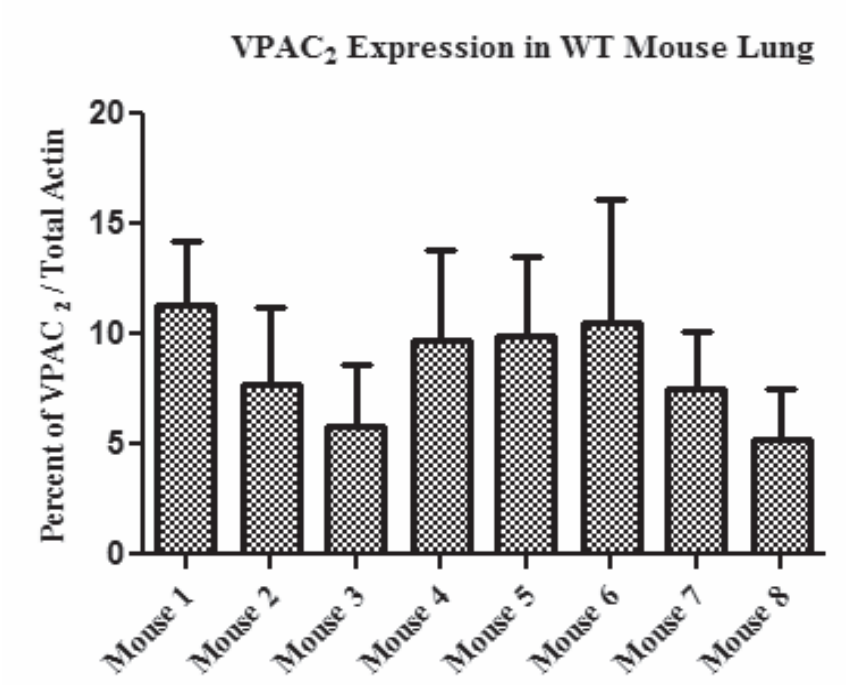
VPAC2 Expression in WT Mouse Lung
Percent of VPAC 2 / Total Actin
20
15
10
5
0
Mouse 1
Mouse 2
Mouse 3
Mouse 4
Mouse 5
Mouse 6
Mouse 7
Mouse 8

Figure 3.9 $VPAC_2$ receptor expression in whole lung tissue lysate from VIP knockout mice (VIPKO). **A)** Representative western blot of 5 VIPKO mouse lung samples revealed with the monoclonial $VPAC_2$ (AS69) antibody. Each lane contains 50 μg of total protein. Membrane was then stripped and re-probed for actin as an internal control (lower panel). **B)** Densitometry values from western blots comparing the percent of the $VPAC_2$ band to actin band ± SEM of n= 3-5 independent experiments on each mouse lung sample. Arrow indicates expected size of $VPAC_2$ band.

A

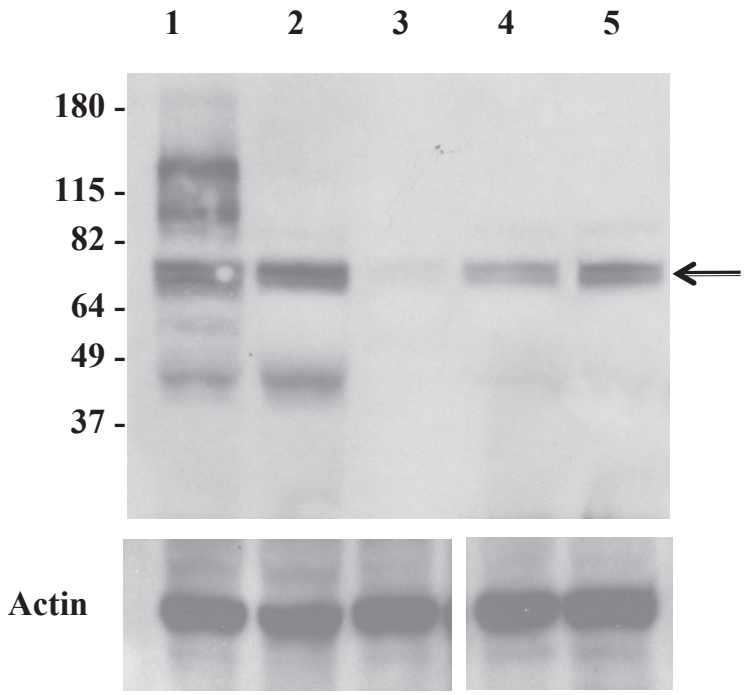
1
2
3
4
5
180 -
115 -
82 -
64 -
49 -
37 -
Actin

B

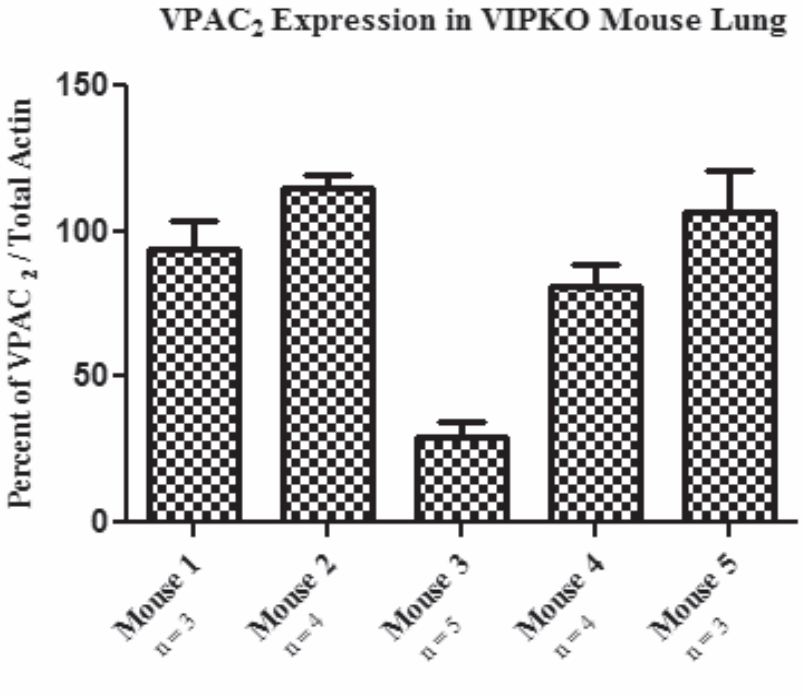
VPAC2 Expression in VIPKO Mouse Lung
Percent of VPAC 2 / Total Actin
150
100
50
0
Mouse 1
n = 3
Mouse 2
n = 4
Mouse 3
n = 5
Mouse 4
n = 4
Mouse 5
n = 3

Figure 3.10 $VPAC_2$ receptor expression in whole lung tissue lysate from VIP knockout treated mice (VIPKOT) that received 500 mg/kg VIP every other day for 3 weeks . **A)** Representative western blot of 5 VIPKOT mouse lung samples revealed with the monoclonial $VPAC_2$ (AS69) antibody. Each lane contains 50 μg of total protein. Membrane was then stripped and re-probed for actin as an internal control (lower panel). **B)** Densitometry values from western blots comparing the percent of the $VPAC_2$ band to actin band ± SEM of n= 3-5 independent experiments on each mouse lung sample. Arrow indicates expected size of $VPAC_2$ band.

A

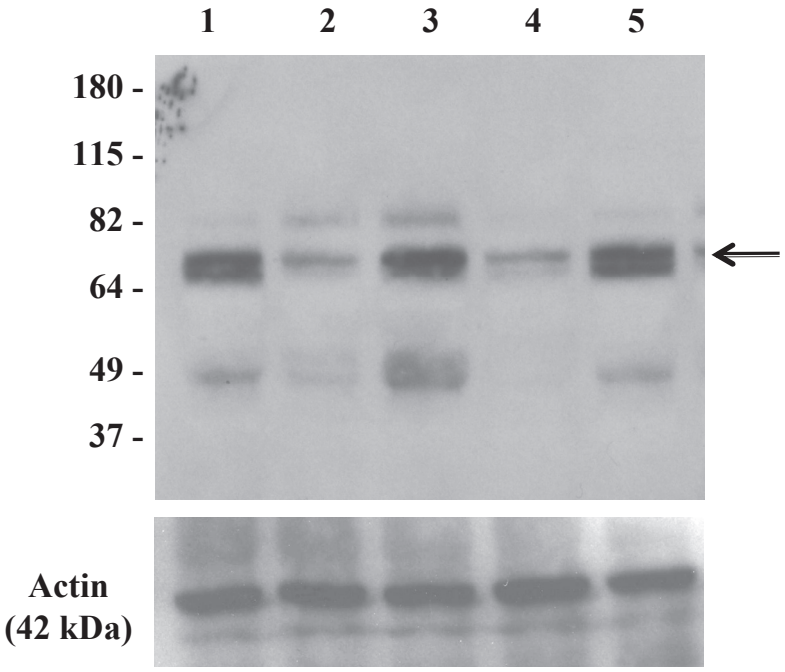
1
2
3
4
5
180 -
115 -
82 -
64 -
49 -
37 -
Actin
(42 kDa)

B

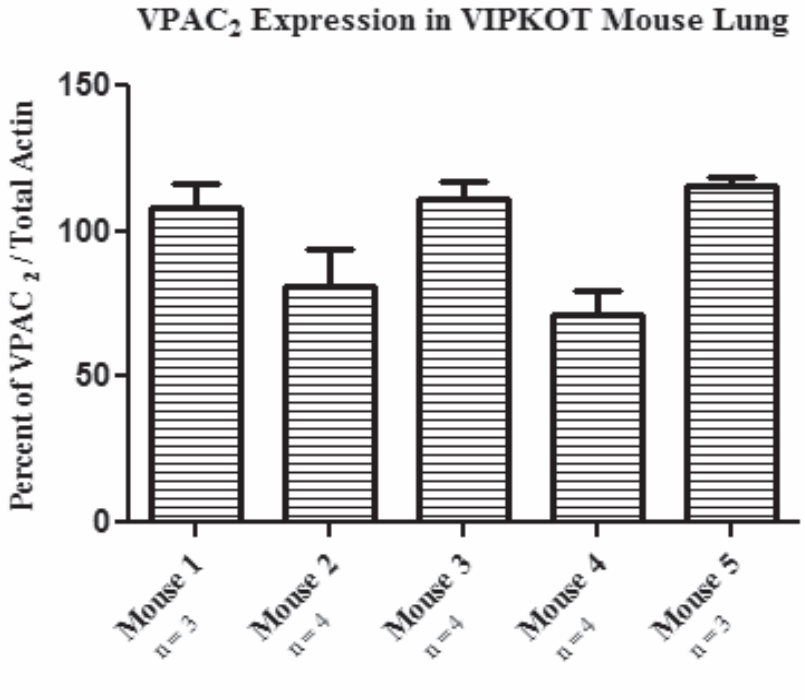
VPAC2 Expression in VIPKOT Mouse Lung
Percent of VPAC 2 / Total Actin
150
100
50
0
Mouse 1
n = 3
Mouse 2
n = 4
Mouse 3
n = 4
Mouse 4
n = 4
Mouse 5
n = 3

Figure 3.11 Average $VPAC_2$ lung expression for all combined samples tested in WT, VIPKO and VIPKO treated groups by western blotting. $VPAC_2$ band was normalized against actin comparing the percent of the $VPAC_2$ band to actin band ± SEM . n= 8 for WT group, n=5 for VIPKO and VIPKOT groups. Statistical analysis for WT vs VIPKO or VIPKOT *** $P < 0.0001$

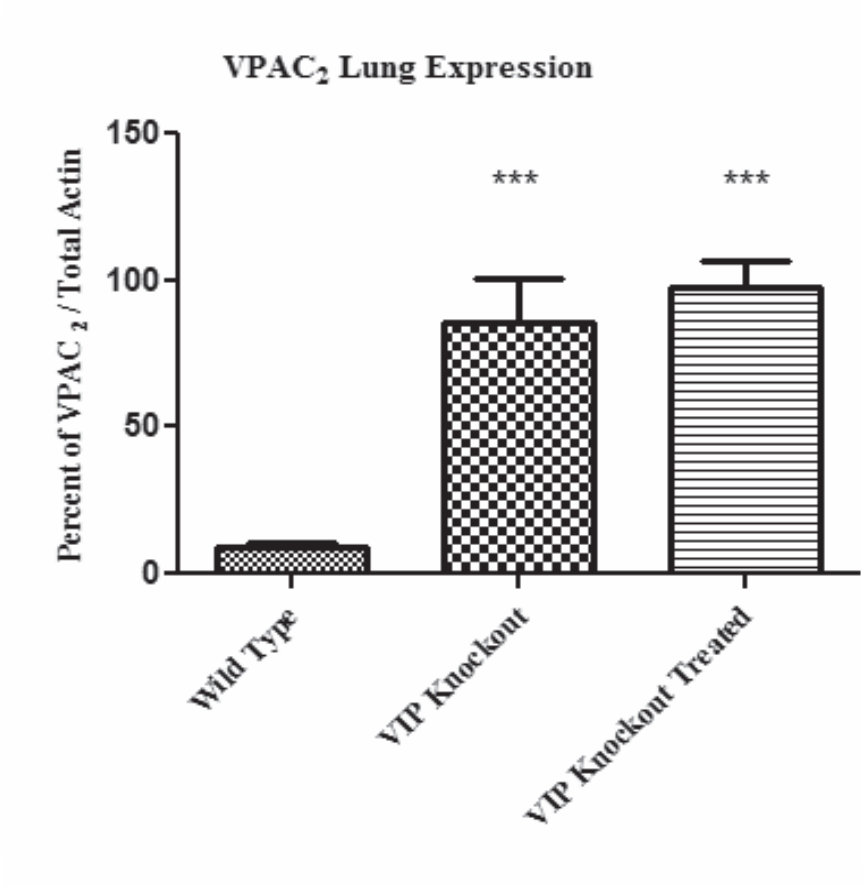
VPAC2 Lung Expression
Percent of VPAC 2 / Total Actin
150
100
50
0
***
***
Wild Type
VIP Knockout
VIP Knockout Treated

Figure 3.12 PAC_1 receptor expression in whole lung tissue lysate from wild type mice. **A)** Representative western blot of 8 wild type mouse lung samples revealed with the monoclonial PAC_1 (1B5) antibody. Each lane contains 50 μg of total protein. Membrane was then stripped and re-probed for actin as an internal control (lower panel). **B)** Densitometry values from western blots comparing the percent of the PAC_1 band to actin band ± SEM of n= 5 independent experiments on each mouse lung sample. Arrow indicates expected size of PAC_1 band.

A

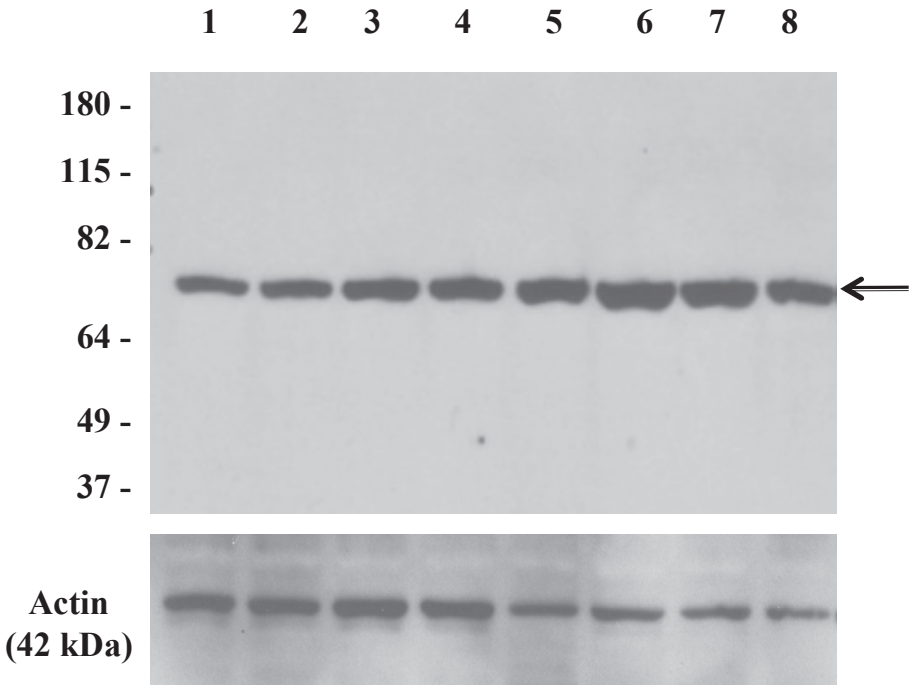
1 2 3 4 5 6 7 8
180 -
115 -
82 -
64 -
49 -
37 -
Actin
(42 kDa)

B

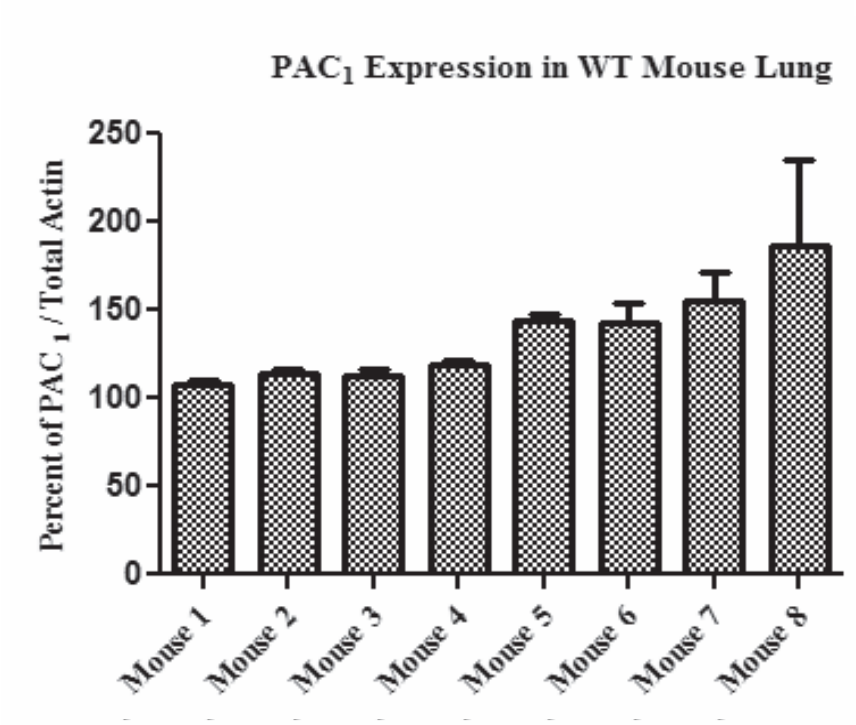
PAC1 Expression in WT Mouse Lung
Percent of PAC 1 / Total Actin
250
200
150
100
50
0
Mouse 1
Mouse 2
Mouse 3
Mouse 4
Mouse 5
Mouse 6
Mouse 7
Mouse 8

Figure 3.13 PAC_1 receptor expression in whole lung tissue lysate from VIP knockout mice (VIPKO). **A)** Representative western blot of 5 VIPKO mouse lung samples revealed with the monoclonial PAC_1 (1B5) antibody. Each lane contains 50 μg of total protein. Membrane was then stripped and probed for actin as an internal control (lower panel). **B)** Densitometry values from western blots comparing the percent of the PAC_1 band to actin band ± SEM of n= 3 independent experiments on each mouse lung sample. Arrow indicates expected size of PAC_1 band.

A

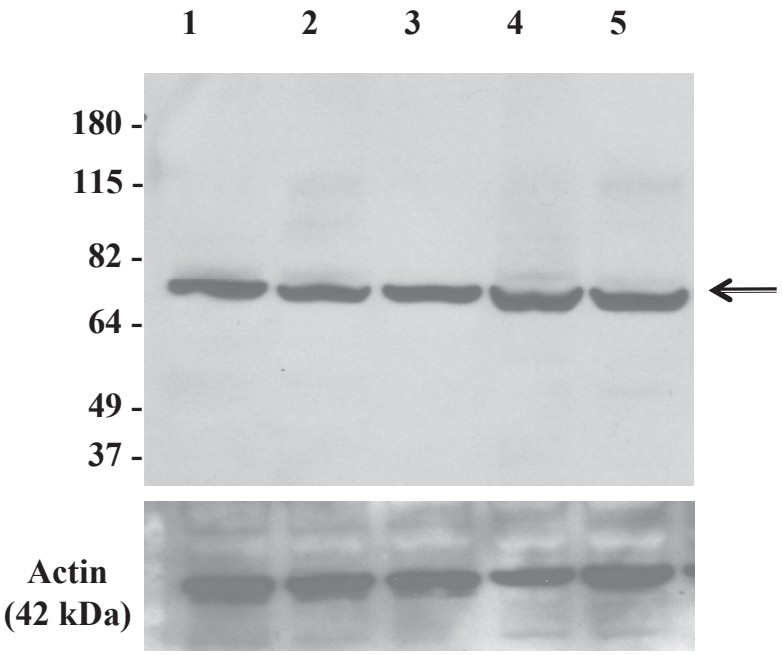
1
2
3
4
5
180 -
115 -
82 -
64 -
49 -
37 -
Actin
(42 kDa)

B

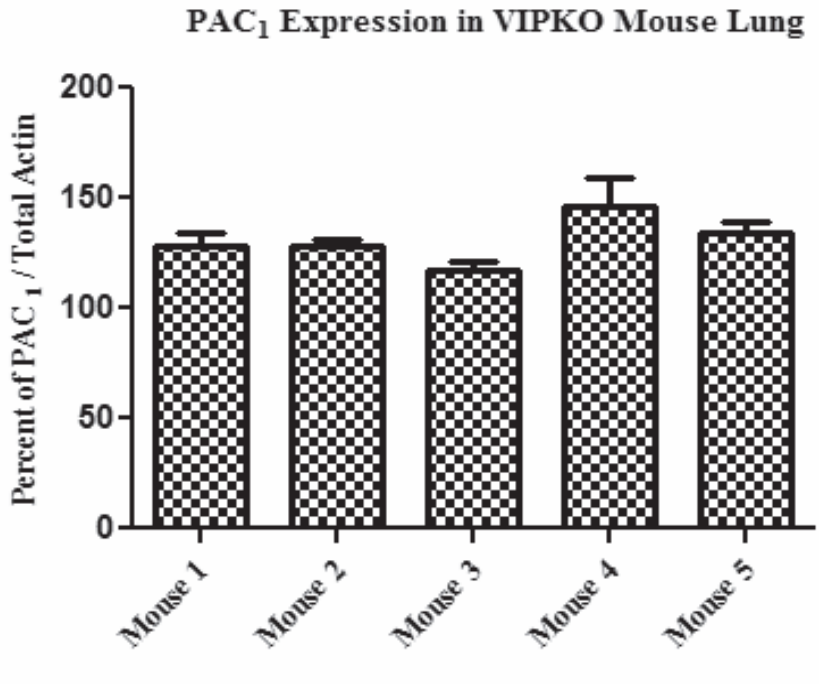
PAC1 Expression in VIPKO Mouse Lung
Percent of PAC 1 / Total Actin
200
150
100
50
0
Mouse 1
Mouse 2
Mouse 3
Mouse 4
Mouse 5

Figure 3.14 PAC_1 receptor expression in whole lung tissue lysate from VIP knockout treated mice (VIPKOT) that received 500 mg/kg VIP every other day for 3 weeks . **A)** Representative western blot of 5 VIPKOT mouse lung samples revealed with the monoclonial PAC_1 (1B5) antibody. Each lane contains 50 μg of total protein. Membrane was then stripped and probed for actin as an internal control (lower panel). **B)** Densitometry values from western blots comparing the percent of the PAC_1 band to actin band ± SEM of n= 3 independent experiments on each mouse lung sample. Arrow indicates expected size of PAC_1 band.

A

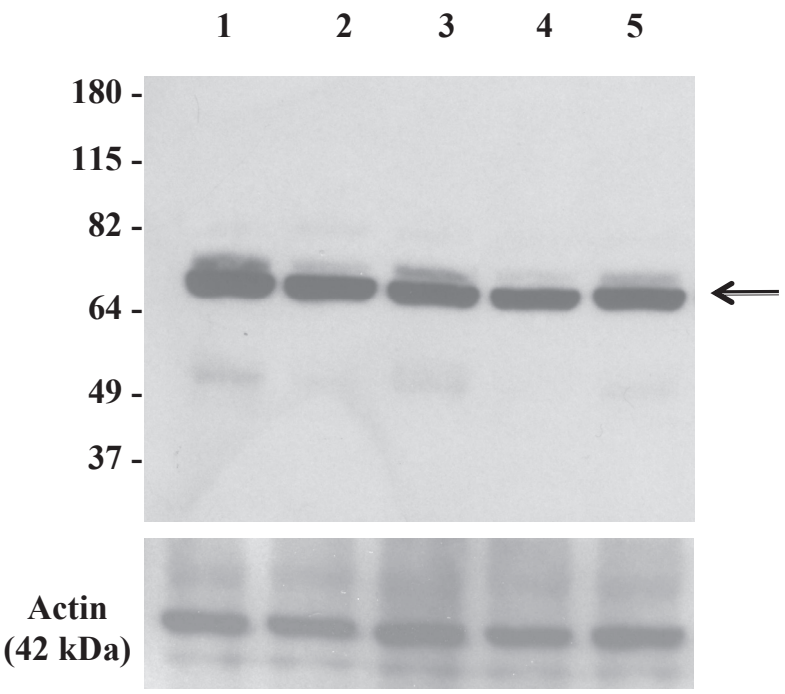
1
2
3
4
5
180 -
115 -
82 -
64 -
49 -
37 -
Actin
(42 kDa)

B

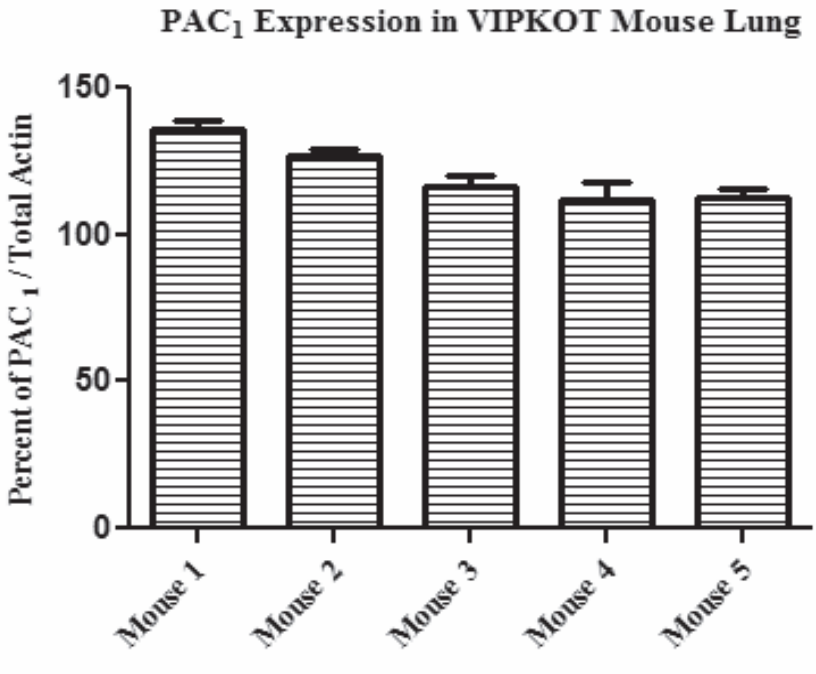
PAC1 Expression in VIPKOT Mouse Lung
Percent of PAC 1 / Total Actin
150
100
50
0
Mouse 1
Mouse 2
Mouse 3
Mouse 4
Mouse 5

Figure 3.15 Average PAC_1 lung expression for all combined samples tested in WT, VIPKO and VIPKO treated groups by western blotting. PAC_1 band was normalized against actin comparing the percent of the PAC_1 band to actin band ± SEM . n= 8 for WT group, n=5 for VIPKO and VIPKOT groups.

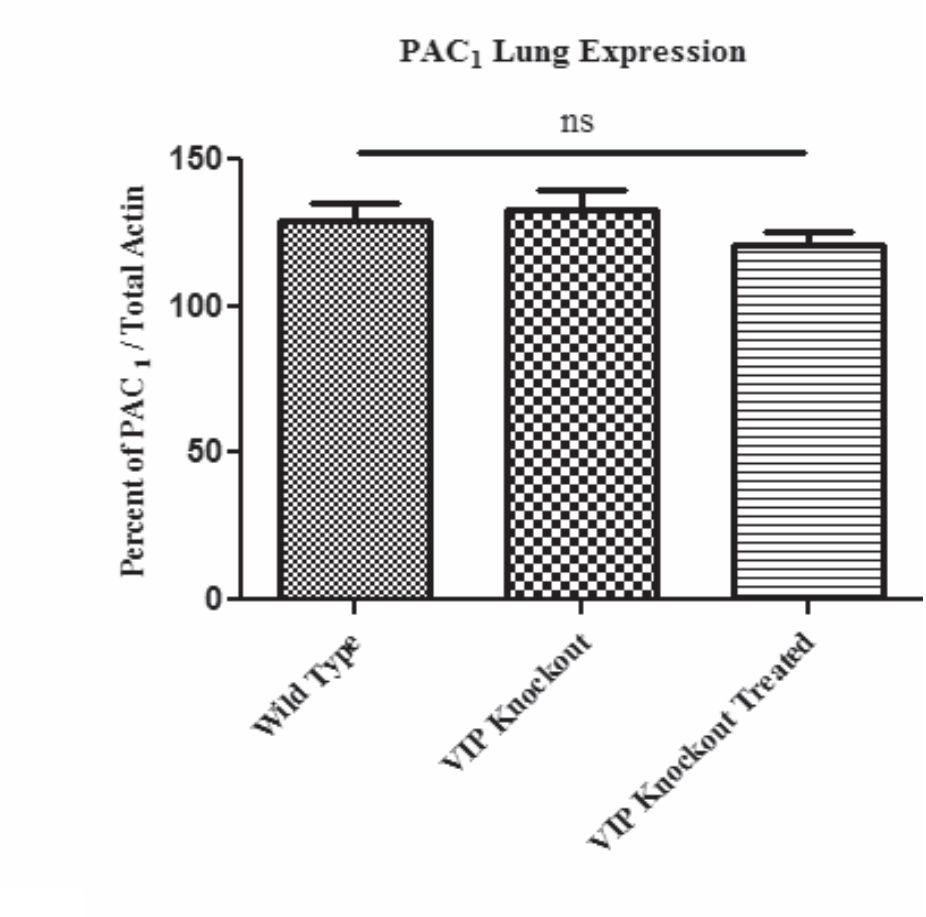
PAC1 Lung Expression
ns
150
100
50
0
Percent of PAC 1 / Total Actin
Wild Type
VIP Knockout
VIP Knockout Treated

Figure 3.16 CFTR protein expression in whole lung tissue lysate from wild type (WT) mice. **A)** Representative western blot of 8 wild type mice lung samples, each lane contained 50 μg of protein and was revealed with monoclonal CFTR (MM13-4) antibody. Membrane was then stripped and probed for actin as an internal control (lower panal). **B) D**ensitometry values from western blots comparing the percent of CFTR protein band to actin band ± SEM of n= 3 for each mouse. Arrow indicates expected CFTR band size.

A

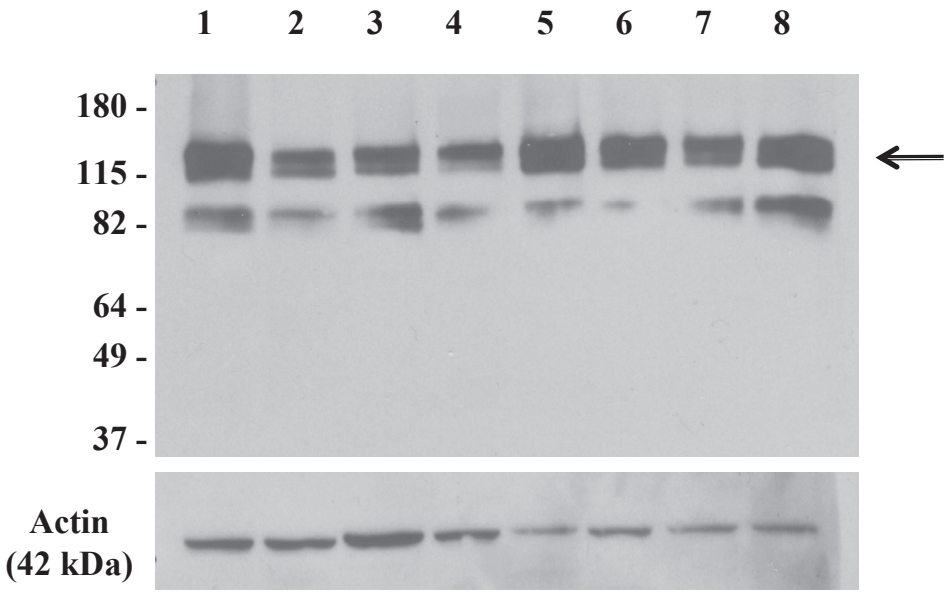
1 2 3 4 5 6 7 8
180 -
115 -
82 -
64 -
49 -
37 -
Actin
(42 kDa)

B

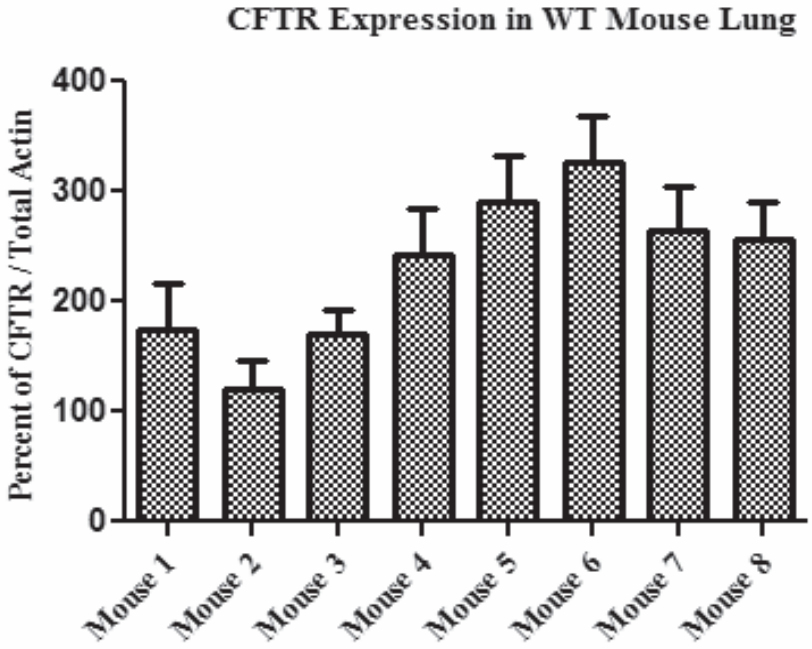
CFTR Expression in WT Mouse Lung
Percent of CFTR / Total Actin
400
300
200
100
0
Mouse 1
Mouse 2
Mouse 3
Mouse 4
Mouse 5
Mouse 6
Mouse 7
Mouse 8

Figure 3.17 CFTR protein expression in whole lung tissue lysate from VIP knockout (VIPKO) mice. **A)** Representative western blot of 5 VIPKO mice lung samples, each lane contained 50 μg of protein and was revealed with monoclonal CFTR (MM13-4) antibody. Membrane was then stripped and re-probed for actin as an internal control (lower panal). **B) D**ensitometry values from western blots comparing the percent of CFTR protein band to actin band ± SEM of n= 3-5 for each mouse. Arrow indicates expected CFTR band size.

A

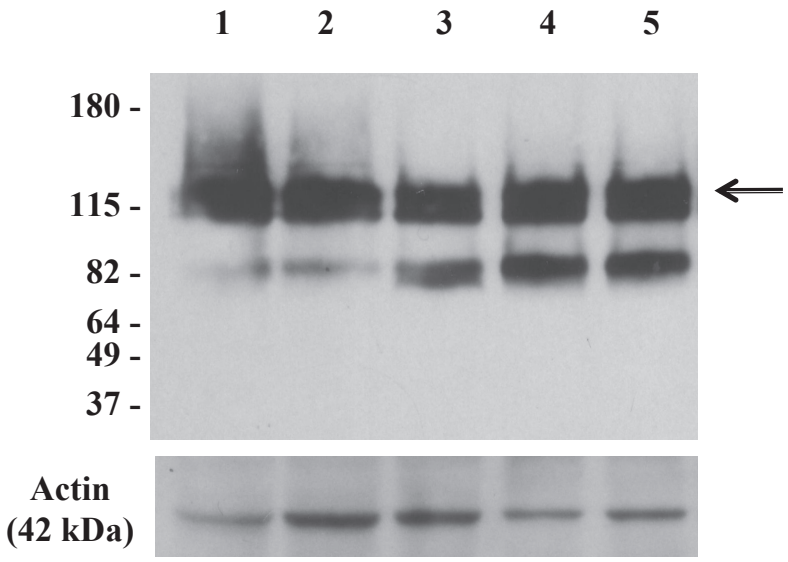
1
2
3
4
5
180 -
115 -
82 -
64 -
49 -
37 -
Actin
(42 kDa)

B

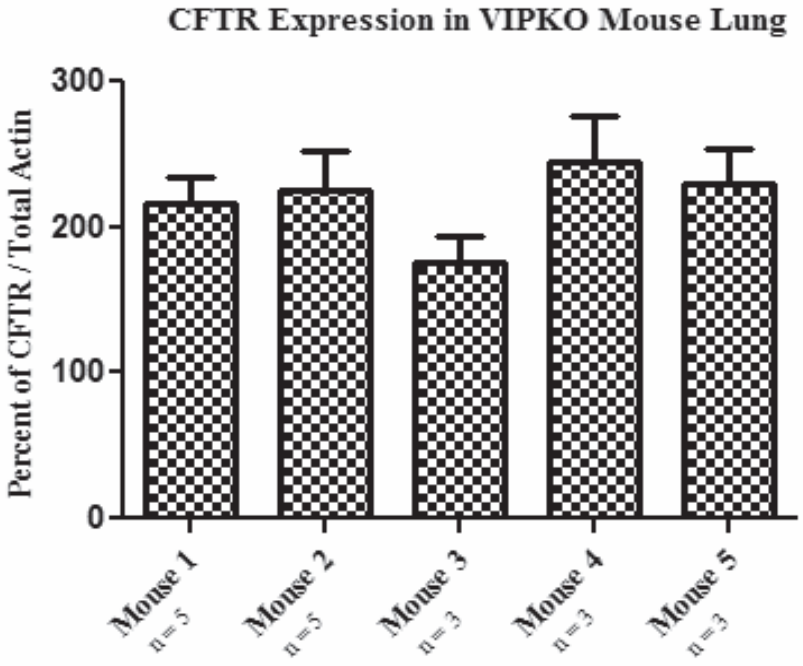
CFTR Expression in VIPKO Mouse Lung
Percent of CFTR / Total Actin
300
200
100
0
Mouse 1
n = 5
Mouse 2
n = 5
Mouse 3
n = 3
Mouse 4
n = 3
Mouse 5
n = 3

Figure 3.18 CFTR protein expression in whole tissue lung lysate from VIP Knockout treated (VIPKOT) mice. **A)** Representative western blot of 5 VIPKOT mice lung samples, each lane contained 50 μg of protein that was reveled with monoclonal CFTR (MM13-4) antibody. Membrane was then stripped and probe for actin as an internal control (lower panel). **B)** Densitometry values from western blots comparing the percent of CFTR protein band to actin band ± SEM of n= 3-4 for each mouse. Arrow indicates expected CFTR band size.

A

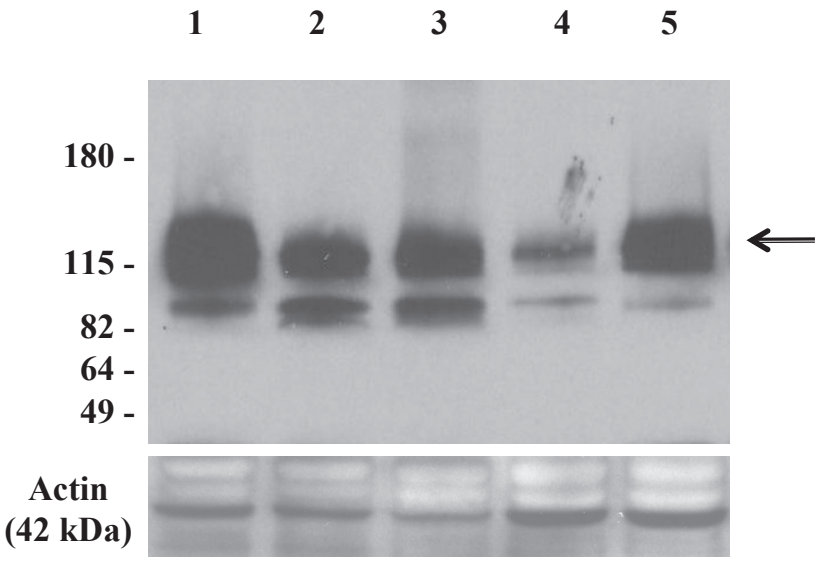
1
2
3
4
5
180 -
115 -
82 -
64 -
49 -
Actin
(42 kDa)

B

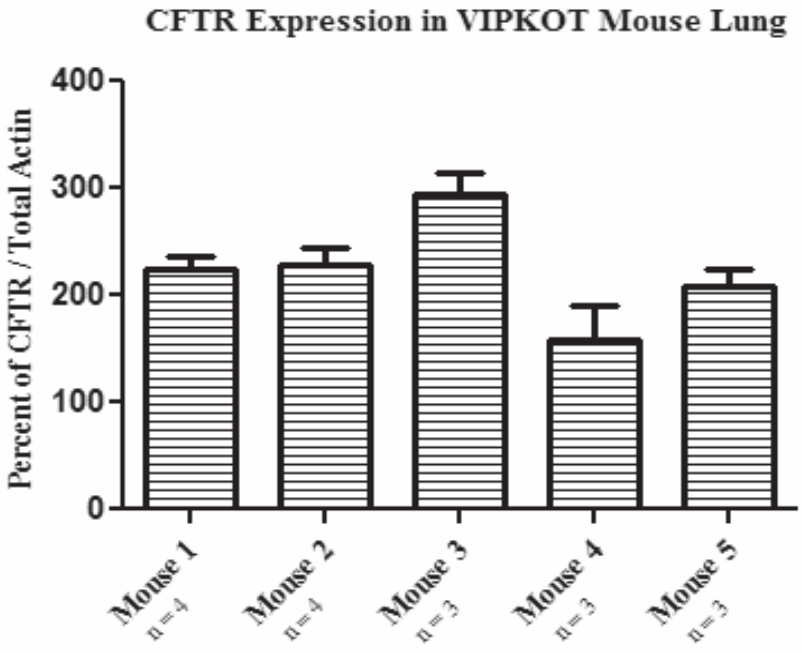
CFTR Expression in VIPKOT Mouse Lung
Percent of CFTR / Total Actin
400
300
200
100
0
Mouse 1
n = 4
Mouse 2
n = 4
Mouse 3
n = 3
Mouse 4
n = 3
Mouse 5
n = 3

Figure 3.19 Average CFTR lung expression for all combined samples tested in WT, VIPKO and VIPKO treated groups with western blotting. CFTR band was normalized against actin comparing the percent of CFTR band to actin band as a percentage ± SEM . n= 8 for WT group, n=5 for VIPKO and VIPKOT groups

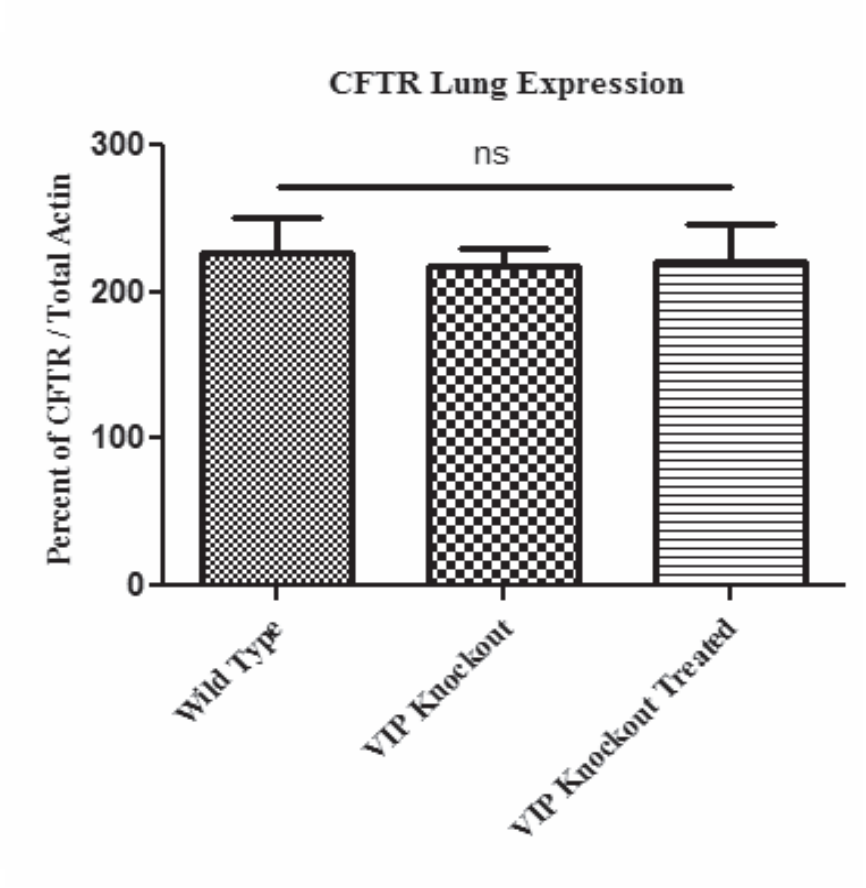
CFTR Lung Expression
ns
300
200
100
0
Percent of CFTR / Total Actin
Wild Type
VIP Knockout
VIP Knockout Treated

Figure 3.20 Positive and negative controls in wild type (WT), VIP knockout (VIPKO) and VIP knockout treated (VIPKOT) C57BL/6 mouse duodenum using RT-PCR after RNA was extracted and converted to cDNA. Positive control primer was designed using the GenBank sequence specific to *Mus musculus* for PKC α and negative controls had no primer added to the reaction . All products were run using 0.8% agarose gel electrophoresis and using the φx molecular marker. **A)** WT duodenum controls, positive control PKC α on the left and negative control on the left. **B)** VIPKO duodenum controls, positive control PKC α on the left and negative control on the left. **C)** VIPKOT duodenum controls, positive control PKC α on the left and negative control on the left. The expected size in base pair (bp) is displayed above each lane.

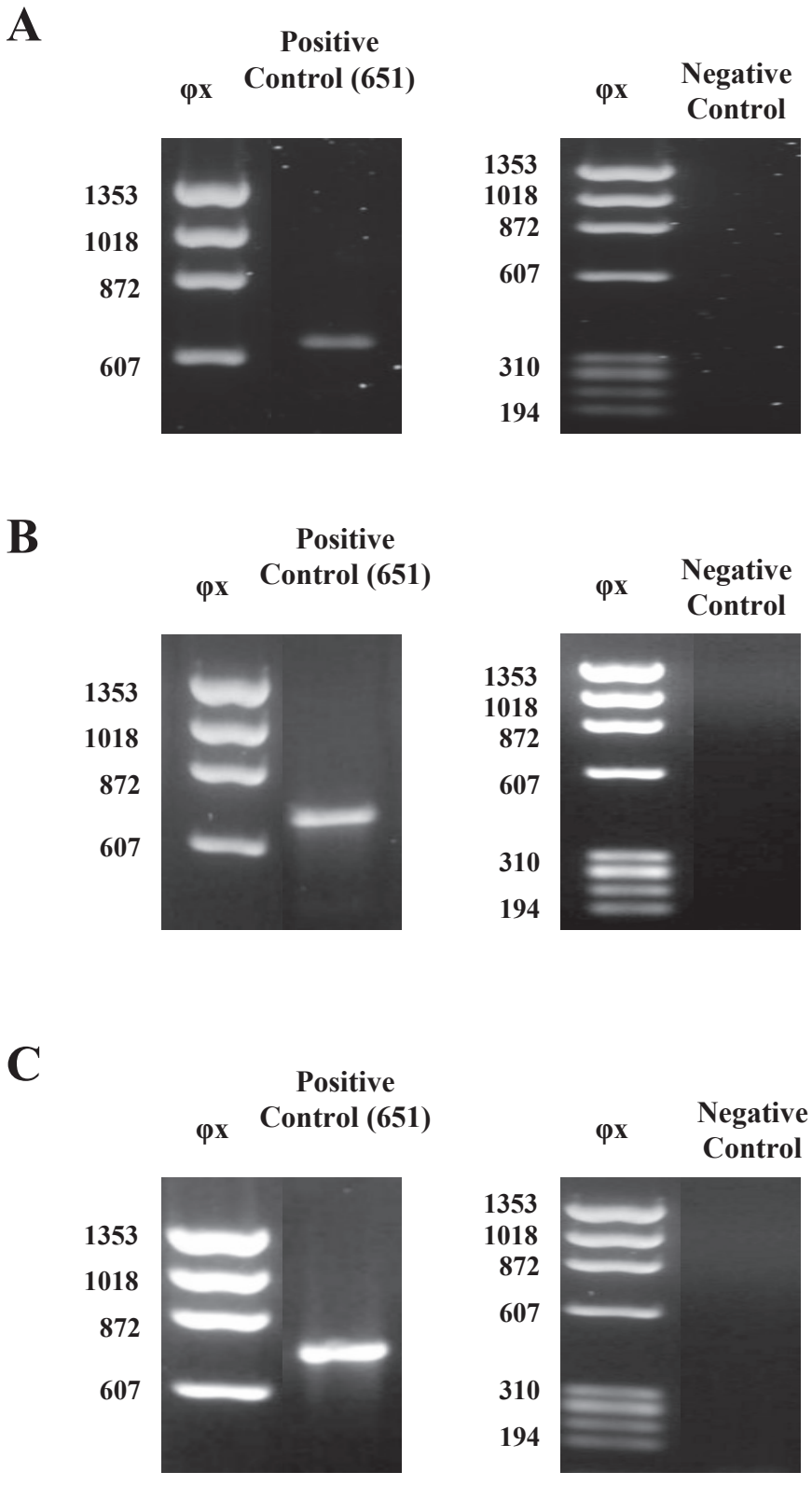
A
φx
Positive Control (651)
φx
Negative Control
1353
1018
872
607
310
194
B
φx
Positive Control (651)
φx
Negative Control
1353
1018
872
607
310
194
C
φx
Positive Control (651)
φx
Negative Control
1353
1018
872
607
310
194

Figure 3.21 Detection of VIP receptor cDNA in wild type (WT), VIP knockout (VIPKO) and VIP knockout treated (VIPKOT) C57BL/6 mouse duodenum using RT-PCR after RNA extraction and conversion to cDNA. All primers were designed using GenBank sequences specific to *Mus musculus* for each VIP receptor and PKC α. All products were run using 0.8% agarose gel electrophoresis and using the φx molecular marker. **A)** $VPAC_1$ receptor cDNA detection in WT (left), VIPKO (center) and VIPKOT (right) mouse duodenum. **B)** $VPAC_2$ receptor cDNA detection in WT (left), VIPKO (center) and VIPKOT (right) mouse duodenum. **C)** PAC_1 receptor cDNA detection in WT (left), VIPKO (center) and VIPKOT (right) mouse duodenum. The expected size in base pair (bp) is displayed above each lane.

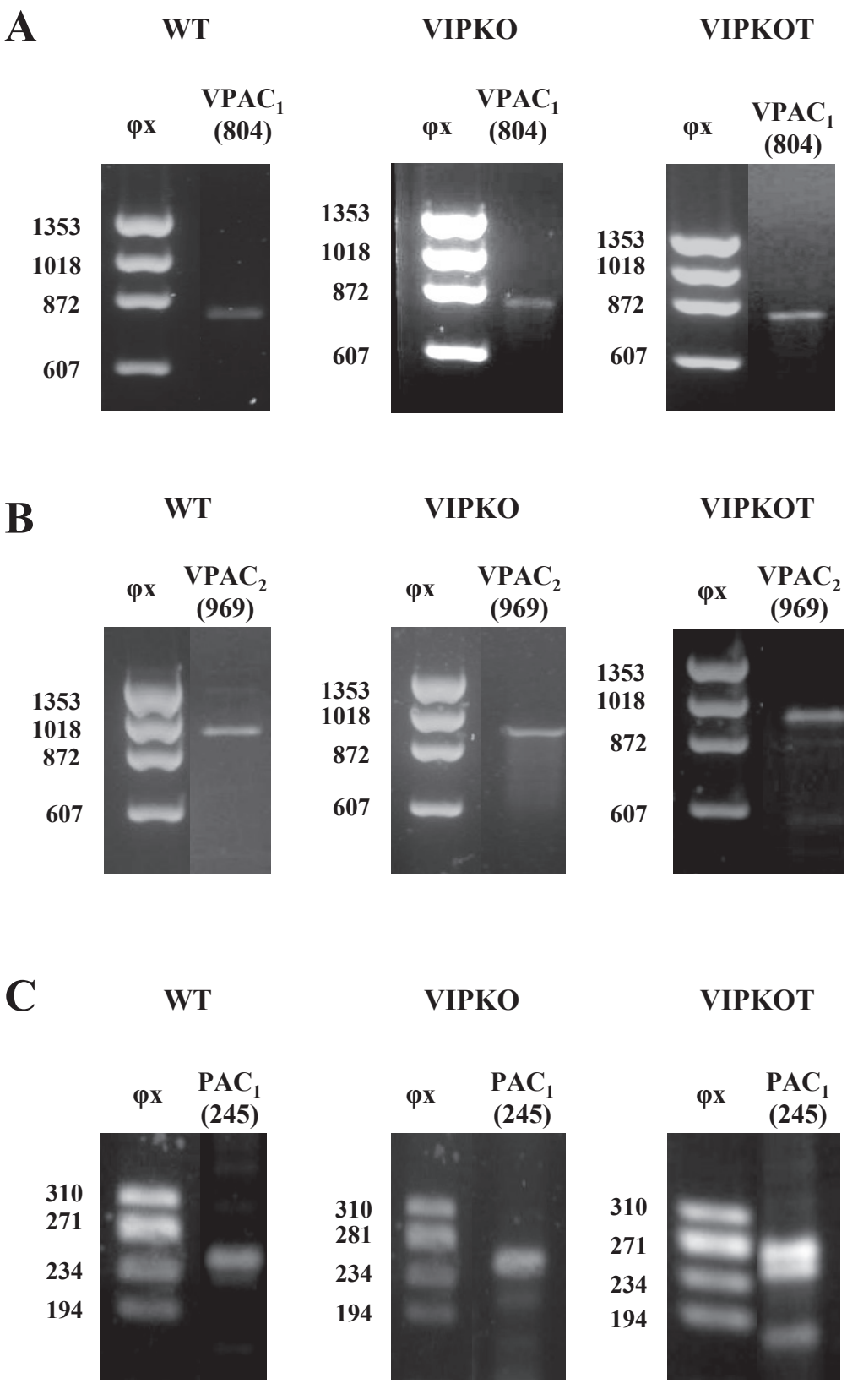
A
WT
VIPKO
VIPKOT
φx
VPAC1 (804)
1353
1018
872
607
B
WT
VIPKO
VIPKOT
φx
VPAC2 (969)
1353
1018
872
607
C
WT
VIPKO
VIPKOT
φx
PAC1 (245)
310
271
234
194
281

Figure 3.22 $VPAC_1$ receptor expression in whole tissue duodenum lysate from **A)** WT, **B)** VIPKO and **C)** VIPKOT mice. Each lane contains 50 μg of protein and was reveled with monoclonal $VPAC_1$ (AS58) antibody. n = 3 independent experiments on each mouse lung sample. Arrow indicates expected size of $VPAC_1$ band.

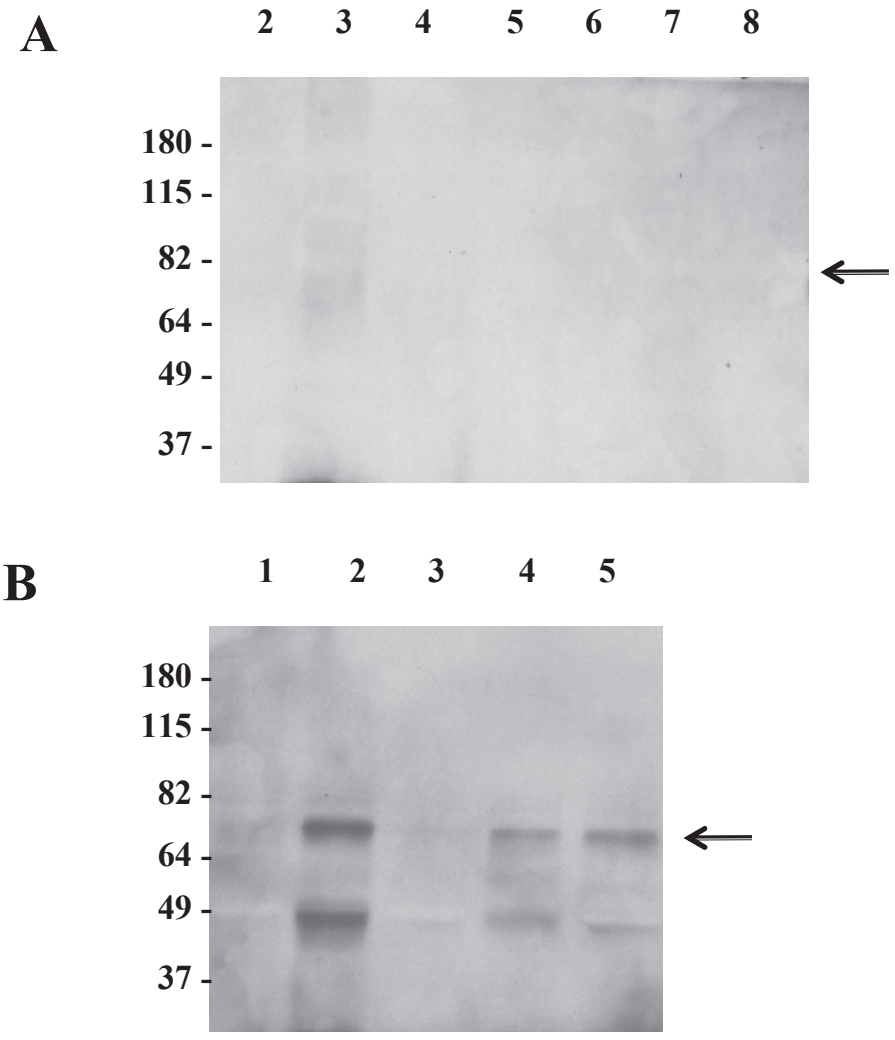
A
2 3 4 5 6 7 8
180 -
115 -
82 -
64 -
49 -
37 -
B
1 2 3 4 5
180 -
115 -
82 -
64 -
49 -
37 -
C
1 2 3 4 5
180 -
115 -
82 -
64 -
49 -
37 -

Figure 3.23 $VPAC_2$ receptor expression in whole tissue duodenum lysate from **A)** WT, **B)** VIPKO and **C)** VIPKOT mice. Each lane contains 50 μg of protein and was reveled with monoclonal $VPAC_2$ (AS69) antibody. n = 3 independent experiments on each mouse lung sample. Arrow indicates expected size of $VPAC_2$ band.

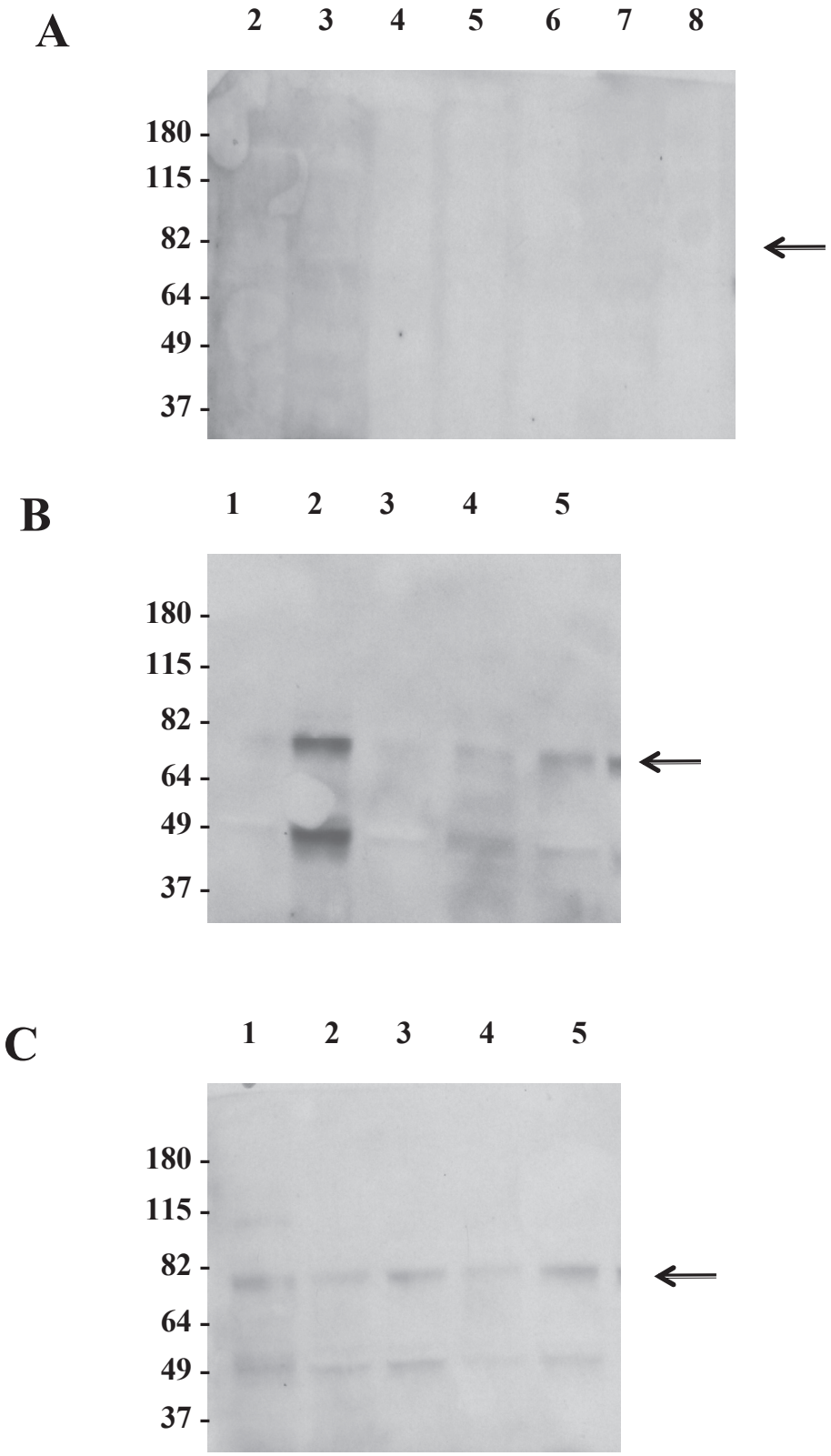
A
2 3 4 5 6 7 8
180
115
82
64
49
37
B
1 2 3 4 5
180
115
82
64
49
37
C
1 2 3 4 5
180
115
82
64
49
37

Figure 3.24 PAC_1 receptor expression in whole tissue duodenum lysate from **A)** WT, **B)** VIPKO and **C)** VIPKOT mice. Each lane contains 50 μg of protein and was reveled with monoclonal PAC_1 (1B5) antibody. n = 3 independent experiments on each mouse lung sample. Arrow indicates expected size of PAC_1 band.

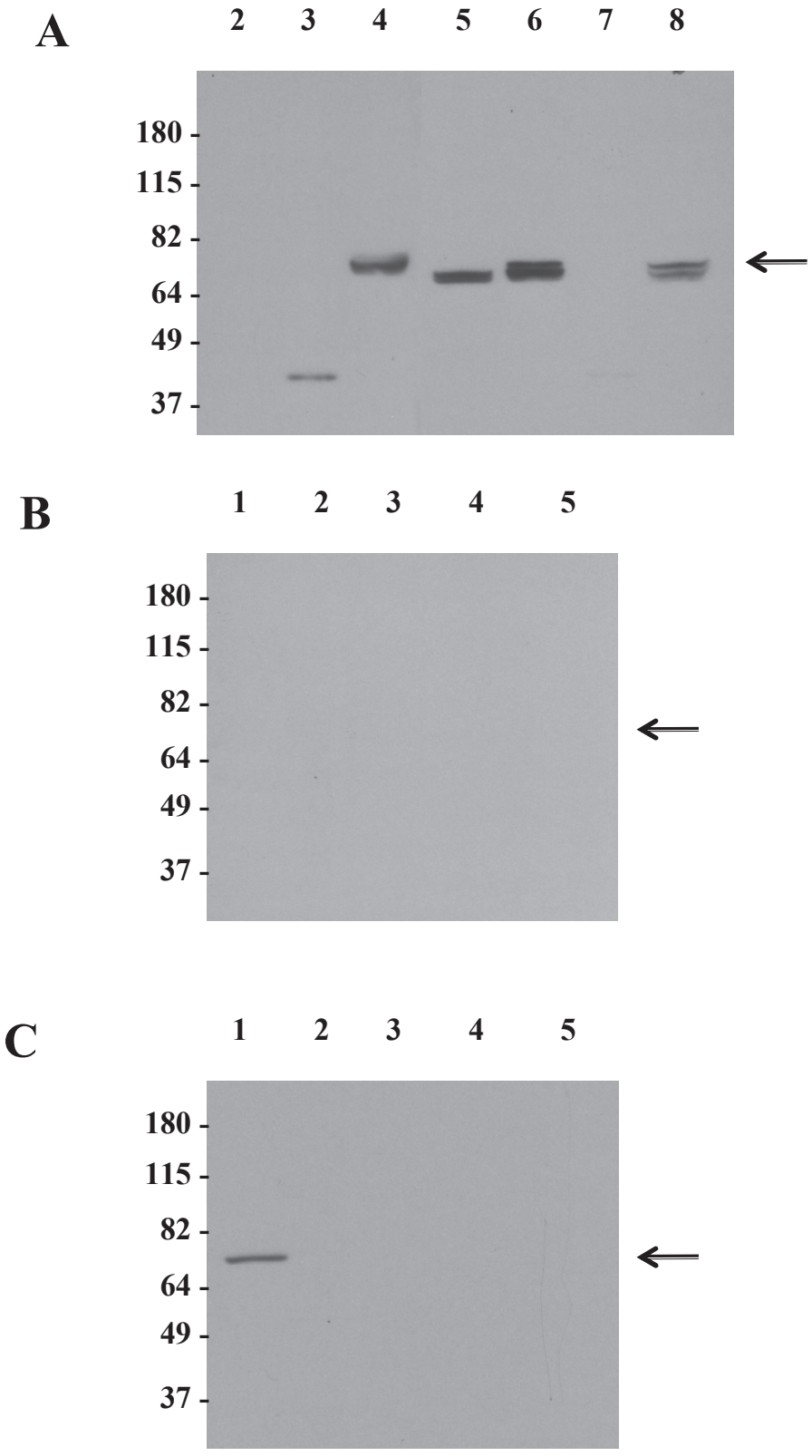
A
2 3 4 5 6 7 8
180
115
82
64
49
37
B
1 2 3 4 5
180
115
82
64
49
37
C
1 2 3 4 5
180
115
82
64
49
37

Figure 3.25 CFTR protein expression in whole tissue duodenum lysate from **A)** WT, **B)** VIPKO and **C)** VIPKOT mice. Each lane contains 50 μg of protein and was reveled with monoclonal CFTR (MM13-4) antibody. n = 3 independent experiments on each mouse lung sample. Arrow indicates expected size of CFTR band.

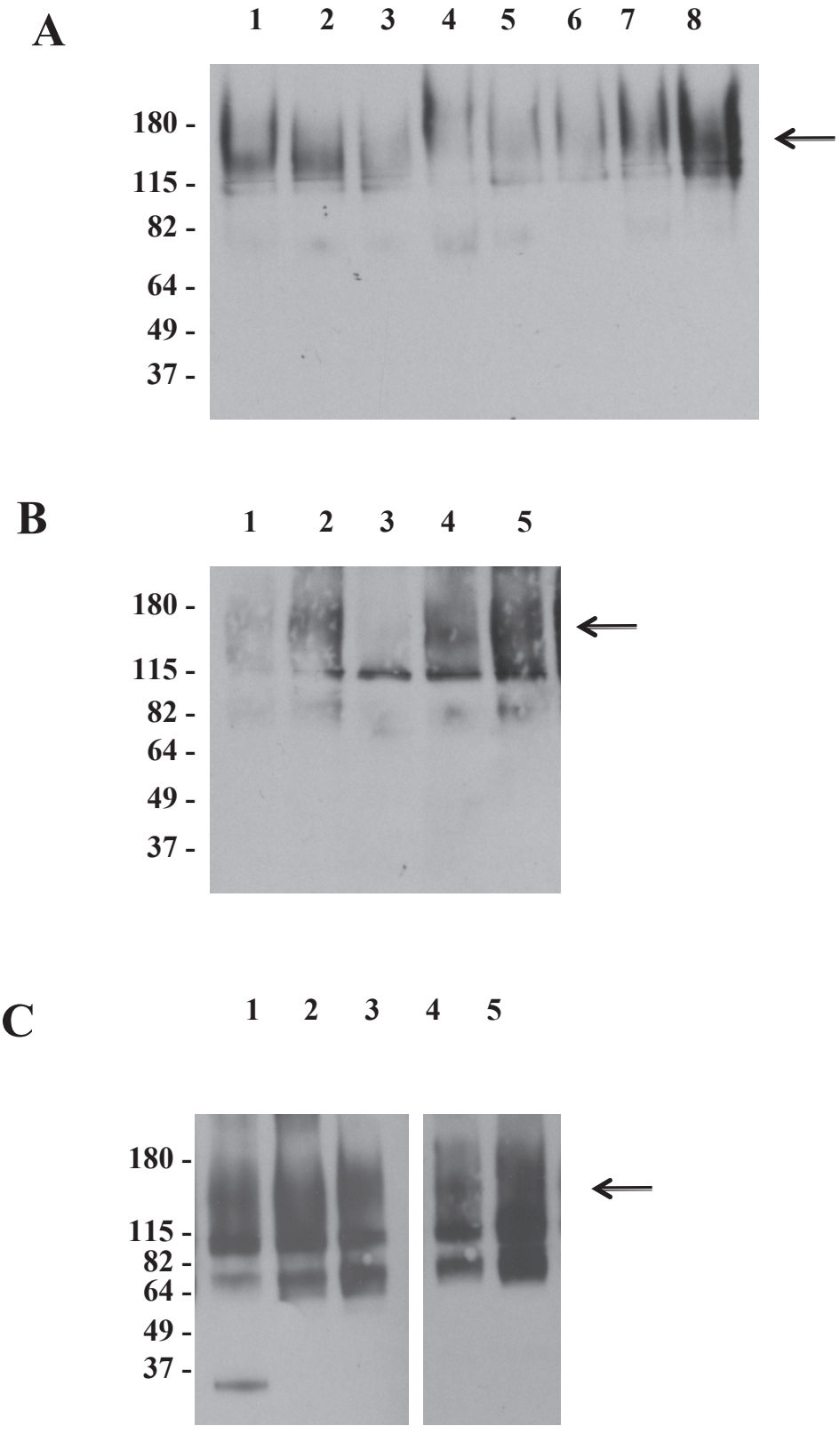
A
1 2 3 4 5 6 7 8
180 -
115 -
82 -
64 -
49 -
37 -
B
1 2 3 4 5
180 -
115 -
82 -
64 -
49 -
37 -
C
1 2 3 4 5
180 -
115 -
82 -
64 -
49 -
37 -